SIMULATION OF THE RECORDED RESPONSE OF UNREINFORCED MASONRY (URM) INFILL BUILDINGS

by

John Kariotis
Kariotis & Associates
South Pasadena, California

Jeff Guh
Delon Hampton & Associates

Gary Hart
Hart Consultant Group

James Hill
James A. Hill & Associates

Nabih Youssef
Nabih Youssef & Associates

and

Doc Nghiem
Department of Building and Safety, City of Los Angeles

Data Utilization Report CSMIP/94-05

California Strong Motion Instrumentation Program

October 1994

This study was conducted at the Kariotis & Associates at South Pasadena and was supported by the Department of Conservation under Contract No. 1091-533.

California Department of Conservation
Division of Mines and Geology
Office of Strong Motion Studies
801 K Street, MS 13-35
Sacramento, California 95814-3531

DIVISION OF MINES AND GEOLOGY
JAMES F. DAVIS
STATE GEOLOGIST

DISCLAIMER

The content of this report was developed under Contract No. 1091-533 from the Strong Motion Instrumentation Program in the Division of Mines and Geology of the California Department of Conservation. This report has not been edited to the standards of a formal publication. Any opinions, findings, conclusions or recommendations contained in this report are those of the authors, and should not be interpreted as representing the official policies, either expressed or implied, of the State of California.

PREFACE

The California Strong Motion Instrumentation Program (CSMIP) in the Division of Mines and Geology of the California Department of Conservation promotes and facilitates the improvement of seismic codes through the Data Interpretation Project. The objective of the this project is to increase the understanding of earthquake strong ground shaking and its effects on structures through interpretation and analysis studies of CSMIP and other applicable strong motion data. The ultimate goal is to accelerate the process by which lessons learned from earthquake data are incorporated into seismic code provisions and seismic design practices.

The specific objectives of the CSMIP Data Interpretation Project are to:

1. Understand the spatial variation and magnitude dependence of earthquake strong ground motion.

2. Understand the effects of earthquake motions on the response of geologic formations, buildings and lifeline structures.

3. Expedite the incorporation of knowledge of earthquake shaking into revision of seismic codes and practices.

4. Increase awareness within the seismological and earthquake engineering community about the effective usage of strong motion data.

5. Improve instrumentation methods and data processing techniques to maximize the usefulness of SMIP data. Develop data representations to increase the usefulness and the applicability to design engineers.

This report is the tenth in a series of CSMIP data utilization reports designed to transfer recent research findings on strong-motion data to practicing seismic design professionals and earth scientists. CSMIP extends its appreciation to the members of the Strong Motion Instrumentation Advisory Committee and its subcommittees for their recommendations regarding the Data Interpretation Research Project.

Moh J. Huang
CSMIP Data Interpretation
Project Manager

Anthony F. Shakal
CSMIP Program Manager

ABSTRACT

The Strong Motion Instrumentation Program of the California Department of Mines and Geology (CSMIP) has obtained records of the response of four buildings with unreinforced masonry (URM) infills. The response was to the Landers, Upland and Sierra Madre earthquakes. The objective of this research was to replicate by computer analysis the CSMIP records.

Three-dimensional elastic computer models were prepared from data obtained from the original construction documents. The URM infills were modeled as diagonal braces in the frame. The stiffness properties of the infills were determined by a nonlinear finite element analysis.

Two of the buildings were steel frame and two were reinforced concrete frame buildings. Two of the buildings had records from two earthquakes. The height of the buildings varied from 5 to 12 stories. All buildings were highly irregular both in plan and vertically.

The values of material properties for use in the nonlinear analyses were estimated and were used as a variable in the procedure for correlation of recorded and calculated data.

Good correlation as to peak displacement was obtained. Good correlation of plots of relative displacement vs. time were obtained for brief periods of time. The damping and stiffness of the building, as recorded, changed during the time of shaking. The elastic model used an effective stiffness and a fixed value of viscous damping.

APPLICATION TO CODES AND PRACTICES

The goal of this research was to provide information for the development of standards and ordinances for reduction of earthquake hazard in frame buildings that have unreinforced masonry infills. Information on how to model the frame and the effect of the infill on the frame stiffness and how to account for stiffness degradation in the frame-infill system was needed. This research has developed a procedure for conversion of the URM infills, in any configuration or shape, into an equivalent diagonal brace. The research has indicated how the effective stiffness of the system can be estimated when the interstory displacements are known. This confirmation of the procedure that includes use of a nonlinear static analysis of the frame and the frame-infill to determine the effective stiffness of the equivalent diagonal brace and a three-dimensional linear-elastic beam element model of the building enables writers of standards to recommend methods of analysis for determination of earthquake hazard.

The research has shown that three-dimensional computer models, excited simultaneously on orthogonal axes, are needed to simulate the response of these highly irregular buildings. These studies found that rotational modes of response may be the primary response mode. In all cases, the maximum displacements were due to combinations of rotational and translational response.

These studies have shown that three-dimensional dynamic analyses are needed to estimate interstory and overall displacements. These studies have shown that the infill within the frame provides the majority of the structural stiffness of this class of buildings and that the synergistic effects of the frame and infill must be used in the modeling of this class of building.

The nonlinear behavior of the masonry infill must be considered in the determination of the effective stiffness of the equivalent brace. The research has shown that the use of nonlinear analysis programs developed by the Technical

Coordinating Committee for Masonry Research (TCCMAR) research can simulate the behavior of unreinforced masonry infills with openings that are contained within steel or reinforced concrete frames.

The research has indicated that insitu testing of the masonry infills is needed for determination of the compressive stress-strain properties of the masonry. In these studies, testing of the masonry was not possible and the material properties of the masonry used in the analyses was a variable. In these studies, the interstory deformations were known and use of masonry properties as a variable could be accommodated. However, for the analysis of existing frame buildings, the materials properties cannot be a variable. The validity of dynamic analyses of infill buildings are dependent on the quality of data that relates the dynamic displacement to the effective stiffness of the infill, and the frame when it is reinforced concrete, at that calculated displacement. This problem has been shown to be solvable by iterative methods. (Kariotis, Feb. 1992, Hart, Feb. 1992a, 1992b). The iterative procedure consists of estimating interstory displacements, calculation of the effective stiffness at that estimated displacement, performing the dynamic analysis using the effective stiffness, comparing the calculated and estimated interstory displacement and then revising the effective stiffness to improve the correlation of estimated and calculated interstory displacements.

The studies have shown that the effective damping of this class of building is a small percentage of critical damping. Experimental testing of masonry infilled frames has shown that the cyclic behavior is severely pinched and that the effective stiffness degrades as the loading cycle is repeated or when the displacement is increased. These hysteretic characteristics indicate that the equivalent viscous damping ratio used in the linear analysis should not exceed 5 percent of critical damping.

The procedures used for simulation of earthquake records in frame buildings

with URM infills may be written into guidelines for the seismic analysis. These guidelines will allow engineers to perform dynamic analyses of complex irregular buildings. Standards that have alternative methods of analysis can be developed when a larger body of analysis data exists. Analyses of existing buildings by the procedures outlined herein will provide the majority of the data needed for development of other methods of analysis than that used herein.

ACKNOWLEDGEMENTS

This research was conducted with funding from the Department of Conservation, Division of Mines and Geology, Office of Strong Motion Studies. Dr. Moh Huang was the Technical Contract Officer. His assistance and the assistance of members of the Strong Motion Instrumentation Program is greatfully acknowledged.

The opinions and conclusions given in this report are those of the writers and do not necessarily reflect the opinions of the contracting agencies.

The contents of this report were developed under contract No. 1091-533 from the California Department of Conservation, Division of Mines and Geology, Strong Motion Instrumentation Program. However, the contents do not necessarily represent the policy of that agency nor endorsement by the State Government.

TABLE OF CONTENTS

SECTION 1

INTRODUCTION

1.1 DESCRIPTION OF THE DATA BASE USED IN THE RESEARCH

The Strong Instrumentation Program of the California Department of Mines and Geology (CSMIP) has instrumented several buildings with unreinforced masonry infills. On June 28, 1992 a magnitude 7.5 M_s earthquake occurred near Landers. The instruments in four of these multistory infilled frame buildings recorded the response of these buildings to this large magnitude event. In addition to the Landers earthquake, two instrumented buildings in Pasadena and Pomona, were shaken by a near small magnitude earthquake, the Sierra Madre and the Upland earthquakes respectively. Building plans and elevations and sensor locations for each building as presented in the Appendices. These appendices are present data that is specific for each building.

The strong motion data used for these studies was obtained from the following reports.

For Station No. 24541 (Pasadena 6-story office building):

a) M. Huang, A. Shakal, et. al. (1991). CSMIP Strong-Motion Records from the Sierra Madre, California Earthquake of 28 June 1991. Calif. Div. of Mines and Geology, Office of Strong Motion Studies, Report No. OSMS 91-03, August 1991.

b) R. B. Darragh, T. Q. Cao, et. al. (1992). First Interim Set of CSMIP Processed Strong-Motion Records from the Sierra Madre, California Earthquake of 28 June 1991. Calif. Div. of Strong Motion Studies, Report No. OSMS 92-01, February 1992.

c) A. Shakal, M. Huang, et. al. (1992). CSMIP Strong-Motion Records from the

Landers, California Earthquake of June 28, 1992. Calif. Div. of Mines and Geology, Office of Strong Motion Studies, Report OSMS 92-09, August 1992.

d) R. Darragh, T. Cao, et. al. (1991). Processed CSMIP Strong-Motion Records from the Landers, California Earthquake of 28 June 1992: Release No. 2. Calif. Div. of Mines and Geology, Office of Strong Motion Studies, Report No. OSMS 92-13, December 1992.

For Station No. 23544 (Pomona 6-story commercial building):

e) CSMIP Staff (1990). Quick Report on CSMIP Strong-Motion Records for the February 28, 1990 Earthquake near Upland, California. Calif. Div. of Mines and Geology, Office of Strong Motion Studies, March 1990.

f) A. Shakal, M. Huang, et. al. (1992). CSMIP Strong-Motion Records from the Landers, California Earthquake of June 28, 1992. Calif. Div. of Mines and Geology, Office of Strong Motion Studies, Report OSMS 92-09, August 1992.

g) R. Darragh, T. Cao, et. al. (1991). Processed CSMIP Strong-Motion Records from the Landers, California Earthquake of 28 June 1992: Release No. 2. Calif. Div. of Mines and Geology, Office of Strong Motion Studies, Report No. OSMS 92-13, December 1992.

For Station No. 24579 (Los Angeles 9-story office building):

h) A. Shakal, M. Huang, et. al. (1992). CSMIP Strong-Motion Records from the Landers, California Earthquake of June 28, 1992. Calif. Div. of Mines and Geology, Office of Strong Motion Studies, Report OSMS 92-09, August 1992.

For Station No. 24581 (Los Angeles 12-story commercial/office building):

i) A. Shakal, M. Huang, et. al. (1992). CSMIP Strong-Motion Records from the Landers, California Earthquake of June 28, 1992. Calif. Div. of Mines and

Geology, Office of Strong Motion Studies, Report OSMS 92-09, August 1992.

The six-story office building in Pasadena (CSMIP Station No. 24541) has 16 channels of instrumentation. The building was constructed in 1906 and has a steel frame infilled with unreinforced brick masonry. The maximum acceleration at the basement level was 0.195g during the Sierra Madre earthquake and 0.04g during the Landers earthquake.

The six-story office building in Pomona (CSMIP Station No. 23544) has 12 channels of instrumentation. The building was constructed in 1923 and has a reinforced concrete frame with unreinforced brick masonry infills. The maximum acceleration at the basement level was 0.13g for the 1990 Upland earthquake and 0.07g for the 1992 Landers earthquake.

The nine-story office building in Los Angeles (CSMIP Station No. 24579) has 18 channels of instrumentation. The building is L-shaped in plan, constructed in 1923, and has a reinforced concrete frame with unreinforced masonry infilled into the frames. The maximum acceleration at the basement level was 0.05g during the Landers earthquake with a duration of significant shaking of about 30 seconds.

The twelve-story commercial/office building in Los Angeles (CSMIP Station No. 24581) has 16 channels of instrumentation. The building was constructed in 1925 and has a concrete encased steel frame and unreinforced brick masonry infills. The maximum acceleration at the basement floor level was 0.04g during the Landers earthquake.

The data provided by the Strong Motion Instrumentation Program was

uncorrected accelerations, instrument-corrected and bandpass filtered acceleration, velocity and displacement vs. time for each channel of instrumentation, response spectra in PSV, PSA, SD and Fourier amplitude spectra presented on tripartite logarithmic plots. Displacements of sensors relative to the lowest level were plotted vs. time for the two Los Angeles Stations.

Plans for the four buildings that were in the possession of the Strong Motion Instrumentation Program were provided for the researchers. Supplemental construction documents were obtained from other sources by the Principal Investigator. The City of Los Angeles was especially helpful in copying file documents of the two Los Angeles buildings and providing these copies to the researchers.

1.2 RESEARCH TEAM

The team consisted of four consulting structural engineering offices and advisors from the Earthquake Safety Division of the Los Angeles Department of Building and Safety. The engineering firms were the Hart Consulting Group, James A. Hill & Associates, Kariotis & Associates, Nabih Youssef & Associates. The personnel that participated in the analysis at the Hart Consulting Group were Gary C. Hart, Rami Elhassan, Mukund Srinivasan and Kevin Wong. The personnel at James A. Hill & Associates were James A. Hill and Brian Unsderfer. John Kariotis, Ayubur Rahman, and Omar Waqfi performed the analyses at Kariotis & Associates. Nabih Youssef, Jeff Guh and Owen Hata performed the analyses at Nabih Youssef & Associates.

Doc Nghiem and David Chang were observers and contributors to the research. They are employed by the Los Angeles Department of Building and Safety and reviewed the progress of this research.

SECTION 2

GENERAL

2.1 STATEMENT OF THE PROBLEM

The data recorded by the Strong Motion Instrumentation Program was the response of buildings that have very significant vertical and plan irregularities. The lateral resistance was provided by the frames and the unreinforced masonry that is infilled into the frame in the exterior walls. The infilled masonry is perforated with windows and doorways. The masonry is multiwythe brick laid in a lime or lime-Portland cement mortar. Cast stone, terra cotta and brick veneer wythes are a part of the masonry infills. The material properties of the masonry could not be obtained by testing. The material properties were estimated by visual comparison with masonry that had been tested by the flat jack method.

The problem was to simulate by a three-dimensional linear-elastic computer analysis the recorded seismic response of these buildings. A real building, under strong shaking, experiences changes in stiffness with nearly every cycle and has hysteretic damping. The effects of stiffness changes and hysteretic damping cannot be directly modeled by a linear system. In summary, the existing building is a complex assembly of materials with nonlinear behavior. The average mechanical properties of the structural materials must be estimated. The effects of many systems in the buildings, such as stairs that are continuous between floors and interior partitioning, cannot be quantified. The problem statement is to reduce these complex buildings to a simple linear-elastic model that has similar dynamic response.

The problem is to establish the validity of the use of three-dimensional linear-elastic computer models, that use effective stiffness and equivalent

viscous damping, to provide an adequate dynamic representation of the infilled frame building.

2.2 GOAL OF THE RESEARCH

The goal of this research is to provide information for the development of standards and ordinances for earthquake hazard reduction in this class of buildings. The research will provide information of how to model the frame, how to include the effect of the infill on the frame and how to account for stiffness degradation in the frame and the frame-infill system. Development of a procedure for conversion of the infill, in any configuration or shape, into an equivalent diagonal brace is the goal. Without procedures for the estimation of effective stiffness of these structural systems, prescription of drift limits and calculation of drift is not possible.

2.3 RESEARCH PLAN

Determination of existing structural systems, the mass of the building and the geometry of the system was completed concurrently with the review of the CSMIP data.

- The existing drawings were reviewed to identify the frame members and the coordinates of their location.
- The weight of each story level above the base of the building was calculated. The center of gravity of each story level was estimated.
- Elevations of each column-beam line and sketches of the location of infilled bays were prepared.
- The size and location of all openings within the infilled bays were noted on the elevations.

This data was developed for each of the four buildings. Concurrently, the recorded data for each building was examined and analyzed.

- The time-displacement histories obtained from the CSMIP records were differenced to determine the average or specific interstory deformation caused by the ground shaking. This interstory displacement was used in the development of the equivalent strut. The records of instruments located on a common floor level that recorded parallel motions were differenced. The difference was converted to rotation by dividing the relative horizontal displacements by the distance between instruments. This data was used to isolate rotational modes and to confirm the assumption that the floor is a rigid body in the horizontal plane.
- The frequency content of instrumental records was analyzed by preparation of 2% and 5% damped spectra and by Fourier analysis methods.

After this raw data was accumulated and analyzed, the investigators elected to analyze indepth the two six-story commercial buildings that are located in Pomona and Pasadena for their response to the Landers earthquake. The buildings were modeled by the SAP 90 linear-elastic three-dimensional program. The floor were considered as rigid in their horizontal plane in this computer model. All beam-column intersections were considered as rigid.

Exterior elevations showing openings in the infills of the buildings were prepared to determine "typical" infill patterns. The parameters for establishing "typical" infills were:

- Moment of inertia and area of the confining frame members.
- Story height and length of the infilled bay.
- Location of the openings relative to the frame and number and size

of the openings.

The initial compressive modulus of elasticity, the tensile cracking stress, the strain associated with peak compressive stress and the peak compressive stress could not be obtained by physical testing of the infills. These values were chosen by experience and/or visual evaluation of the exposed masonry.

The force-displacement relationship for each of the "typical" infill panels was calculated by use of a nonlinear finite element program developed by Robert D. Ewing, Ahmad El-Mustapha and John Kariotis (FEM Version 1.08) (Ewing, R.D., et al, 1990) as a part of their NSF-sponsored TCCMAR research. A pair of diagonal braces having the effective stiffness of the infill within the bay of the infilled frame was substituted for the unreinforced masonry. This effective stiffness was determined by the following process.

- For each typical infill bay configuration, the confining frame and the masonry was analyzed by use of the nonlinear FEM developed by TCCMAR research. The stress-strain relationship of the URM was estimated by experience gained from test data obtained in comparable buildings.
- The force-displacement relationship of the frame and its infill was calculated by incrementally displacing the assembly. This analysis determines the stiffness degradation of the system due to cracking and strain in the frame and infill.
- The confining frame was then analyzed without any infill with the FEM program.
- The force-displacement relationships of the infilled frame and the frame alone were differenced.
- The area and modulus of elasticity of the equivalent diagonal braces was calculated to provide an effective system stiffness

corresponding to the secant stiffness at the maximum story displacement determined by the evaluation of the CSMIP displacement records.

- These braces were added to the three dimensional frame model of the building.

The computer model was excited by the selected basement time-histories. Motions on the orthogonal axes were applied simultaneously.

The process of obtaining a best-fit computer replication was an iterative process. The viscous damping used in the linear-elastic model was established using the best available data. The computed periods of the linear-elastic model were compared to estimated periods extracted from the CSMIP data. Rotational periods for the SAP model and for the CSMIP data were compared. The parameters that were modified to improve the fit were the effective stiffness of the reinforced concrete frame members, the effective stiffness of steel beams for the effects of the semi-rigid connectors to the columns, the effective stiffness of the diagonal struts that represent the infills and the percent of critical damping.

These parameters are variables as the materials properties of the structural elements are estimated, not quantified by physical testing. The percent of critical damping used in the SAP model is estimated as probable for the peak displacement taken from the CSMIP data. The SAP model used estimated values of damping for modes and displacements. This representation is technically inadequate to replicate the hysteretic damping in the existing structure.

SECTION 3

ANALYSIS

3.1 AVAILABLE DATA

The data available to the researchers consisted of the building plans on file, plans and elevations showing the location of all instruments, and the processed records of each of the instruments. Additional data as to the existing construction of the buildings was obtained from the files of the City of Los Angeles and from the owners of the buildings. There were visible conflicts between the existing construction of CSMIP Station No. 23544 in Pomona as shown on the original construction documents and the observations of the exterior walls. The light well on the west begins at the second floor level rather than the mezzanine level as shown on the drawings. There is a conflict as to the construction of the frame that extends from the main floor to the second floor level at the south end. The original drawings show that these columns are reinforced concrete. A supplemental drawing shows a structural steel girder at the second floor level supported by steel columns encased in concrete.

Additions have been made to CSMIP Station No. 24541 in Pasadena. These additions tie the two wings of the U-shape together at all levels and add weight to the buildings. Construction documents and results of investigations made during the preparation of this addition were available to the researchers.

A presentation of the available instrumental data is given in the Appendices for each building.

3.2 ANALYSIS OF THE AVAILABLE DATA

The time-displacement data of instruments located at different levels was differenced to obtain maximum relative displacements. When the relative

displacement includes several stories, the overall displacement was distributed uniformly over each intervening story. For CSMIP Station No. 23544, the available relative displacement data was for the first to second floor level. The majority of this displacement at the north wall was assigned to the mezzanine-second floor height as this level is perforated with windows. The wall below the mezzanine level is nearly solidly infilled.

Analyses of the spectra of the recorded data was made by Fourier analyses and by differencing the spectrum of a record above the base of the building from the spectrum of the recorded base motion that had been selected as the input at the base of the building. These analyses provided estimates of period of response modes.

Estimates of equivalent viscous damping was made by analysis of the recorded response of the building. These estimates of damping were used for initial analyses but were revised to improve the quality of fit. The damping in the building is hysteretic and previous analytical research conducted as a part of the TCCMAR research program (Waqfi and Kariotis, 1992) has shown that hysteretic damping cannot be readily simulated by viscous damping. The damping force used in a linear-elastic analysis is related to the instantaneous velocity and as this velocity changes during the time-history analysis the damping force changes. Experimental testing of infilled frames has shown that the effective stiffness of the system changes in each successive cycle and that the damping occurs only on the unloading cycle. Insitu compressive testing of multiwythe masonry also indicates that each loading cycle causes a nonrecoverable strain. The experimental testing of infills shows that the system has a virgin envelope and a stabilized envelope that represents the force-displacement relationship after several cycles to the same displacement. The CSMIP data includes this hysteretic behavior; the linear-elastic response data was calculated using a

damping force that is related to the velocity of each of the story masses.

Instruments at the edges of the building that are oriented in parallel were differenced. This difference was converted to rotation in radians by dividing by the distance between the instruments. This data was used to estimate frequencies of rotational response.

3.3 METHODOLOGY OF THE ANALYSES

3.3.1 GENERAL

The research plan described in Section 2.3 was followed for each building. The unique conditions of each building required that special investigations be made for each building. These special investigations included studies of the sensitivity of the calculated response to global stiffness changes that are related to the material properties of the masonry infills and to the cracking of the concrete moment frame and to the viscous damping used. Probable damped modal frequencies were estimated from the CSMIP data. The SAP analyses may not have equivalent damped modal frequencies. The modal frequencies and the percent of critical damping generally had to be changed for each analysis to provide an improved fit to the probable modal frequencies and the recorded relative displacements.

3.3.2 INFILLED REINFORCED CONCRETE FRAMES

The CSMIP Station Nos. 24579 in Los Angeles and 23544 in Pomona have reinforced concrete frames. Station No. 23544 has a severe plan irregularity below the second floor level and a lesser degree of plan irregularity from the second floor to the roof level. A mass irregularity is at the roof level. The lateral resistance at the east and south is provided by the concrete frame and

minimal infills. The percentage of the gross moment of inertia of the columns at this level that should be used as effective stiffness was a parameter that was investigated. Station No. 24579 is an L-shaped building that has a single story garage structure constructed in the portion of the property not occupied by the nine-story building. Reinforced concrete walls separate the garage occupancy from the office occupancy. These reinforced concrete infills were analyzed by methods identical to those used for unreinforced masonry infills. The effect of changing the modulus of elasticity of the concrete frames without infill independent from changing the effective area of the masonry strut was investigated.

3.3.3 INFILLED STEEL FRAMES

The CSMIP Station No. 24541 in Pasadena and 24581 in Los Angeles have structural steel frames and multiwythe brick masonry infills. Station No. 24541 has a severe plan and stiffness irregularity below the second floor. The south and east street fronts have only frames to resist lateral displacements. The west wall at the first floor has infilled panels that have a small window in each bay. The north end is highly perforated with openings. Above the second floor, the infilled walls at the perimeter of the light well add stiffness, especially in the north-south direction. The exterior walls have more symmetry in plan above the second floor except that the east and south walls are thicker. This moves the probable rotational center of the building above the second floor in the opposite direction from the probable location below the second floor.

Station No. 24581 is nearly symmetrical in plan in the north-south direction. A significant plan irregularity exists in the east-west direction. The floor beams are encased in concrete adding stiffness to the frame system. The columns of both buildings are encased in brick or clay tile. The floor beams

in Station No. 24541 support a clay tile arch system topped with an unreinforced concrete slab. No contribution of this floor system to beam stiffness was used.

3.4 ANALYSIS OF THE INFILLS

3.4.1 GENERAL

The masonry infill within the steel or reinforced concrete frame resists shear distortion of the frame. Experimental testing of solid infills have shown that the behavior of the infill can be represented by a compression-only strut extending from the upper to lower corners of the bay of the frame. Experimental testing of infills with openings has shown that the presence of openings changes the effective stiffness of the infill. The effect of the infill with openings was represented by pinned-end struts placed diagonally in the frame for all opening configurations. The area in this diagonal was determined from the nonlinear finite element analysis.

All buildings have an offset in the multiwythe masonry from the steel or reinforced concrete frame. A single wythe of the masonry on the exterior of the building bypasses the frame. No gaps between the frame and the infill were assumed.

3.4.2 MATERIAL PROPERTIES

The nonlinear finite element model must be programmed with material behavior and this material behavior should be determined by physical testing. The testing should have stress-strain relationships that approximate the state of stress and strain in the infill. The materials properties needed for the nonlinear analysis of an infill are:

- Tensile cracking strain. This property is assumed to be isotropic.

- Initial modulus of compression.
- Strain at peak compressive stress. This should be the strain caused by cyclic loading in compression.
- Peak compressive stress.
- Mechanical and physical properties of the confining frame if structural steel.
- Properties of the concrete such as described for the masonry if the confining frame is reinforced concrete.
- Assumption of a tension stiffening model for the reinforced concrete elements.

The nonlinear finite element analyses assumes that the peak uniaxial compressive stress in the masonry was 1200 psi and that this peak stress occured at 0.004 inches per inch strain. The stiffness of the infill calculated by this assumption was a variable and was modified by the analyst to improve the fit of the calculated data to the recorded data. The modifications were constrained in that all infill elements must be equally adjusted.

3.4.3 MODELING OF THE INFILL AND CONFINING FRAME

The choice of element size used in the nonlinear analysis is critical. Small elements must be used in critical stress and strain zones adjacent to the confining frame. The reinforcement in a reinforced concrete frame may use a smeared model, that is the quantity of reinforcement is uniformly distributed over the gross area. The steel member may be represented by flange and web or by an appropriately sized rectangle. When the column has its strong axis parallel to the plane of the infill it was represented by flange and web. When the weak axis was parallel to the plane of the infill it was represented by a rectangle of equal moment of inertia and area.

3.4.4 ADAPTATION OF THE FEM RESULTS TO THE SAP MODEL

The nonlinear analysis of reinforced concrete frames is a two-part analysis. The frame is first analyzed without infills. The second analysis is of the frame and the masonry infill. The force-displacement plots of the monotonic loading is differenced and used as the effective stiffness of the diagonal members that represent the infill. In these analyses, the relative displacement at each story level has been determined by use of the CSMIP displacement data. The estimated or specific story displacement is used in conjunction with the FEM analysis to determine a secant stiffness. This is converted as shown in Figure B.15 of Appendix B to a pair of struts of elastic material that is identical to the material used for the beams and columns.

These analyses initially did not analyze the steel frames without infill. The area of the diagonal members was determined directly from the nonlinear analysis of the masonry and the confining steel frame. However, the dynamic analysis of CSMIP Station No. 24581 found that the stiffness of the steel frame, when of substantial member size, must be deducted from the results of the nonlinear FEM analysis.

3.5 MODELING OF THE BUILDING

3.5.1 GENERAL

All beams that frame into the building columns were included in the model. If one end of a beam framed into another beam, a pinned-end was used for that end in the model. All beam-column joints were considered rigid as the infill prevents rotation of the beam relative to the column. This assumption was used for the structural steel systems regardless of the detailed connection. The analyses of CSMIP Station No. 24581 found that the stiffness of the steel beams

in the frame must be adjusted to less than 100% to account for the flexibility of the beam-column connection.

The diagonal members were given pinned-ends to eliminate any contribution to flexural stiffness. Approximately 80 percent of the stiffness of the diagonal members as determined from the FEM analysis was used as the initial elastic stiffness. This was chosen to estimate the stiffness on reloading to a stabilized force-displacement envelope. The base of the building was taken as the level of the first floor. This assumption was made as reinforced concrete perimeter walls are below this level. All columns were considered fixed at this level.

The CSMIP basement records were applied at the first floor level. This assumption and the assumption of a fixed base building, that is no rotation of the building on the supporting soils, will increase the effective stiffness of the computer model of the building over that of the existing building.

3.5.2 SELECTION OF DAMPING RATIOS

There are three critical unknowns as to the dynamic response of these buildings. These are:

- Translational stiffness on the x and y axes.
- Rotational stiffness at levels of plan irregularity.
- Damping that occurred during the recorded time.

Matching of the CSMIP time-displacement records would require that all three of these critical unknowns be calculable. The translation and torsional stiffness was calculated for the computer model using "typical" infilled bays. All infilled bays were given a diagonal strut. The stiffness of the strut was estimated from the "typical" bays analyzed by the finite element program. The damping force used in the linear-elastic computer model is a viscous damper that

functions full time during the time-history analysis. The percentage of critical damping is calculated for the frequency of each mode and the damping force is related to the calculated velocity. The actual damping is hysteretic and does not have a damping force acting opposite to the loading force on a loading cycle. The real damping is due to nonlinear cyclic distortion of the masonry infill.

The stiffness of the building could be modified to match a period obtained by the review of the CSMIP data and then the damping ratio could be modified to match the amplitude of the calculated displacement. A reasonable fit to some of the recorded data for a limited period of time could be obtained by this procedure. However, the damping ratios used in the analyses would probably be larger than that expected for the recorded displacement. The damping ratio used in these analyses was limited to five percent of critical damping for the higher modes as correlation of calculated and recorded data was not improved for increased damping. Less than five percent of critical damping for the principal modes was a parameter used in correlation of calculated data with recorded data.

3.5.3 PROCEDURE FOR CORRELATION OF ELASTIC ANALYSIS RESULTS WITH RECORDED DATA.

The data recorded in the building was the response of a building founded on soils at a story height below the base elevation that was used in the linear-elastic model. The added story height and flexibility of the soils increased the recorded damped building period over that calculated by the linear-elastic model. The top displacement was increased over that calculated by the computer model but the amount of increase cannot be quantified at this time.

It is expected that the frequency of the rotational modes will be less affected by the added story height and soil flexibility than translational modes. Somewhat more confidence can be had in matching periods of rotational modes as these modal frequencies can be estimated from the plots of rotation vs. time.

All parameters that affect displacement and modal frequencies are subject to modification. However, the periods calculated by the SAP model should always be less than those deduced from the CSMIP data. The least expected stiffness of the infills was restricted to about eighty percent of that determined by the nonlinear analysis and the upper bound of the damping ratio used in the linear-elastic model was five percent of critical damping. Cyclic testing of infilled frames by Flanagan (March 1933) and others has indicated that the secant stiffness on the second cycle to the same displacement is less than that measured on the virgin cycle.

SECTION 4

RESULTS OF THE ELASTIC ANALYSES

4.1 GENERAL

Four appendices present the results of the analyses in detail. This section summarizes that data.

4.2 CSMIP STATION NO. 23544 IN POMONA, LANDERS EARTHQUAKE

A damping ratio of 2% of critical was used for this analysis. The effective stiffness of the diagonal members used was 100% of that calculated by the FEM analysis. The effective stiffness of the reinforced concrete beams was taken as 70% of that calculated using the concrete section. Sixty percent of the stiffness of the concrete columns above the second floor and 35% of the stiffness of the concrete columns below the second floor was used in the frame members to estimate the reduction in stiffness due to cracking of the concrete.

A comparison of the relative displacements recorded and calculated is given in Table 4.1. The values from the CSMIP data and calculated by SAP have very good correlation in peak value.

TABLE 4.1

COMPARISON OF RELATIVE DISPLACEMENTS FOR STATION NO. 23544, LANDERS EQ.

DIRECTION	FLOOR & LOCATION	CHANNELS	CSMIP DATA MAX. INCHES	SAP DATA MAX. INCHES
N-S	Mid 2nd Fl.	5-6	0.36	0.36
E-W	S. 2nd Fl.	9-12	1.33	1.38
E-W	N. 2nd Fl.	10-12	0.76	0.68
N-S	Mid Roof	2-6	0.59	0.61
E-W	S. Roof	7-12	1.86	2.00
E-W	N. Roof	8-12	1.47	1.32
N-S	W. Roof	3-6	0.37	0.42
N-S	W. Roof	4-6	0.36	0.42

The comparison is plotted in time in Figures A.11 through A.18 in Appendix A. This correlation shows that the correlation is reasonable for the instrument located near to the center of mass (Channel 2). The channels that recorded translational and rotational modes (7 and 9) show that the SAP model over predicts the displacement in the beginning of the shaking but has better correlation from 25 seconds to 45 seconds.

4.3 CSMIP STATION NO. 23544 IN POMONA, UPLAND EARTHQUAKE

The Upland earthquake preceded the Landers earthquake. The ground motion recorded at the base of the building during the Upland earthquake was used to excite the SAP model that was correlated to the Landers data. This was done as the building had been damaged by the Upland earthquake. The visible damage was at the north wall above the mezzanine floor level.

A comparison of the relative displacements recorded and calculated is given in Table 4.2. A better correlation is made with peak values than with the plots of displacement-time shown in Figures A.19 - A.24.

TABLE 4.2

COMPARISON OF RELATIVE DISPLACEMENTS FOR STATION NO. 23544, UPLAND EQ.

DIRECTION	FLOOR & LOCATION	CHANNELS	CSMIP DATA MAX. INCHES	SAP DATA MAX. INCHES
N-S	Mid 2nd Fl.	5-6	0.63	0.56
E-W	S. 2nd Fl.	9-12	1.28	1.52
E-W	N. 2nd Fl.	10-12	0.95	1.17
N-S	Mid Roof	2-6	1.09	1.05
E-W	S. Roof	7-12	1.83	2.05
E-W	N. Roof	8-12	1.90	2.08
N-S	W. Roof	3-6	0.68	0.71
N-S	W. Roof	4-6	0.70	0.71

The SAP model cannot cope with the stiffness change, as shown in Figure A.24. This channel records the motion at the second floor level directly above the location of the damage visible after the Upland earthquake.

4.4 CSMIP STATION NO. 24541 IN PASADENA, LANDERS EQ.

All response modes of this building with significant mass coupling are torsional. The torsional stiffness above the second floor greatly exceeds the torsional stiffness below the second floor. The stiffness of the infill panels was taken directly from the FEM analyses with no reduction in stiffness due to cyclic loading. The stiffness of the structural steel frame was not deducted from the infilled system stiffness as was done for a later analysis of a building with a much heavier steel frame. The material properties used for the masonry were identical to those used for the other buildings. It is probable that the properties used exceed those that would be established by testing.

The SAP model generally over estimated the dynamic displacements at the second floor level and under estimated the displacements at the roof. Five percent damping was used for all modes. Six modes of response were used in the SAP model. The relative displacements shown in Table 4.3 have a reasonable agreement. Rotational displacements are plotted in Figures B.5, B.10 A and B.

TABLE 4.3

COMPARISON OF RELATIVE DISPLACEMENTS FOR STATION NO. 24541, LANDERS EQ.

DIRECTION	FLOOR & LOCATION	CHANNELS	CSMIP DATA MAX. INCHES	SAP DATA MAX. INCHES
N-S	W. 2nd Fl.	1-16	0.24	0.26
N-S	E. 2nd Fl.	2-16	0.90	1.34
E-W	N. 2nd Fl.	11-13	0.80	1.05
E-W	S. 2nd Fl.	12-13	0.75	0.85
N-S	W. Roof	3-16	1.40	1.06
N-S	E. Roof	4-16	2.00	1.97
E-W	N.W. Roof	5-13	2.50	2.00
E-W	N.E. Roof	6-13	2.50	2.00
E-W	Mid Roof	7-13	2.02	1.57
E-W	S. Roof	8-13	1.35	1.35

4.5 CSMIP STATION NO. 24541 IN PASADENA, SIERRA MADRE EQ.

The comparison of measured and calculated displacements is shown in Table 4.4. The stiffness model used for these predictions is that used for predicting the displacements caused by the Landers earthquake. The quality of the predictions when plotted in time vs. displacements in Figures B.11 and B.12 are better in their phase relationship to the recorded data than the time-displacement plots for the Landers earthquake.

TABLE 4.4

COMPARISON OF RELATIVE DISPLACEMENTS FOR STATION NO. 24541, SIERRA MADRE EQ.

DIRECTION	FLOOR & LOCATION	CHANNELS	CSMIP DATA MAX. INCHES	SAP DATA MAX. INCHES
N-S	W. 2nd Fl.	1-16	0.20	0.20
N-S	E. 2nd Fl.	2-16	0.90	0.86
E-W	N. 2nd Fl.	4-13	0.50	0.75
E-W	S. 2nd Fl.	12-13	0.50	0.60
N-S	W. Roof	3-16	1.60	0.84
N-S	E. Roof	4-16	1.60	1.15
E-W	N.W. Roof	5-13	1.50	1.52
E-W	N.E. Roof	6-13	1.50	1.52
E-W	Mid Roof	7-13	0.98	1.02
E-W	S. Roof	8-13	0.80	0.91

4.6 CSMIP STATION NO. 24579 IN LOS ANGELES, LANDERS EQ.

The comparison of measured and calculated displacements is shown in Table 4.5. The calculated data was for six modes that have more than 90 percent mass participation. The stiffness of the infilled masonry was determined by differencing the stiffness of the infilled frame and the bare reinforced concrete frame. Seventy percent of the strut stiffness calculated by the FEM analysis was used for all diagonal strut elements. Eighty-five percent of the stiffness of the uncracked concrete sections was used for frame stiffness.

TABLE 4.5

COMPARISON OF RELATIVE DISPLACEMENTS FOR STATION NO. 24579, LANDERS EQ.

DIRECTION	FLOOR & LOCATION	CHANNELS	CSMIP DATA MAX. INCHES	SAP DATA MAX. INCHES
N-S	S.W. 2nd Fl.	8-6	0.18	0.16
E-W	S.W. 2nd Fl.	9-5	0.16	0.17
E-W	N. 5th Fl.	10-5	1.15	1.13
E-W	S.W. 5th Fl.	11-5	0.60	0.54
N-S	S.W. 5th Fl.	12-6	0.55	0.49
N-S	W. 5th Fl.	13-6	0.91	0.94
E-W	N. Roof	14-5	2.22	2.06
E-W	S.W. Roof	16-5	0.96	1.01
N-S	S.W. Roof	17-6	0.87	0.88
N-S	W. Roof	18-6	1.56	1.77

The calculated response at the roof at sensor No. 14 has good correlation with maximum displacement but as shown in Figure C.11, the calculated displacement appears to deviate from the recorded displacements at about 19-20 seconds into the record. The recorded data has a frequency change at this time. This is also shown in the record of sensor No. 18, Figure C.14.

4.7 CSMIP STATION NO. 24581 IN LOS ANGELES, LANDERS EQ.

The comparison of measured and calculated displacements is shown in Table 4.6. The SAP model consistently over-predicts the transverse displacement in the center of the building except at the roof level at the base of the penthouse. The infills in the penthouse frame were not included in the SAP model. The transverse motions that are significantly affected by translation and rotation, Channels 11 and 13, Figures D.9 and D.10, are predicted in amplitude but are out-of-phase. The error could be attributed to prediction of rotational modes and damping.

TABLE 4.6

COMPARISON OF RELATIVE DISPLACEMENTS FOR STATION NO. 24581, LANDERS EQ.

DIRECTION	FLOOR & LOCATION	CHANNELS	CSMIP DATA MAX. INCHES	SAP DATA MAX. INCHES
N-S	W. Mezzanine	5-3	0.37	0.32
N-S	Mid Mezzanine	6-3	0.19	0.25
N-S	E. Mezzanine	7-3	0.38	0.35
E-W	Mid Mezzanine	8-4	0.11	0.11
N-S	Mid 4th Fl.	9-3	0.57	0.80
E-W	Mid 4th Fl.	10-4	0.60	0.42
N-S	W. 12th Fl.	11-3	2.56	2.25
N-S	Mid 12th Fl.	12-3	2.28	2.31
N-S	E. 12th Fl.	13-3	2.10	2.12
E-W	Mid 12th Fl.	14-4	2.48	2.57
N-S	Mid Roof	15-3	2.51	2.38
E-W	Mid Roof	16-4	2.57	2.63

4.8 SUMMARY OF THE RESULTS OF THE ANALYSES OF INFILLED REINFORCED CONCRETE FRAMES

The reinforced concrete frame building has an additional unknown that is unique to this class of construction. The effective stiffness of the concrete frame member must be estimated. The reduction in frame stiffness due to cracking caused by dead and live loading must be estimated and the validity of this estimate is not easily established. The damping associated with a concrete frame is generally believed to exceed that of a steel frame, however the pinched hysteretic behavioral characteristics of reinforced concrete elements may cause the effective damping to be less than that expected for steel frames.

The frame model of CSMIP Station No. 23544 did not use the reinforced concrete joists in the floor at the location of the column as a part of the frame in the E-W direction. The effective stiffness of the infills were not reduced to account for probable stiffness on second cycle vs. first cycle of loading. These effects may be offsetting for translational stiffness but could have significant effect on rotational stiffness. The damping was the minimal expected

to improve the correlation of the amplitude of the calculated displacement with the recorded displacement.

The post-analysis review of the data indicates that the frame stiffness in the E-W direction should be increased to include the effects of floor joists as a part of the frame system and the stiffness of the infills should be decreased to lengthen the rotational periods. A damping of between 2 and 5 percent would decrease the predicted amplitude of the N-S displacement.

The model of CSMIP Station No. 24579 also used lesser effective infill stiffness, greater effective frame stiffness, and lower damping ratios than the expected median values. Instruments that recorded rotational modes were not well correlated with calculated data in time or in phase. A better match was made with channels that were less affected by rotation.

4.9 SUMMARY OF THE RESULTS OF THE ANALYSES OF INFILLED STEEL FRAMES

CSMIP Station No. 24541 has been subjected to two earthquakes since installation of the accelerometer array. The earthquakes were the 1991 Sierra Madre and the 1992 Landers event. The SAP model replicated the rotational response to the Sierra Madre earthquake with surprising accuracy, Figure B.11A and B.11B. The calculated response at the west wall to the Sierra Madre earthquake has a reasonable match at the second floor and a poor match at the roof level. The SAP model used the effective stiffness of the brace as determined from the FEM analysis of the frame and infill and did not reduce the stiffness to account for reduced stiffness in recycling.

The stiffness of the frame and infill and the frame was differenced for calculation of the effective stiffness of the infill for CSMIP Station No. 24581 but not for No. 24541. The effective stiffness of the floor beams was also reduced to compensate for the reduced local stiffness at the beam-column

connection. The comparative time-histories at the second floor have good general correlation as the SAP model calculates only six modes of response. The building has near symmetry in the longitudinal direction and the longitudinal response at the roof, Figure D.13, is replicated.

The studies have shown that the steel frame and concrete frame building should be modeled by the same procedure. The effective stiffness of the infill should be based on the difference of the stiffness of the infilled frame and the base frame. The beam stiffness should be reduced to account for cracking in concrete beams due to loading prior to the earthquake or to account for reduced stiffness at the beam-column joint in steel frames.

SECTION 5

CORRELATION OF DATA FROM ELASTIC ANALYSIS WITH RECORDED DATA

5.1 CORRELATION OF DATA

The results of the preliminary calculation of the response of the instrumented building was correlated with the recorded data by adjustment of the effective stiffness of the frame members, the effective stiffness of the diagonals that represent the infill and the damping. The number of modes used to calculate the response was reduced to 3 or 6 principal modes. When six modes of response were used, the maximum damping of 5 percent of critical was used for modes 4, 5, and 6, lesser damping was used for the 3 principal modes.

Rules for correlation were established. The rules were:

- The effective stiffness of the infills was a variable as no testing of the materials had been done. However, the stiffness of all infills must be changed by the same percentage.
- The stiffness of frame members, beams or columns can be changed to represent cracking of reinforced concrete members or semi-rigid beam column connections, but all frame members must be treated identically. An exception to this was reduction of the effective stiffness of reinforced concrete column sections when no infill was within that line at that story level.
- Damping was a variable, however upper and lower bounds of effective damping were set at 2 and 5 percent of critical damping.

5.2 PROBABLE REASONS FOR DEVIATION OF CALCULATED DATA FROM RECORDED DATA

5.2.1 GENERAL

The linear-elastic three-dimensional model calculates the displacement vs.

time relationship for the number of modes specified and uses concepts of viscous damping to represent energy dissipated on each loading and unloading cycle. The SAP model is fixed at the specified base which was the floor of the first story.

The CSMIP data was recorded in a building that had stiffness changes in parts of the buildings during the earthquake. The building was embedded into the soils and the base of the building was not fixed at the foundation-soil interface. The damping in the building was hysteretic.

A difference of the calculated response and recorded response was expected. Prior research conducted in the TCCMAR program, (Waqfi & Kariotis, 1992) has shown that the peak displacements of a nonlinear and a linear dynamic analysis can be matched for a portion of the record. The linear-elastic model that was used in this analytical research revised its stiffness at each time step and used mass-proportional damping in lieu of hysteretic damping. The SAP model used in these studies had a constant stiffness for each computer run. The previous study indicated that the linear-elastic model would predict maximum relative displacement and match the portion of the time-displacement record when the stiffness of the SAP model matched the instantaneous stiffness of the nonlinear building if the selected viscous damping represented the hysteretic damping.

5.2.2 MODAL FREQUENCIES

A plot of the relative displacement of stories was obtained by differencing the displacements obtained by integration of the acceleration records. This record includes the displacements due to all modes of vibration. Rotational modes can be separated from translational modes by differencing the displacement of sensors at that floor that recorded displacements on one axis of the building. A similar analysis of the calculated response can be made. The frequency content of these rotational modes can be estimated by averaging the time to repeat

several cycles of response.

If the stiffness of the SAP model above the first floor matched the stiffness of the building above the first floor, the calculated undamped fundamental period of the SAP model would be less than the measured fundamental period of the building. This difference can be attributed to the added basement stories and soils flexibility. The calculated damped period of the SAP model would be less than the recorded damped period. This difference would be due to the difference of viscous damping and hysteretic damping.

In summary, correlation of rotational damped periods can be obtained by inspection of rotational response but this does not assure that the instantaneous stiffnesses of the building and the effective stiffnesses of the SAP model are identical.

5.2.3 DAMPING

The damping in the building was hysteretic. That is, the plot of the unloading force-displacement relationship is not similar to the loading branch. The damping associated with unreinforced masonry infills is due to inelastic behavior when loaded in compression. This behavior has been shown by insitu testing by flat jacks. This behavior of the infill material causes the load-displacement relationship to become pinched in a manner similar to that of reinforced concrete and masonry elements. This hysteretic behavior is shown by experimental testing by Flanagan (March 1993) and others.

The damping used in the linear-elastic analyses is a combination of damping proportional to the stiffness and mass matrices. The proportion of each cannot be controlled by the user of the program. The damping force acts on loading and unloading and is linear with the velocity at each time step. The hysteretic damping can be represented by viscous damping if the magnitude of displacement

predicted by the model having hysteretic damping is similar to the viscous damped model. However, the damped frequency of hysteretic model will not be identical to the frequency of the model having viscous damping. The effects of hysteretic damping have been shown by other studies (Waqfi & Kariotis, 1992) to be less dependent on the magnitude of displacement. The value of damping used in the three dimensional linear-elastic studies was chosen by information obtained by Fourier analyses and by experience.

The correlation attempted to approximate damped frequencies of the analyses and the data. Damping values were adjusted within a narrow range, 2 to 5 percent of critical, to correlate the maximum values of calculated displacements with those recorded.

5.2.4 NONLINEAR MATERIALS BEHAVIOR

The study used a linear-elastic model to predict the dynamic response of a building with nonlinear materials properties. If the maximum displacement caused by the ground motion were unknown, an iterative procedure would have to be used to solve the stiffness-dynamic displacement relationship. For this problem, the relative displacement must be assumed and an effective stiffness calculated for this assumed displacement. The linear-elastic model calculates dynamic displacements for these stiffness assumptions. The stiffness assumptions previously used are modified by use of the data obtained by the nonlinear finite element analyses to have an effective stiffness that is compatible with the calculated dynamic displacements. This iterative process continues until closure is obtained.

The near-elastic properties of the materials may be used with a spectrum that is appropriate for an average return period of about 100 years. The stiffness is then adjusted as previously discussed to be appropriate for this

intensity of loading. Spectra with increasing average return periods are then used as loading for the system with the stiffness found appropriate for a lesser intensity of earthquake shaking. The stiffness is adjusted (decreased) for each increase in dynamic loading. This procedure may require less iteration cycles as the logic in estimating the reduction of stiffness for each element is more straightforward.

In these studies the relative displacements were known. The effective stiffness was obtained from the nonlinear finite element analyses for the known displacement. This effective stiffness was based on assumed materials properties such as cracking stress and effective compression modulus. The rule adopted was that all infill related stiffness properties could be revised within a range of 100 to 70 percent of the effective stiffness properties estimated from the nonlinear analyses. The effective stiffness of the reinforced concrete frame members was estimated as a percentage of the stiffness based on cross-sectional properties.

The effective stiffness of the infilled panels and the frames were modified to obtain a reasonable correlation between the damped frequencies of the model and that derived from studies of the CSMIP data. Stiffness changes can be detected by examination of the CSMIP data. The Pomona and Pasadena buildings did have significant stiffness degradation during the Upland and Sierra Madre earthquakes and some stiffness degradation during the Landers earthquake. CSMIP Station No. 24579 shows a stiffness degradation during the Landers earthquake at about 19-20 seconds into the record.

The principal effects of nonlinear behavior are related to equivalent damping rather than changes in effective stiffness. As the effective primary mode stiffness of the building changes, the linear-elastic model can have at some time a near-identical effective primary mode stiffness. Studies of the

comparative dynamic response of nonlinear models and linear models have shown that the initial dynamic conditions at the beginning of an excitation have little effect on subsequent dynamic behavior. This behavior allows the simulation of a nonlinear building or nonlinear dynamic response model by an equivalent linear-elastic dynamic response model for a limited period of time.

SECTION 6

CONCLUSIONS

6.1 CONCLUSIONS ON CORRELATION

The research has shown that the maximum relative displacements taken from the recorded data can be simulated with the linear-elastic three-dimensional computer model. The time of occurrence of this peak displacement and the direction of this peak displacement can be replicated with lesser quality. The time-displacement history can be replicated for a limited duration of time for some locations in the structure.

The quality of correlation improved with the study of each building as experience in choosing how to modify the variables that affects the response of the building was gained. The studies also found that the linear elastic computer model has inherent limitations on replication of the dynamic response of a building that had stiffness degradation during the length of the record and had damping due to material behavior.

The conclusion of this research is that the combination of a static nonlinear finite element analysis and linear-elastic three-dimensional dynamic analysis can replicate the measured response of frame buildings with unreinforced masonry infills. The basis for this conclusion is that highly irregular buildings were modeled by these computer programs and correlations having a reasonable degree of accuracy were made. The research did not include physical testing of materials or onsite verification of the information shown on the construction documents. The data used was based on the experience of the researchers.

The probable deviation of calculated data from real data includes that used for mass, location of center of mass, effective stiffness of systems, stiffness

degradation caused by prior earthquakes, distribution of stiffness in plan and elevation, substitution of viscous damping for hysteretic damping and modeling error in assuming the building is fixed at the first floor level. The most significant reason for error is believed to be due to distribution of stiffness in plan and elevation and use of viscous damping. The study has shown that rational estimates of each unknown value or quantity can be made. And that simplified analyses using these values and quantities can simulate the measured response with a degree of accuracy that assures the ability of the analytical procedure that was used in this research to determine the probable dynamic response of infilled frame buildings.

6.2 RECOMMENDATIONS FOR ANALYSIS OF INFILLED FRAME BUILDINGS

6.2.1 GENERAL

The material properties of the unreinforced masonry materials should be determined by insitu testing. The flat-jack procedure (Kariotis & Nghiem, 1993) is recommended for determination of the stress-strain relationship. The application of compressive load on the masonry should be cyclic to determine the strain limit of the masonry. Nonlinear analyses of infilled frames have found that the results are somewhat insensitive to the stress limit state of the masonry but that the allowable displacement of the infilled frame (that displacement at which strength degradation commences) is more sensitive to the tolerance of the masonry for strain.

The number of infilled frames that should be analyzed is dependent on the panel heights, height-width ratio of the panel, size of confining frame members, and size and location of openings within the frame. A suggested method is to analyze what are considered to be representative panels with average properties.

Panels that have variation in one parameter only are analyzed to determine the sensitivity of the effective stiffness to that parameter. As an example, only 23 panels were analyzed to determine the effective stiffness of CSMIP Station No. 24581. This building is 12 stories in height and has about 40 infilled bays in each story level.

The size of mesh used to model the infill and represent the frame members should consider the recommendations made by the Infill Subcommittee of the Existing Building Committee of the Structural Engineers Association of Southern California (Rahman, Md. A., 1993).

The frame and its infill is modeled as an independent element as shown in Figure B.15. The frame with and without the infill is displaced incrementally at the top. The nonlinear analysis plots the force-displacement relationship and provides a major event file that indicates cracking, angle of crack, compressive strain and average tensile strain and occurrence of peak strain in an element.

The difference of the behavior of the bare frame and the infilled frame is used to calculate the effective stiffness of the substitute diagonal members. Figure B.15 shows that the infill functions as a compression member to restrain the shear deformation of the confining frame. It is recommended that two tension-compression members be used to minimize effects that would be caused by choosing a direction of the inclination of the diagonal members.

Fully reversing cyclic testing (Flanagan and Bennett, 1993) (Klinger and Bertero, 1976) has shown that the secant stiffness on reloading to the same displacement is reduced from stiffness on the first loading to that displacement. It is suggested that 80 percent of the effective stiffness as determined by the nonlinear analyses be used to represent the probable effective stiffness for repeated cycles.

The three-dimensional model uses all frame members in the model that frame into or are adjacent to the columns. The latter case, adjacent to columns, is for concrete frame structures as torsional stiffness of concrete beams may be substantial. All horizontal members are considered to be fixed to the column. The exterior frame that is containing the infill is included in the model. The ends of the equivalent diagonal elements are pinned at the column-beam joints.

In these studies, the relative displacements were known and the effective stiffnesses were estimated for those relative displacements. In the case of a dynamic analysis of an existing infilled frame building the earthquake loading is prescribed by a spectrum. Use of a 475 year average return period and mean dynamic amplification factors is recommended. The three-dimensional model is excited on the x and y axes simultaneously and the results are combined by the SRSS method. It is recommended that 5% damped spectral values be used.

Initial relative displacements are assumed for each story level and the effective stiffness is calculated for this displacement in accordance with the procedures previously described. The displacements of the dynamic analysis model will probably be different than that displacement used to determine the effective stiffness. The results of the first analysis are used to estimate a more appropriate effective stiffness for the second analysis. The iterative process continues until a reasonable correlation exists between the estimated displacement and the calculated displacement.

If the calculated displacement exceeds a prescribed drift limit or the acceptable displacement of several of the infilled panels, supplemental stiffening elements can be added to the model and the iterative process continued to an acceptable solution.

6.2.2 INFILLED STEEL FRAMES

Steel beams in the floor are commonly encased in concrete making the beam composite with the floor for dead and live loading. The steel beams are generally connected to the columns with semi-rigid connections. The preliminary analyses of CSMIP Station No. 24581 used 130 percent of the moment of inertia of the bare beam as its probable stiffness. This was corrected to 85 percent of the moment of inertia of the bare beam to improve the correlation. The semi-rigid connection decreases the stiffness of the beam for a short length of the beam but is in an area of high moment. The semi-rigid connection can be included in the nonlinear analysis of the frame and the infill and frame by making the connection an element. The reduced stiffness of the connection can be incorporated in the SAP model but use of an effective stiffness for the full length of the floor beam is recommended.

Columns in steel frame buildings may be encased in concrete. The columns in the steel frame buildings analyzed in these studies had brick or clay tile encasement. It is recommended that the added stiffness of the concrete encasement be considered when it occurs.

6.2.3 INFILLED CONCRETE FRAMES

The reinforced concrete frame is modeled in the nonlinear finite element program with appropriate properties. If the columns have reinforcement contained in a spiral the reinforcement can be smeared. If the beam or column has concentrated reinforcement at its edges, this reinforcement should be contained within an element.

The nonlinear analysis of the bare frame can be utilized as a guide for selection of appropriate cracked stiffnesses of the concrete frame. An alternate is to use the SAP data and Formula (9-7) of the 1991 Edition of the Uniform

Building Code to estimate the effective moment of inertia of the beams and columns. The estimates of moment, M_a, should include dead load effects. The axial load on the columns increases their stiffness and the stiffness of columns given by Formula (9-7) of the UBC must be used with caution. Axial load effects can be introduced into the nonlinear analysis. These studies did not use axial load effects in the nonlinear analyses.

6.3 LIMITATIONS OF THE RECOMMENDED PROCEDURES

These analyses were made of buildings that had limited stiffness degradation during the time of recorded shaking. No strength degradation was indicated by the nonlinear analyses of the infills for the measured relative deformations. The recommended procedure can be extrapolated to analyses that have more significant stiffness degradation but have not been shown to be applicable to systems that have strength degradation.

SECTION 7

RECOMMENDATIONS FOR CONTINUING RESEARCH

7.1 SELECTION OF CANDIDATES FOR INSTRUMENTATION

These four buildings had the majority of structural features that are common to the inventory of these buildings in California. The construction data for one of these buildings was unavailable and in the same instance, CSMIP Station No. 23544, an exterior visual survey found discrepancies between the construction documents and the existing building. The selection of candidates for instrumentation should include criteria such as.

- Availability of complete architectural and structural construction documents.
- Verification that the building is represented by the available data.

These buildings, if steel frame, are fully described by 3 sets of drawings. The architectural drawings provide data for analyses of the infilled panels and for calculation of building mass. The structural steel drawings provide frame member sizes and coordinates. The concrete drawings provide data on building mass and encasement of the structural steel frame. All of these drawings are needed for analysis.

Reinforced concrete frame buildings have the member sizes and locations shown on plans, sections and schedules. The reinforcing schedules of columns and beams are needed to estimate post-cracked stiffnesses.

7.2 PLANNING OF INSTRUMENTATION PATTERN

These studies have found that separation of rotational modes from translation modes was beneficial in correlation studies. This indicates that location of sensors at the edge of the building is preferred to locations in the

center of the building. Concentration of sensors at a building level to record translational and rotational motion at that level is superior to distribution of fewer sensors vertically.

The location of the instrument relative to the edge of the building should be shown on the CSMIP data if the sensors are not at the edge of the building.

The instrumentation pattern should be planned to capture an expected dynamic response. It is suggested that a relative stiffness analysis for static loading be made of the building prior to fixing the location of sensors. This preliminary analysis could confirm that the pattern of sensors will record the expected response.

7.3 ONSITE INVESTIGATION AND MATERIALS TESTING

The onsite investigation should confirm that the existing drawings adequately describe the existing building. The dynamic response of these buildings with URM infills is sensitive to the materials behavior and properties. A minimal material testing program is warranted to remove uncertainty from the correlation of calculated response to measured response.

SECTION 8

BIBLIOGRAPHY

CSMIP Staff (1990). Quick Report on CSMIP Strong-Motion Records for the February 28, 1990 Earthquake near Upland, California. Calif. Div. of Mines and Geology, Office of Strong Motion Studies, March 1990.

Darragh, R., Cao, T., et. al. (1991). Processed CSMIP Strong-Motion Records from the Landers, California Earthquake of 28 June 1992: Release No. 2. Calif. Div. of Mines and Geology, Office of Strong Motion Studies, Report No. OSMS 92-13, December 1992.

Darragh, R.B., Cao, T.Q., et. al. (1992). First Interim Set of CSMIP Processed Strong-Motion Records from the Sierra Madre, California Earthquake of 28 June 1991. Calif. Div. of Strong Motion Studies, Report No. OSMS 92-01, February 1992.

Ewing, R.D., El-Mustapha, A.M. and Kariotis, J.C. (Dec. 1987, Revised June 1990). FEM/I, A Finite Element Computer Program for the Nonlinear Static Analysis of Reinforced Masonry Building Components, TCCMAR Report No. 2.2-1.

Flanagan, R.D. and Bennett, R.M. (March 1993). Large-Scale Testing of Structural Clay Tile Infilled Frames. Proceedings of the 1993 Annual Conference of the Canadian Society of Civil Engineers. Martin-Marietta Energy Systems, Inc. Center for Phenomena Engineering.

Hart, G.C. et al (Feb. 1992 a) Seismic Performance Study. DPC Gymnasium. Elastic Time History Analysis Using SAP 90. TCCMAR Report No. 2.1-8.

Hart, G.C. et al (Feb. 1992 b) Seismic Performance Study. TMS Shopping Center. Elastic Time History Analysis Using SAP 90. TCCMAR Report No. 2.1-9.

Huang, M., Shakal, A., et. al. (1991). CSMIP Strong-Motion Records from the Sierra Madre, California Earthquake of 28 June 1991. Calif. Eiv. of Mines and Geology, Office of Strong Motion Studies, Report No. OSMS 91-03, August 1991.

Kariotis, J.C. and Waqfi, O.M. (Feb. 1992) Trial Designs Made in Accordance With Tentative Limit States Design Standards for Reinforced Masonry Buildings. TCCMAR Report No. 9.1-2.

Kariotis, J.C. and Nghiem, D. (1993). In-Situ Determination of the Compressive Stress-Strain Relationship of Multi-Wythe Brick Masonry. Proceedings of the Structures Congress 1993, Vol. 2, pp. 1421-1426. American Society of Civil Engineers.

Klinger, R.E. and Bertero, V.V. (Dec. 1976). Infilled Frames in Earthquake-Resistant Construction, University of California, Berkeley, CA. Report No. EERC 76-32.

Rahman, Md.A. (1993). Special Modeling Considerations in the Finite Element Analysis for Unreinforced Masonry Infill. A Workshop for the Seismic Retrofit of Infilled Frame Buildings. Structural Engineers Association of Southern California.

Shakal, A., Huang, M., et. al. (1992). CSMIP Strong-Motion Records from the Landers, California Earthquake of June 28, 1992. Calif. Div. of Mines and Geology, Office of Strong Motion Studies, Report OSMS 92-09, August 1992.

Waqfi, O.M. and Kariotis, J.C. (April 1992) Comparison of the Dynamic Response of a Damped MDOF Nonlinear Beam Model with an Equivalent SDOF Hysteretic Model. TCCMAR Report No. 2.3-6.

APPENDIX A

SIMULATION OF THE RESPONSE OF CSMIP STATION NO. 23544 TO THE LANDERS AND UPLAND EARTHQUAKES

SECTION A1

INTRODUCTION

A new method of modeling unreinforced masonry infill walls with diagonal brace elements was investigated. The effective strut was obtained by equating the strut stiffness to the equivalent stiffness of the walls. A six story commercial building located in Pomona, California and instrumented by the California Strong Motion Instrumentation Program (CSMIP) was used to study the applicability of this modeling technique. The lateral force resisting system of the building consists of a reinforced concrete frame and unreinforced masonry infill walls. A three dimensional linear elastic beam element model of the structure was developed, based upon the recorded response of the building to the Landers earthquake of June 28, 1992. This model was subjected to the recorded ground motion of the Upland earthquake of February 28, 1990. The results of the computer simulation were compared to the recorded response of the building.

SECTION A2

BUILDING DESCRIPTION

CSMIP Station no. 23544 is a six story commercial building with a penthouse and basement level. It was designed in 1923 and is located in Pomona, California. At the ground floor the building measures 65 feet by 120 feet in plan and 71 feet in height, excluding the penthouse.

The floor and gravity framing consist of 3 inch thick reinforced concrete slab and reinforced concrete beams, girders and columns. The foundation consists of spread reinforced concrete footings. The lateral force

resisting system is a reinforced concrete frame with unreinforced masonry infill walls.

The basement is enclosed by a 12 inch thick concrete wall. This perimeter wall extends 7 feet 6 inches beyond the wall above, along the east side of the building. The mezzanine level consists of an L-shaped floor diaphragm that runs along the north and west walls. At the second floor a portion of the building along the west wall is setback creating a U-shaped floor plan. The northwest wing has approximate dimensions of 26 feet in the north-south direction and 19 feet in the east-west direction. The dimensions of the southwest wing are approximately 49 feet in the north-south direction and 19 feet in the east-west direction. The penthouse is located above this wing.

The south and east walls have many large openings from the ground level to the second floor. The west wall of the southwest wing is solid from the ground level to the top of the penthouse, except for a few small openings. The north wall is solid at the ground floor and perforated with windows from the mezzanine level to the roof.

The plan irregularities below the second floor causes the center of rotation to be located near the northwest corner of the building at the lower levels. Thus, the response of the building will contain a significant rotational component.

SECTION A3

RECORDED EARTHQUAKE RESPONSE OF BUILDING

The recorded data from the Landers and Upland earthquakes were used in this investigation. A three dimensional linear elastic beam element model of

the building was developed using the Landers record. The Upland record was used to verify the modeling technique.

The Landers earthquake of June 28, 1992, with a magnitude of 7.5 M_S, is the largest event to occur in California since 1952. The main shock occurred at 4:58 AM PDT near Landers, located in the Mojave Desert about 43 km north of Palm Springs and 80 km east of San Bernardino. The estimated location of the epicenter is 34.217°N, 116.433°W and a focal depth of 9 km. Analysis by USGS and Caltech indicates that the earthquake had a right-lateral strike-slip mechanism.

Station No. 23544 is instrumented with 12 sensors. Figure A.1 shows the location and direction of measurement of these sensors. The second floor was instrumented such that the effect of the mezzanine level on the building response may be studied. The sensors measuring the roof response in the north-south direction along the west wall yields additional information concerning rotational motion and the effect of the solid wall on the building response.

The maximum recorded ground acceleration at the site was 0.07g in the north-south direction. The peak ground acceleration in the east-west and vertical directions were 0.05g and 0.03g respectively. A peak response acceleration of 0.19g in the east-west direction and 0.15g in the north-south direction was recorded at the roof.

The maximum relative displacements of the roof, with respect to basement level, were 0.59 inches in the north-south direction, 1.86 inches and 1.47 inches in the east-west direction at the south and north walls respectively. At the second floor the maximum relative displacements were, in the north-south direction 0.36 inches, in the east-west direction, 1.33 inches and 0.76 inches at the south and north walls.

A large percentage of the roof displacement occurs between the second and ground floors. At the second floor, the east-west displacement at the south wall is larger than at the north. This is attributed to the contribution of rotation to the motion and the stiff walls at the north end.

No significant differences were found between the ground motion record of channels 11 and 12. Both channels recorded motion in the east-west direction at opposite ends of the basement. The ground motion recorded by channel 12 was selected for use in the analytical study as it was placed together with channel 6.

Figure A.2 shows the rotational motion of the roof with respect to ground. This motion was derived by taking the difference of the relative motion of the roof, with respect to base, in the east-west direction at the south and north wall and dividing this difference by the length of the building. From this figure the period of rotation was found to be approximately 1.3 seconds. Figure A.3 shows the rotational motion of the second floor with respect to ground. Figures A.4-A.6 show the relative displacement of the roof with respect to the second floor, in the north-south direction, the east-west direction at the south and north wall respectively. The maximum relative displacement in the north-south direction was found to be 0.23 inches, in the east-west direction 0.71 inches at the north wall and 0.51 inches at the south wall.

The Upland earthquake of February 28, 1990, was a near small magnitude event. The maximum recorded ground acceleration at the site was 0.13g in the north-south direction. The peak ground acceleration in the east-west and vertical directions were 0.10g and 0.06g respectively. A peak response acceleration of 0.34g in the east-west direction and 0.30g in the north-south direction was recorded at the roof.

The maximum relative displacements of the roof, with respect to basement level, were 1.09 inches in the north-south direction, 1.83 inches and 1.90 inches in the east-west direction at the south and north walls respectively. At the second floor the maximum relative displacements were, in the north-south direction 0.63 inches, in the east west direction, 1.28 inches and 0.95 inches at the south and north walls.

SECTION A4

COMPUTER MODEL

A three dimensional beam element computer model of the building was developed (Figure A.7). The floor plates of the building were modeled as rigid horizontal diaphragms. The frame joints were assumed fixed at the basement level and continuous elsewhere. The effective stiffness of the concrete frame was estimated by considering the frame member sizes and the interstory drift.

Due to the 42 inch average depth of the spandrel beams, it was assumed that these beams would not experience significant cracking and a 30% reduction of gross area was assigned to these members. The recorded data shows that a large portion of the roof displacement occurs between the second and ground floors. This can be attributed to the severe plan irregularity below the second floor, where the lateral resistance at the east and south walls are provided by the concrete frame and minimal infills. Above the second story the floor heights are uniform and there are no large wall openings, whereas below the second floor there are many along the south and east walls. It was assumed that the columns above the second floor did not experience as much

cracking as those below. A reduced area of 60% of gross was assumed for columns above the second level and 35% of gross for columns below.

In the computer model of the building the unreinforced masonry infill walls were modeled as diagonal brace elements. The properties of these members were selected such that the computed strut stiffness equaled the equivalent stiffness of the walls. A study of these walls was conducted using a nonlinear finite element model. From these studies force-deformation curves were produced. These curves were used to find the equivalent stiffness of the walls by calculating a deformation, from CSMIP records, and computing the corresponding secant stiffness.

The interstory drifts for the upper levels of the building were calculated by using the maximum relative displacement between the roof and second floor and assuming a linear deflected shape. Similarly, by taking the maximum relative displacement between the second floor and ground level the interstory drift of the lower levels were ascertained. These values of interstory drifts were used in conjunction with the force-deformation curves to compute the equivalent stiffness of the infill walls.

The building was damaged in the Upland earthquake. An on site inspection revealed cracking in the north wall above the mezzanine floor level. Due to this damage and the large measured displacements at the second floor, the effective stiffness of the diagonal members below the second floor level, as calculated by the nonlinear finite element analysis, were reduced by 20%.

In the nonlinear model of the walls the material properties of the masonry and the reinforcement in the frame were taken as :

For masonry,	
compressive strength	1.2 ksi
compressive strain	0.004 in/in

elastic modulus (tension)	4000 ksi
cracking strength	0.1 ksi
tensile cracking strain	0.00025 in/in
For steel,	
yield stress of reinforcement	40 ksi

The material behavior used in the nonlinear finite element analysis was assumed as testing was not a part of the research.

A damping value of 2% of critical was used in the analysis. This value was estimated from the roof level response. The first three periods of the building model are 1.04s, 0.7s and 0.51s. Figures A.8-A.10 show the first, second and third mode shapes of the building. The first mode is a translation in the east-west direction, the second a rotation and the third a north-south translation. Only the first three modes were used in the analysis.

SECTION A5

COMPARISON OF ANALYTICAL RESULTS TO CSMIP DATA

A comparison of the relative displacements, recorded and calculated, for the Landers earthquake, is given in Table A-1. The recorded data and the simulation results have very good correlation in peak value. The peak simulated response is within 15% of the recorded value.

The results of the computer simulation are shown in Figures A.11-A.16. Figures A.11, A.13 and A.15 show the recorded displacements along with the simulated response at the roof. Figures A.12, A.14 and A.16 show the recorded response together with the simulated response at the second floor. Figures

A.11 and A.12 are the displacements in the north-south direction, Figures A.13 and A.14 are the displacements at the south wall in the east-west direction, Figures A.15 and A.16 are the displacements in the east-west direction at the north wall.

The displacement obtained from the simulation is in good agreement with the recorded data in the north-south direction. The amplitude and phase relationship are reasonably correlated at the roof and second floors. In the east-west direction the simulated and recorded data are not in good agreement at either the roof or second level. The motion in this direction is influenced by the rotational mode of the building.

The rotational mode is dependent on the building geometry and the distribution of stiffness. Figures A.17 and A.18 show the recorded and simulated rotation of the roof and second floor respectively. The figures indicate that the computer model does not adequately approximate the rotational response of the building. An improved estimate of the rotational mode would result in better correlation of east-west displacements. The north-south displacements are less affected by the rotational motion, as the sensor measuring this motion is located next to a stiff wall.

The ground motion recorded at the basement of the building during the Upland earthquake was used to excite the building model that was correlated to the Landers data. A comparison of the relative displacements, recorded and calculated, is given in Table A-2. Peak values are well correlated. Displacement time histories (Figures A.19-A.24) are not in good agreement. The building sustained damage to the north wall during the event. This manifests itself as a change in stiffness. A linear analysis cannot simulate this occurrence.

SECTION A6

CONCLUSION

Unreinforced masonry infill walls were modeled as diagonal brace elements in a three dimensional linear elastic beam element model. The effective strut was obtained by equating the strut stiffness to the equivalent stiffness of the walls. The recorded response to the Landers earthquake of 1992 was used in the development of the analytical model.

The simulation results were compared to the recorded response of the building. The peak displacements from the simulation compared favorably to the recorded data in both the Landers and Upland cases. The displacement time histories were not well correlated. An improved estimate of the rotational mode would result in a better correlation of the displacements.

The issue of selecting the appropriate value of damping was not investigated, although it significantly affects the response. It was found that the assumed value of viscous damping does not adequately approximate the hysteretic damping inherent in the building.

In analyzing the recorded response of the building it was found that a sensor located along the east wall of the roof measuring motion in the north-south direction would help identify the rotational and translational modes.

LOCATION	CHANNEL	MIN. DISPL. (in.)	MAX DISPL. (in.)
2nd FLOOR N-S	5	-0.23	0.36
SAP90		-0.24	0.36
2nd FLOOR E-W S. WALL	9	-1.33	1.19
SAP90		-1.28	1.38
2nd FLOOR E-W N. WALL	10	-0.63	0.76
SAP90		-0.68	0.52
ROOF N-S	2	-0.36	0.59
SAP90		-0.41	0.61
ROOF E-W S. WALL	7	-1.86	1.63
SAP90		-1.92	2.00
ROOF E-W N. WALL	8	-1.15	1.47
SAP90		-1.32	1.10

Table A-1 Peak displacement values of recorded and simulated response to Landers Earthquake.

LOCATION	CHANNEL	MIN. RELATIVE DISPL. (in.)	MAX. RELATIVE DISPL. (in.)
2nd FLOOR N-S	5	-0.63	0.53
SAP90		-0.54	0.56
2nd FLOOR E-W S. WALL	9	-1.28	1.07
SAP90		-1.41	1.52
2nd FLOOR E-W N. WALL	10	-0.67	0.95
SAP90		-1.16	1.17
ROOF N-S	2	-1.09	0.95
SAP90		-0.88	1.05
ROOF E-W S. WALL	7	-1.83	1.54
SAP90		-1.98	2.05
ROOF E-W N. WALL	8	-1.37	1.90
SAP90		-2.01	2.08

Table A-2 Peak relative displacement values of recorded and simulated response to Upland Earthquake.

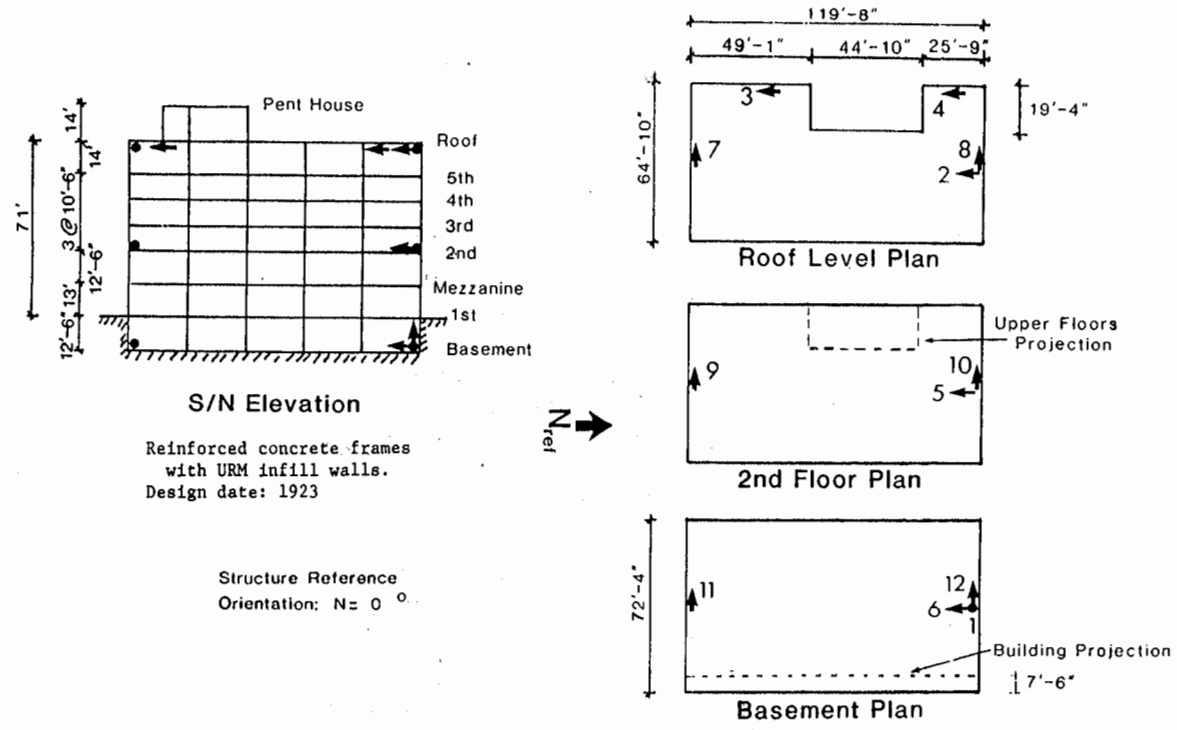

Figure A.1 Sensor locations for CSMIP Station no. 23544.

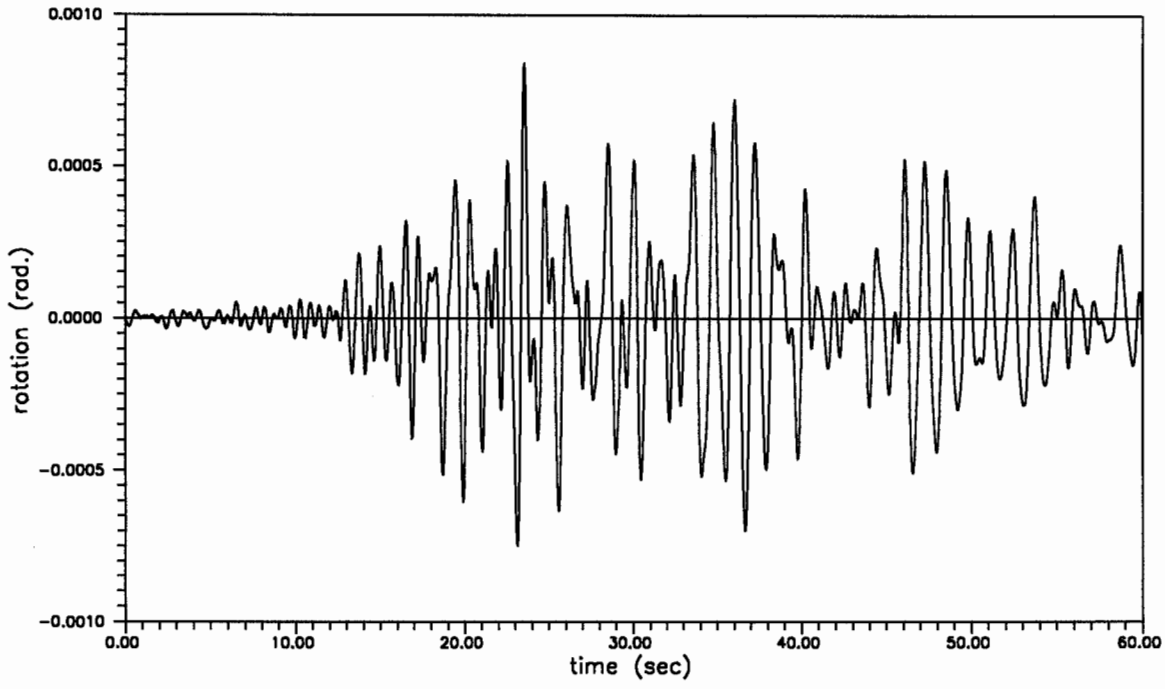

Figure A.2 Rotation of roof with respect to base.

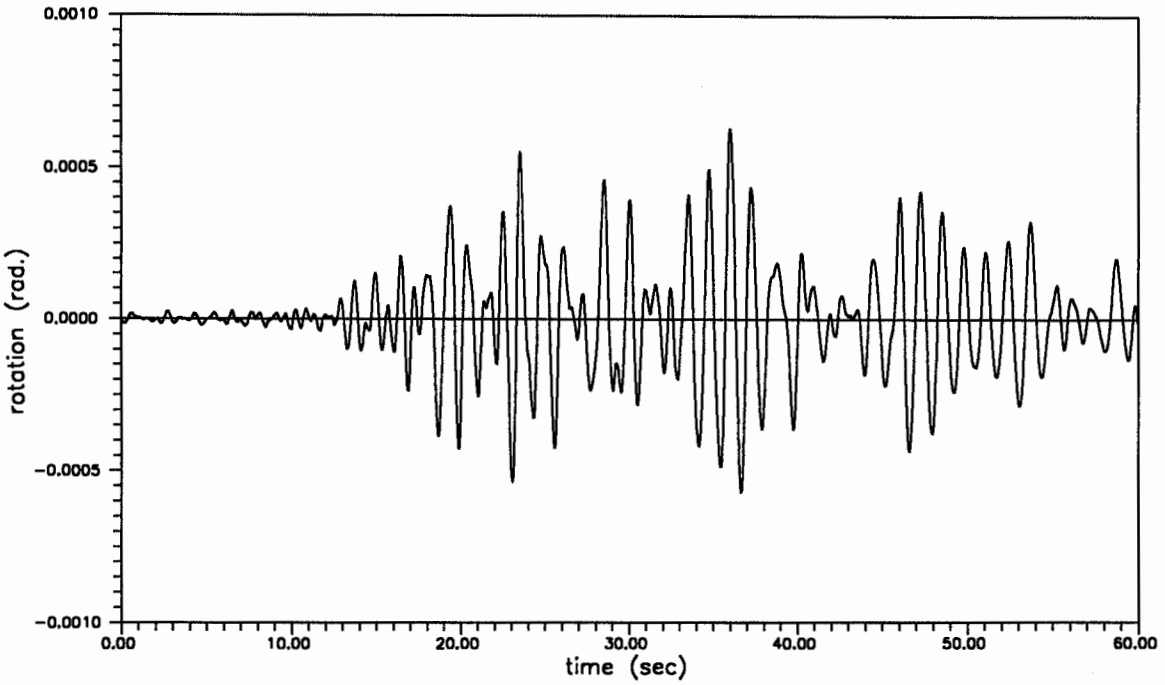

Figure A.3 Rotation of second floor with respect to base.

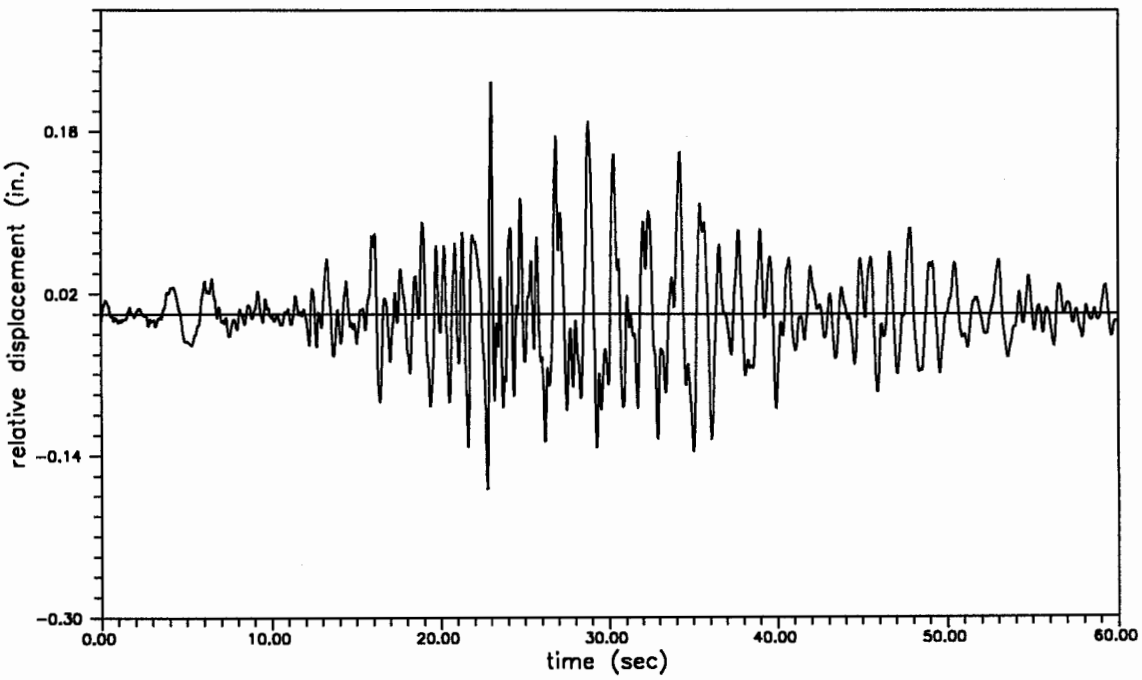

Figure A.4 Relative displacement of roof with respect to second floor in north-south direction.

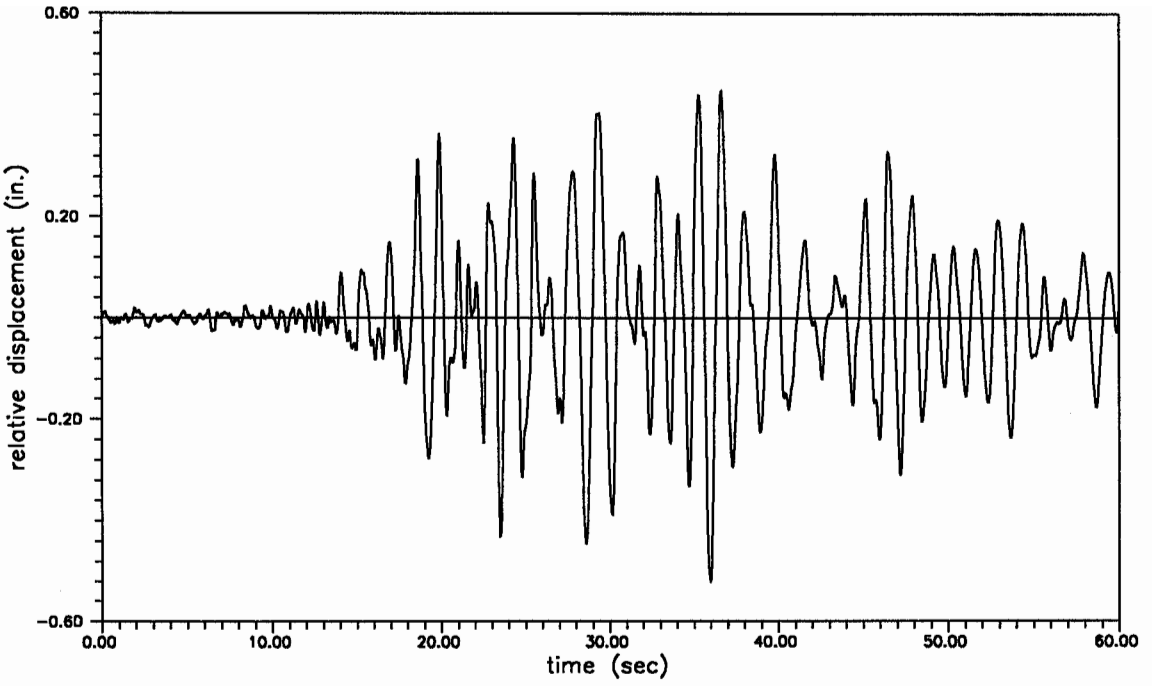

Figure A.5 Relative displacement of roof with respect to second floor in east-west direction at south wall.

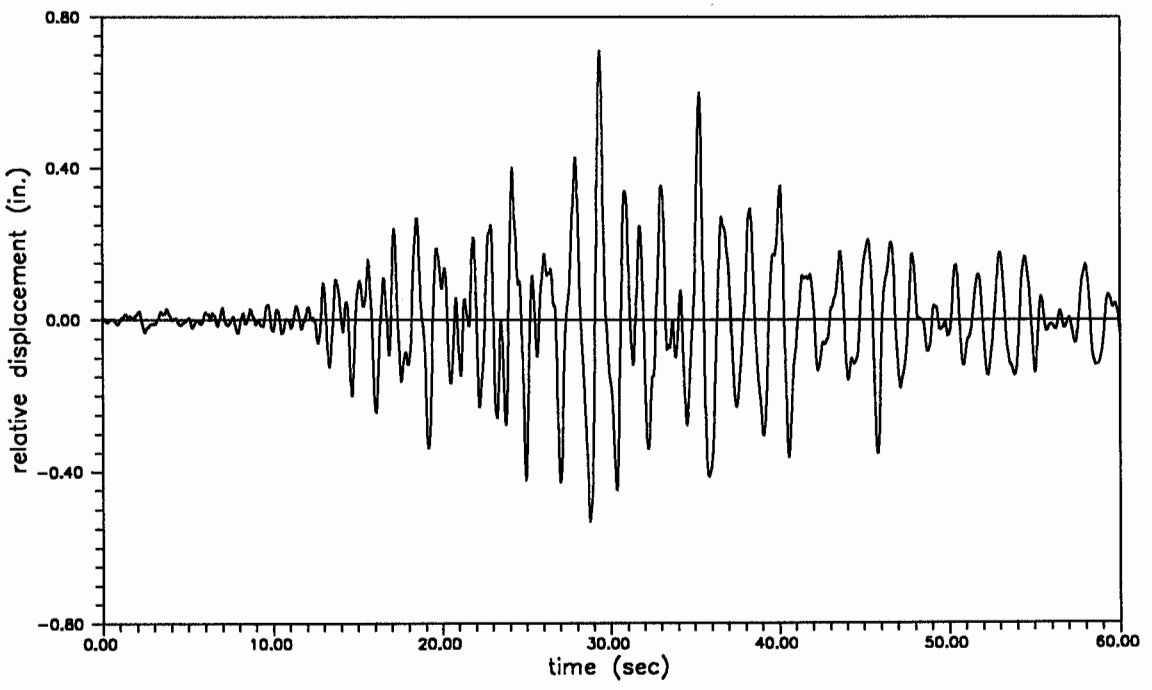

Figure A.6 Relative displacement of roof with respect to second floor in east-west direction at north wall.

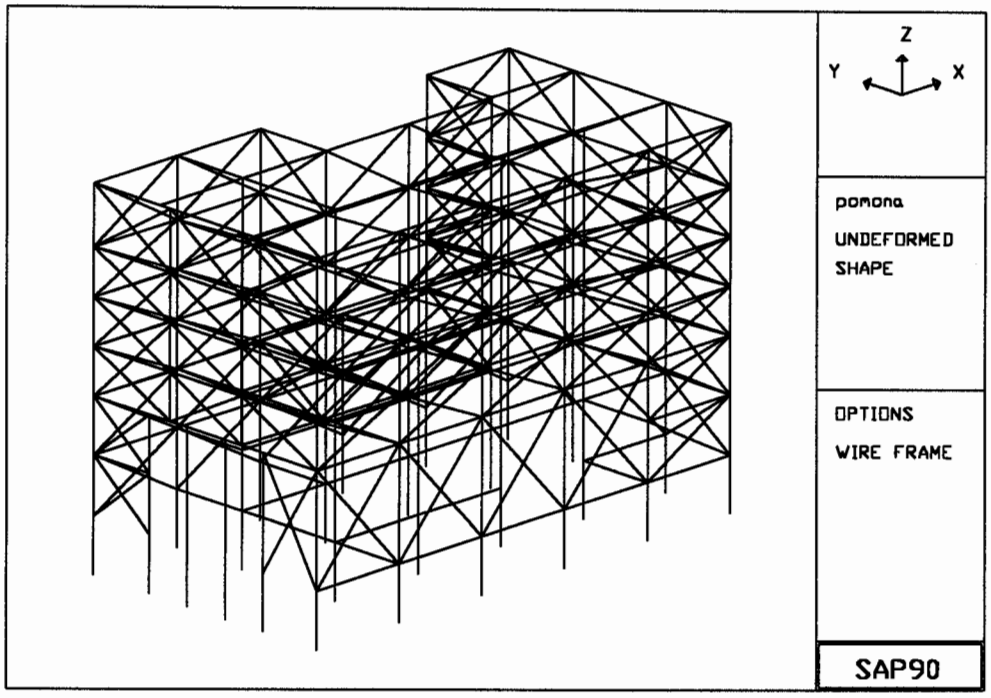

Figure A.7 Three dimensional computer model of six story commercial building.

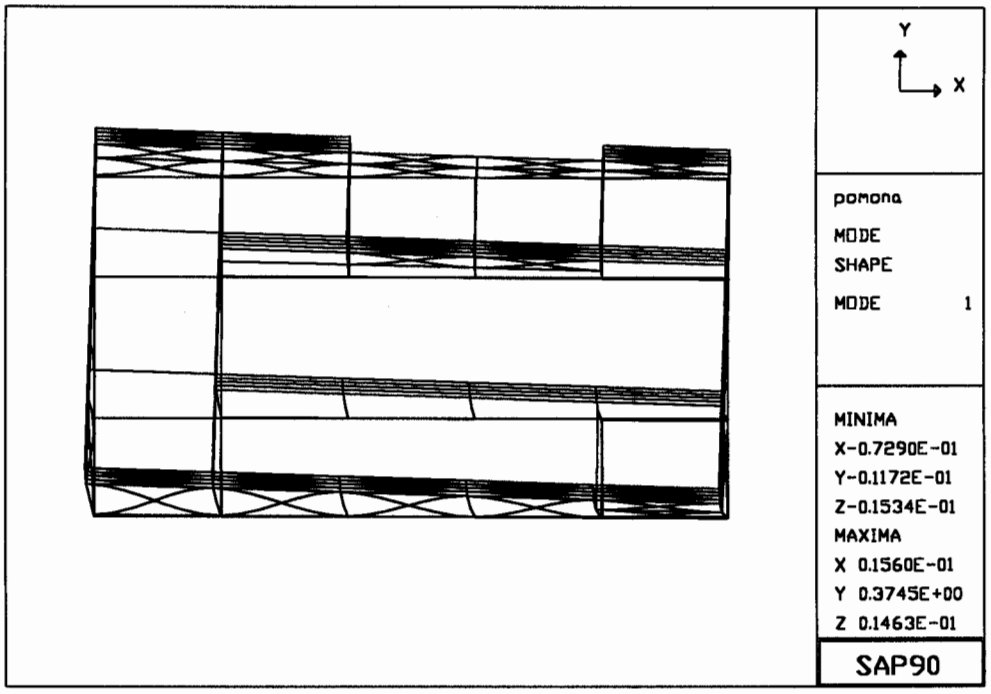

Figure A.8 First mode, translation in east-west direction, period of 1.04s.

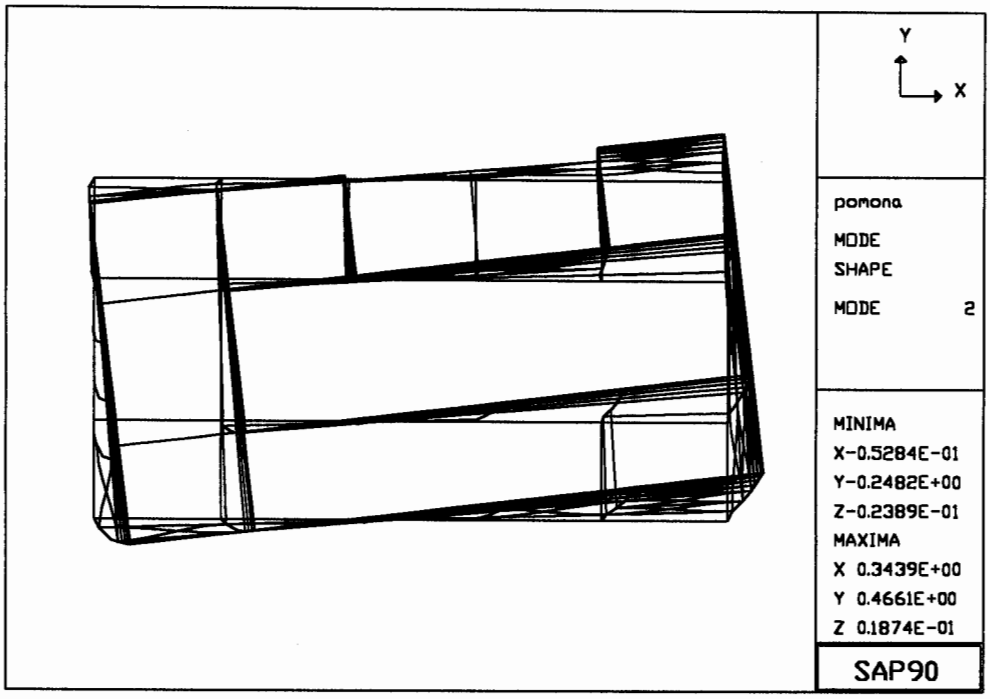

Figure A.9 Second mode, rotation, period of 0.71s.

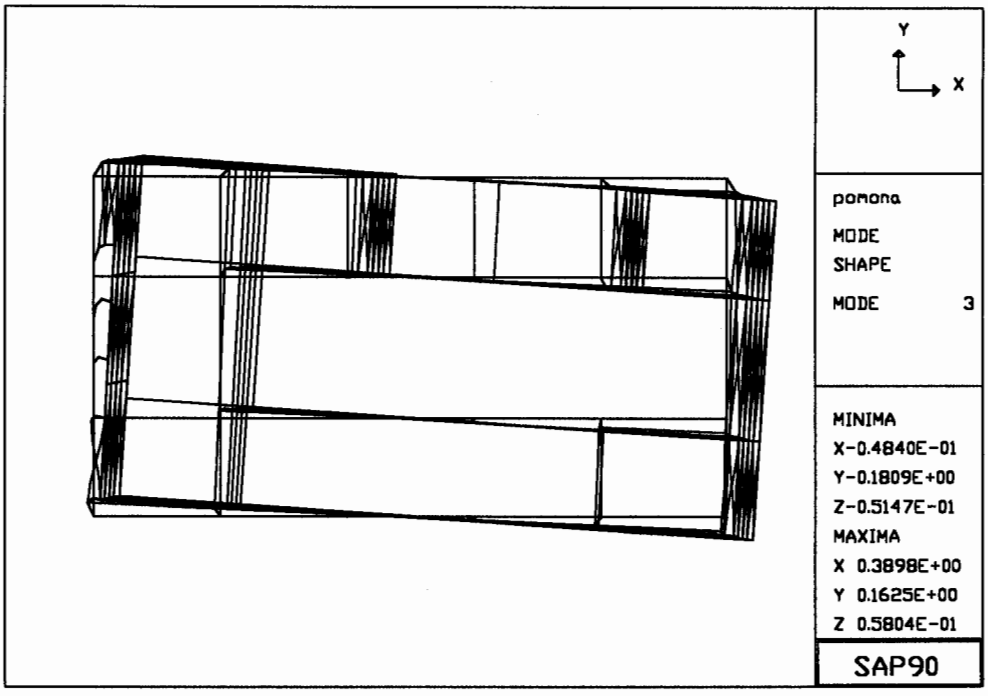

Figure A.10 Third mode, translation in north-south direction, period of 0.51s.

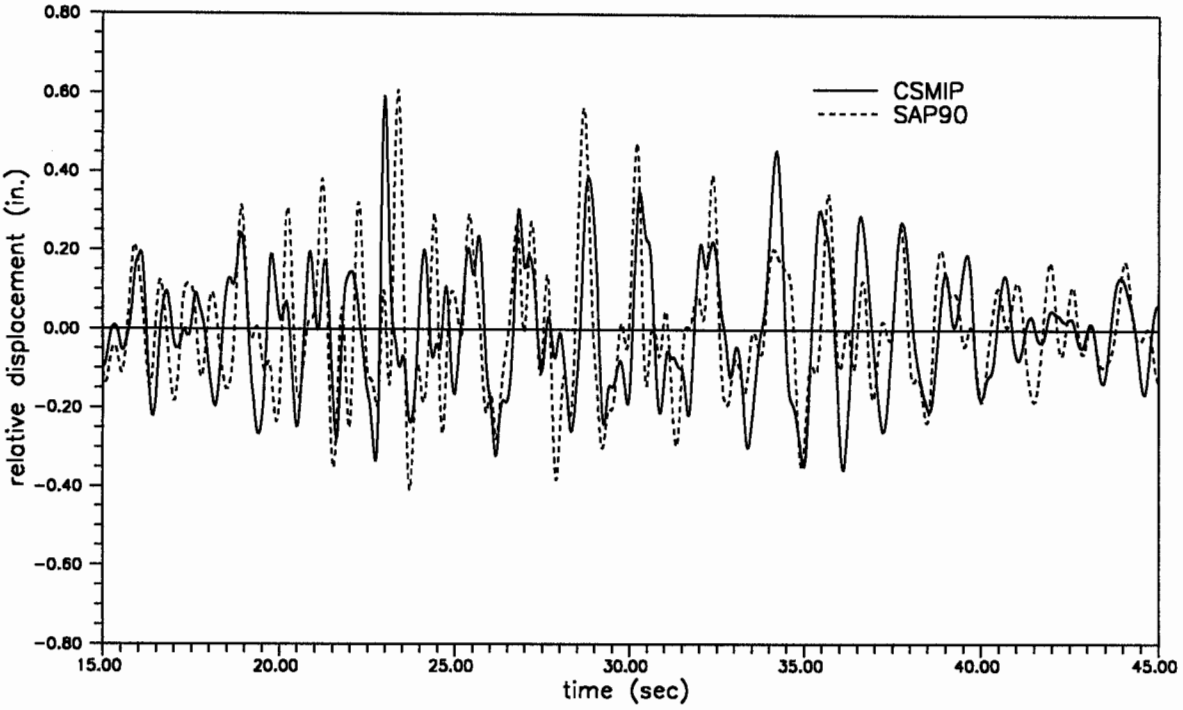

Figure A.11 Recorded (channel 2) and simulated displacement of roof with respect to base (channel 6) in the north-south direction (Landers).

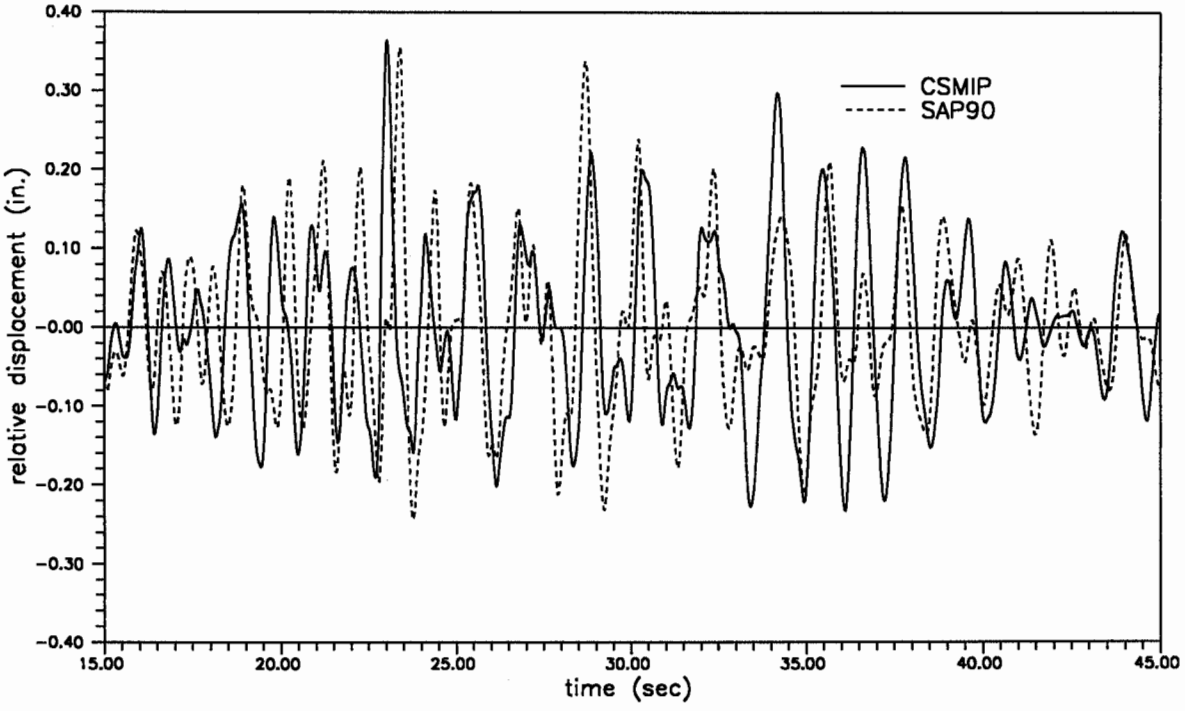

Figure A.12 Recorded (channel 5) and simulated displacement of the second floor with respect to base (channel 6) in the north-south direction (Landers).

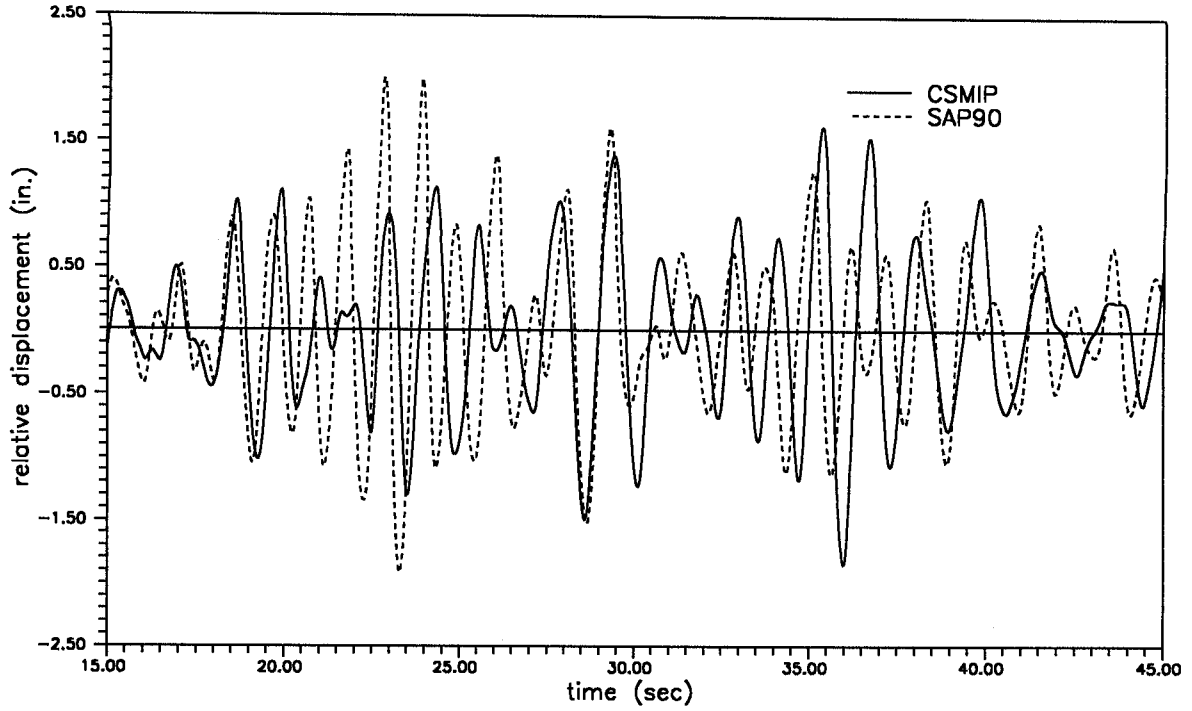

Figure A.13 Recorded (channel 7) and simulated displacement of roof with respect to base (channel 11) in the east-west direction at south wall (Landers).

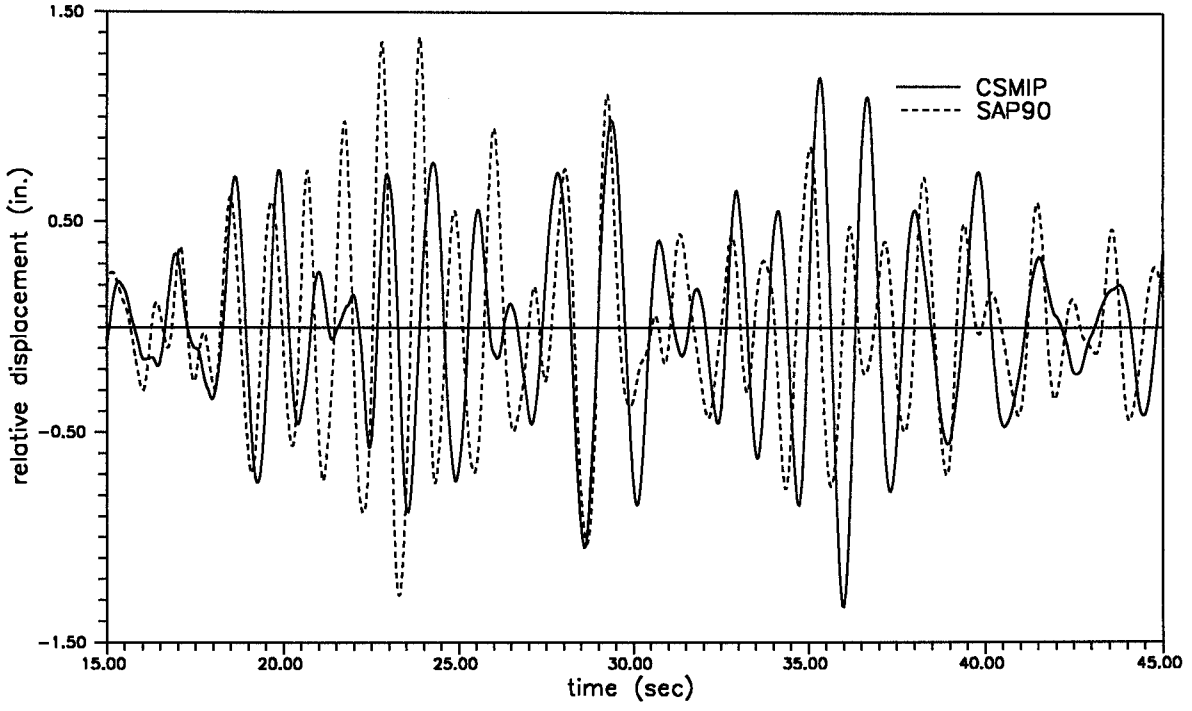

Figure A.14 Recorded (channel 9) and simulated displacement of the second floor with respect to base (channel 11) in the east-west direction at south wall (Landers).

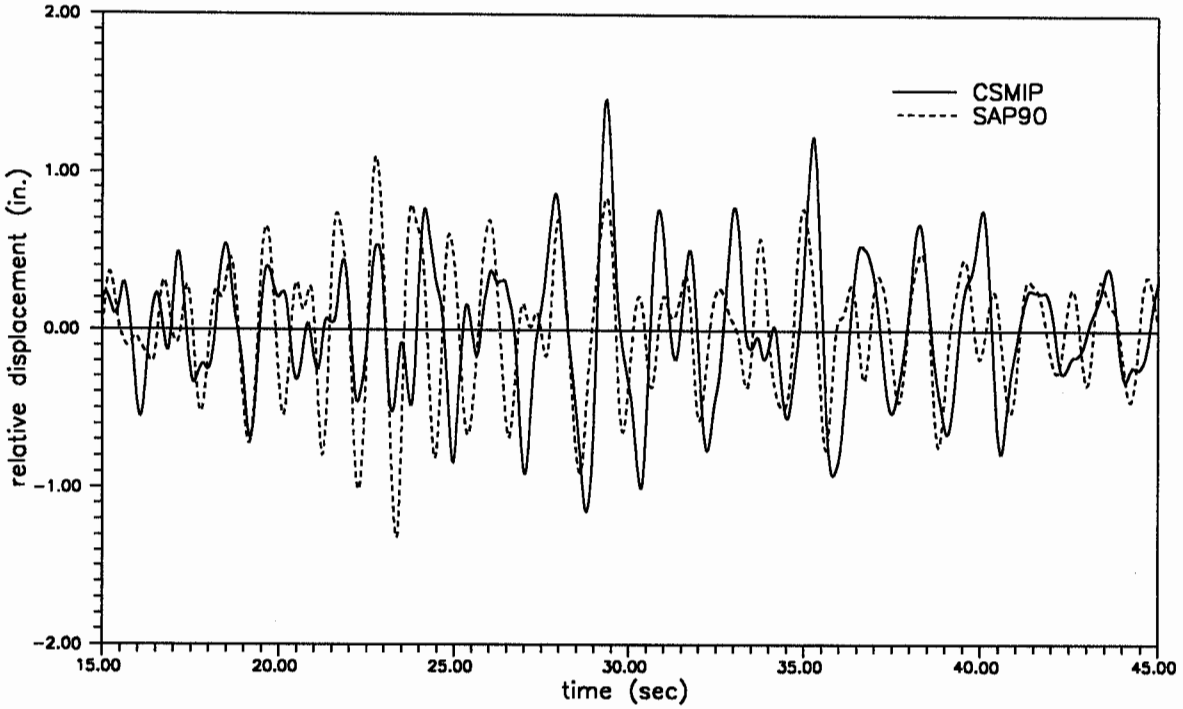

Figure A.15 Recorded (channel 8) and simulated displacement of roof with respect to base (channel 12)in the east-west direction at north wall (Landers).

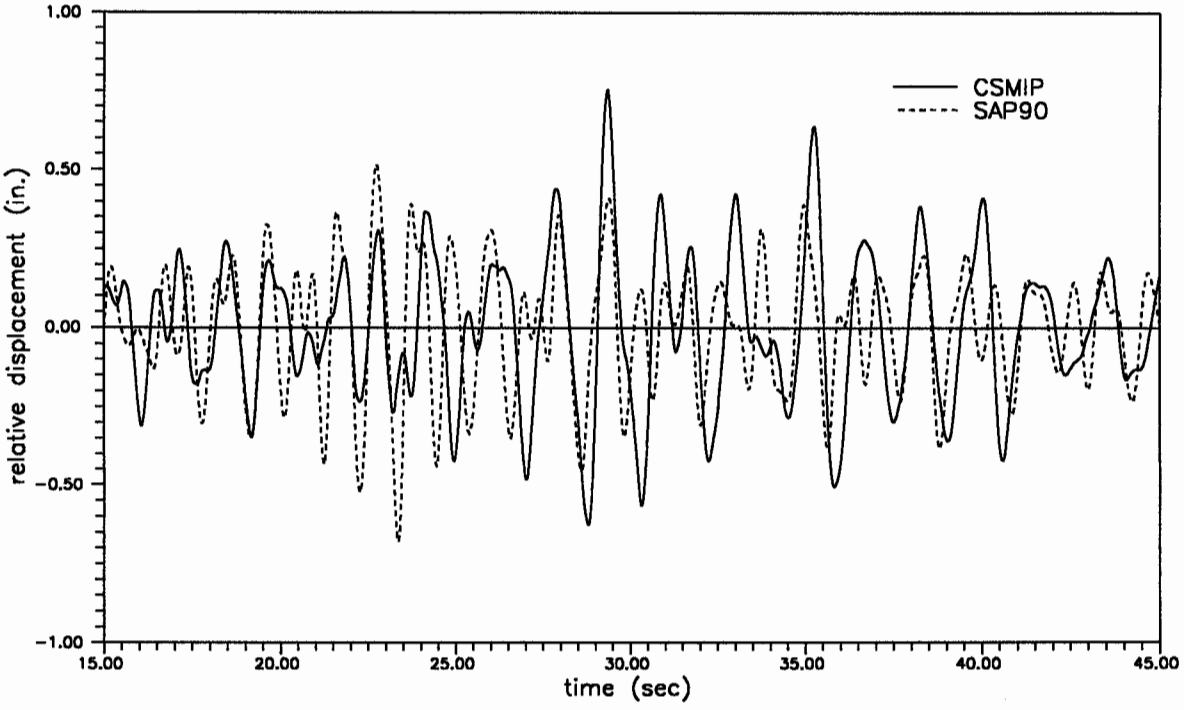

Figure A.16 Recorded (channel 10) and simulated displacement of the second floor with respect to base (channel 12) in east-west direction at north wall (Landers).

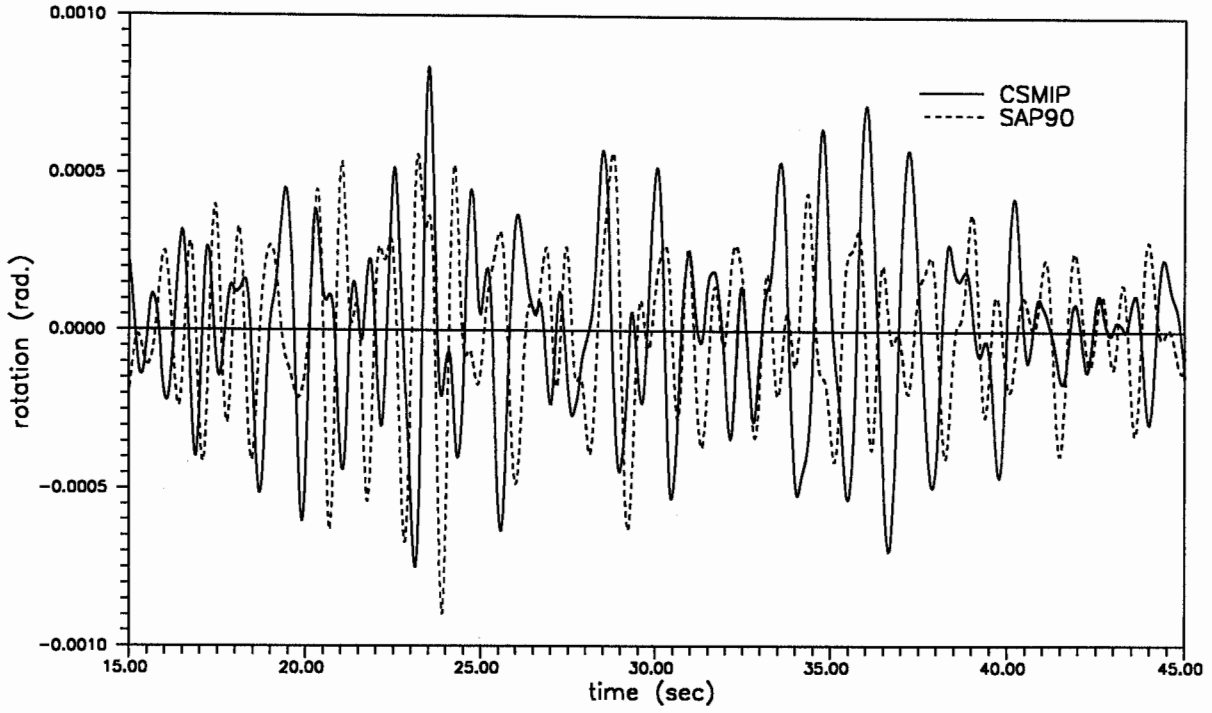

Figure A.17 Recorded and simulated rotation of roof (Landers).

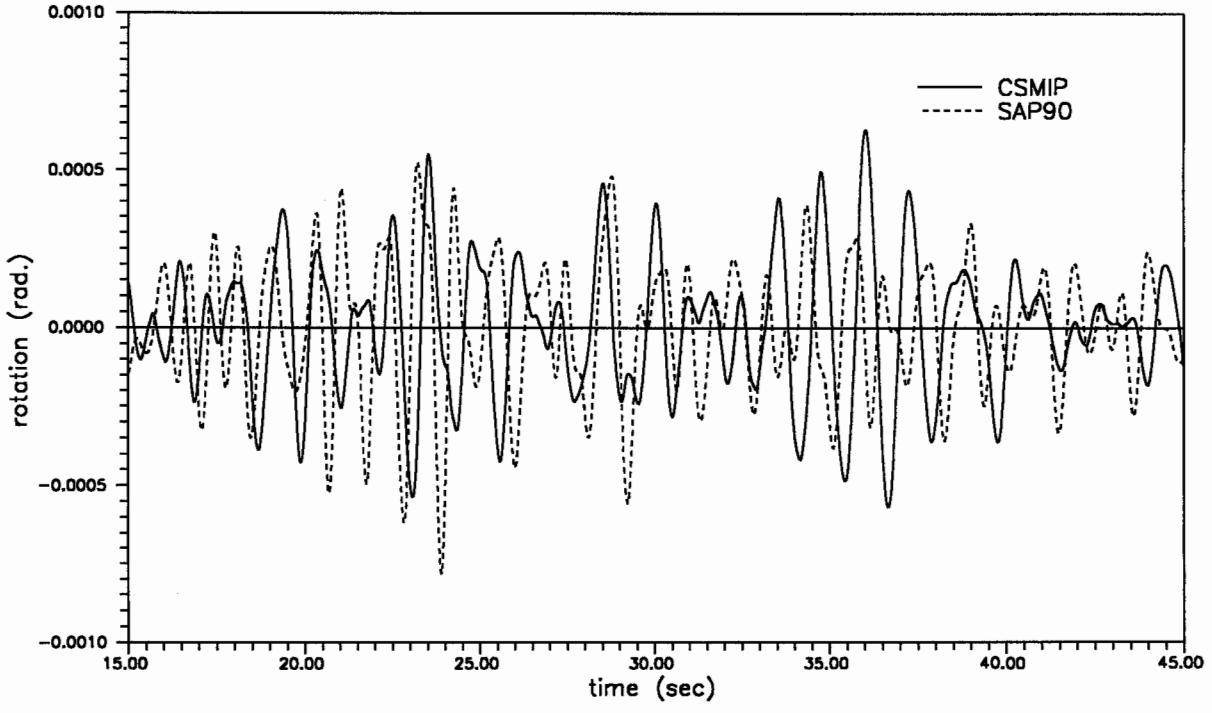

Figure A.18 Recorded and simulated rotation of second floor (Landers).

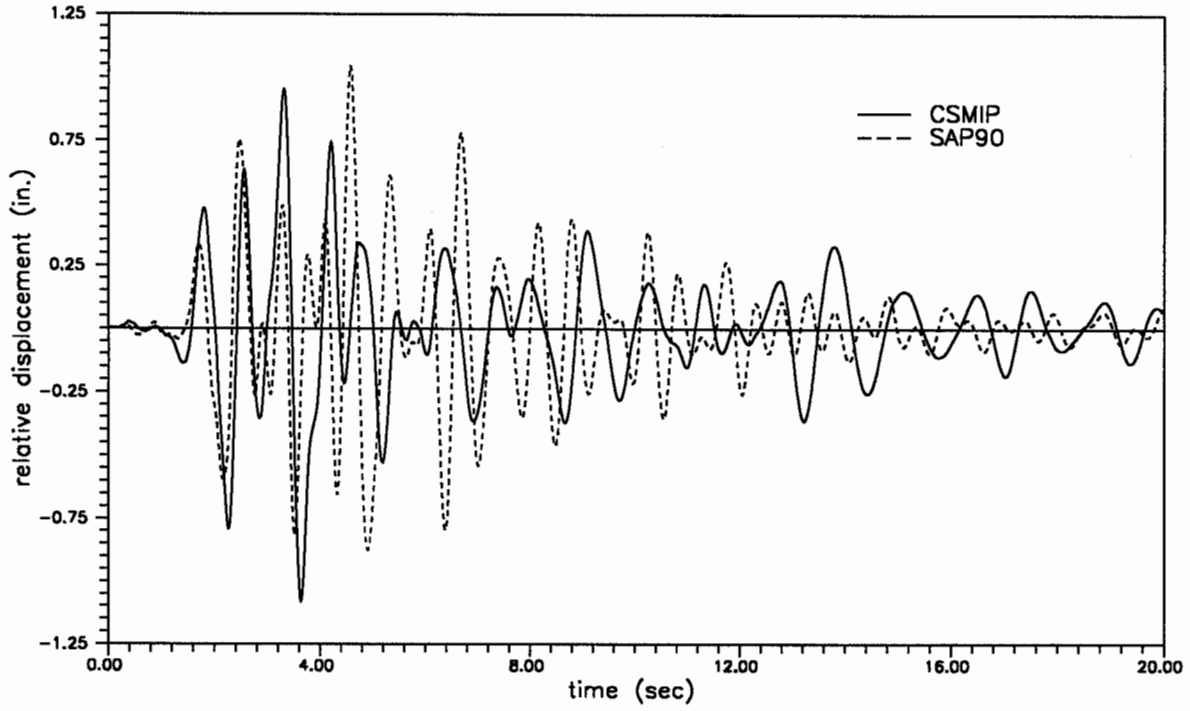

Figure A.19 Recorded (channel 2) and simulated displacement of roof with respect to base (channel 6) in north-south direction (Upland).

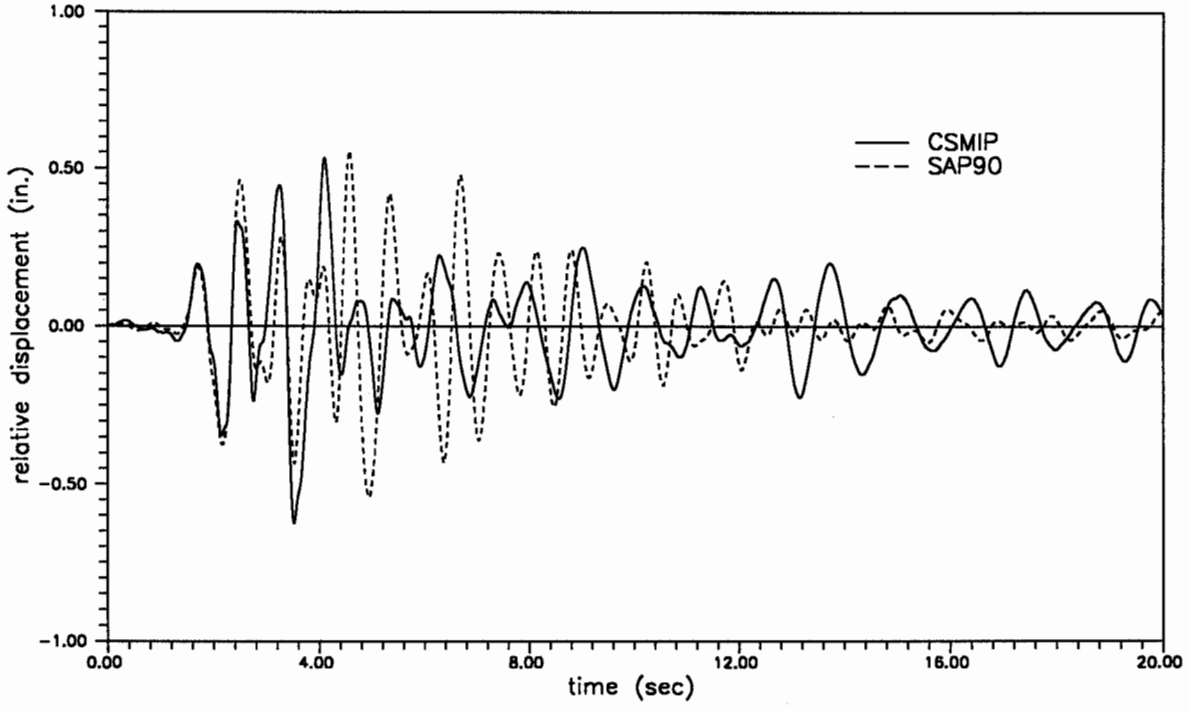

Figure A.20 Recorded (channel 5) and simulated displacement of the second floor with respect to base (channel 6) in north-south direction (Upland).

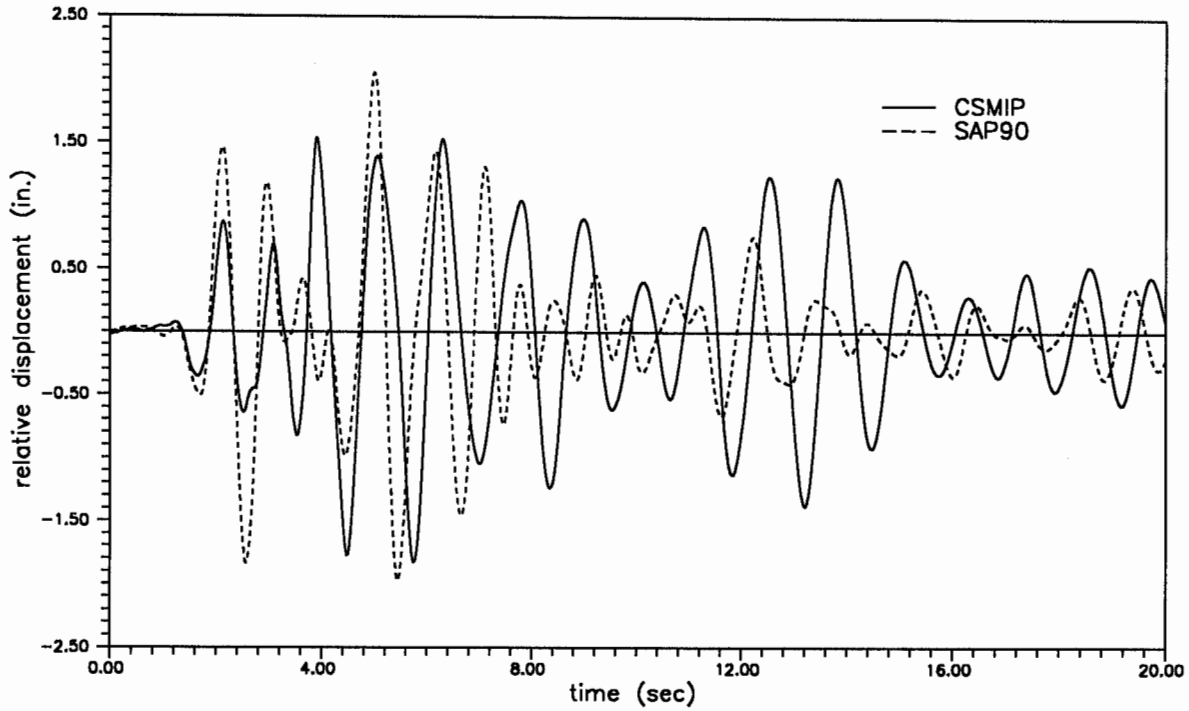

Figure A.21 Recorded (channel 7) and simulated displacement of roof with respect to base (channel 11) in east-west direction at south wall (Upland).

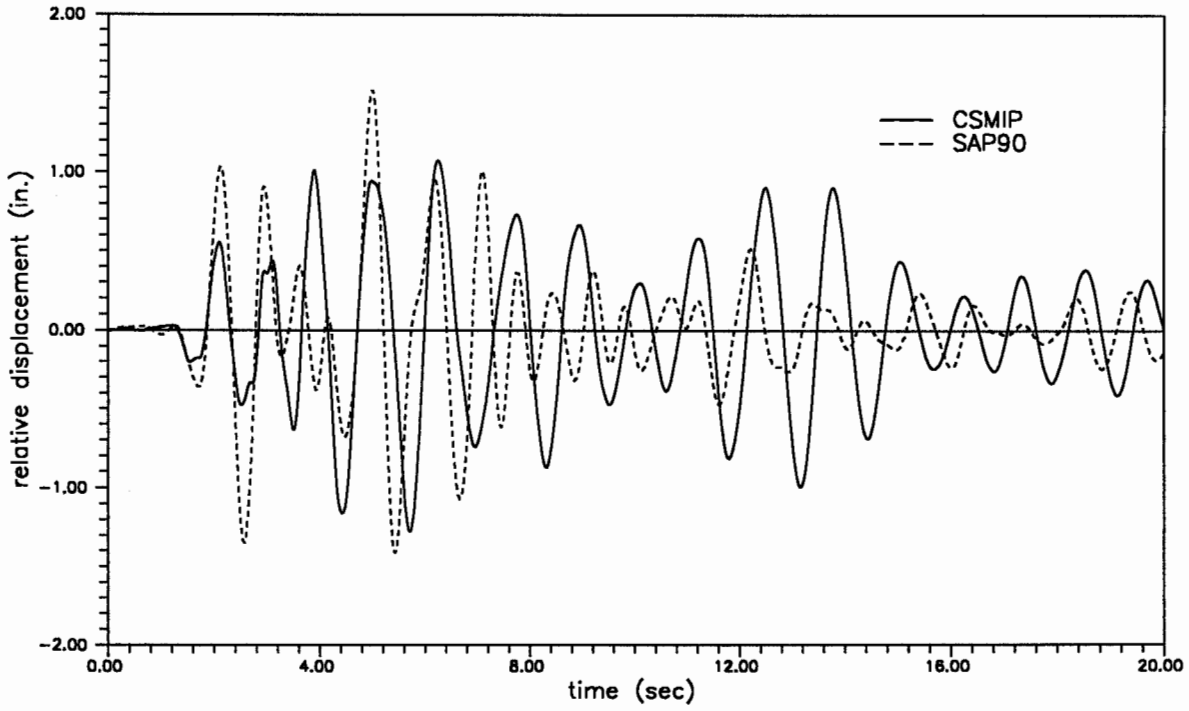

Figure A.22 Recorded (channel 9) and simulated displacement of the second floor with respect to base (channel 11) in the east-west direction at south wall (Upland).

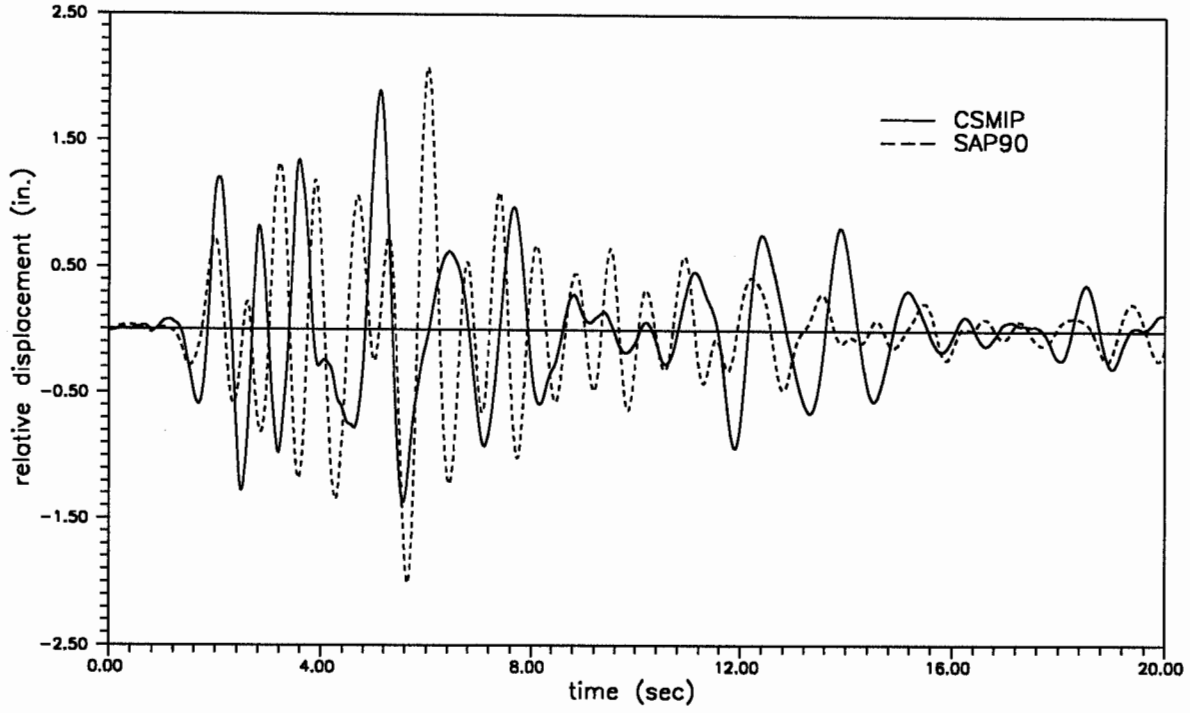

Figure A.23 Recorded (channel 8) and simulated displacement of roof with respect to base (channel 12) in east-west direction at north wall (Upland).

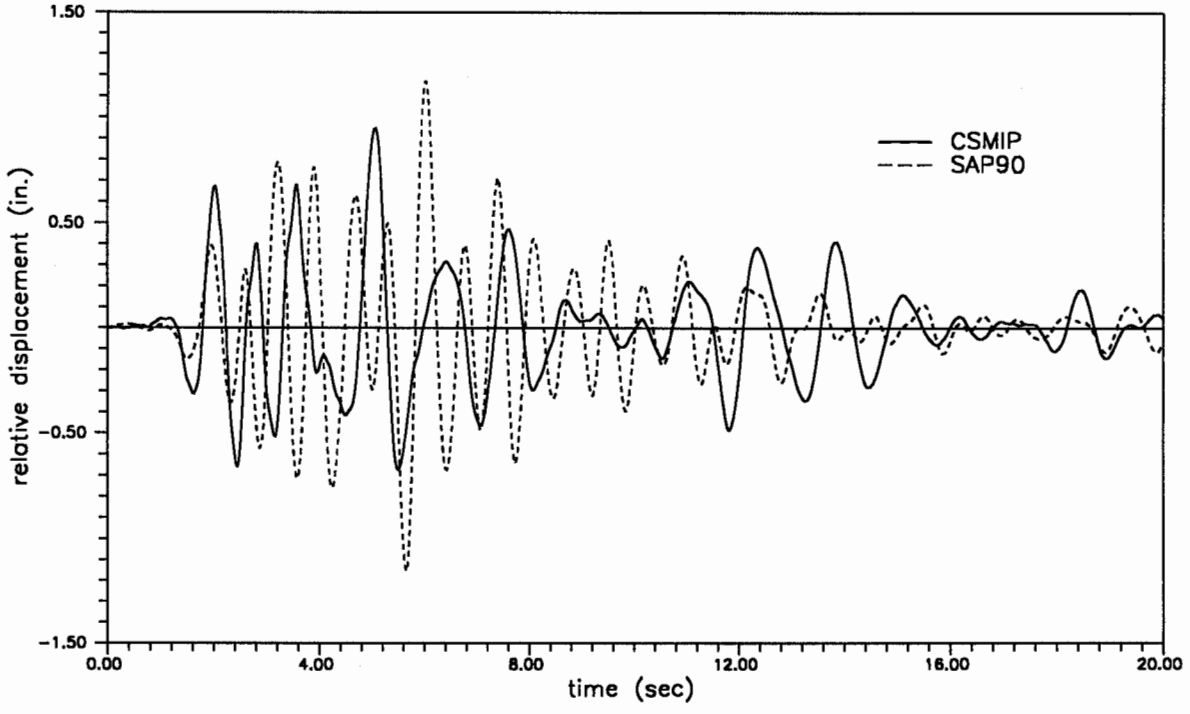

Figure A.24 Recorded (channel 10) and simulated displacement of the second floor with respect to base (channel 12) in east-west direction at north wall (Upland).

APPENDIX B

SIMULATION OF THE RESPONSE OF

CSMIP STATION NO. 24541 TO

THE LANDERS AND THE SIERRA MADRE EARTHQUAKE

SECTION B1

INTRODUCTION

B1.1 SCOPE OF THE ANALYSIS

The intent of this study is to evaluate the ability to model infill frame structures using a combination of linear and nonlinear analytical procedures. These procedures included the use of the SAP90 frame program and the FEM program to model the building structure. Using time-histories and response spectra analysis, the results of the analytical study were compared to the results recorded at the building during the Landers and Sierra Madre event. CSMIP Station No. 24541 is one of the four buildings selected for this program.

B1.2 DESCRIPTION OF THE BUILDING

The building is a 6 story structure with one basement level and is located in the Pasadena area. The lateral load resisting system is made up of a steel frame and the exterior unreinforced masonry infill material within the frame system. No testing was done on the materials and, therefore; the properties were assumed based on experience.

B1.3 COMPUTER MODEL OF THE BUILDING

The SAP90 computer model utilized the bare steel beams and columns. Their connections were considered rigid. The column support was taken at the first floor with a fixed configuration ignoring the basement level. The concrete floors and roof were modeled as rigid diaphragms. The infill was modeled using a nonlinear FEM program and represented with equivalent diagonal braces.

B1.4 CSMIP DATA

The time history data supplied by CSMIP consisted of the Landers record and the Sierra Madre record. A thorough analysis was accomplished based on

the Landers records and the final model was used for a comparison to the Sierra Madre records.

SECTION B2

DESCRIPTION OF THE BUILDING

B2.1 TYPE OF LATERAL FORCE RESISTING SYSTEM

CSMIP Building No. 24541 is located in Pasadena, California. The floor plans and elevations as provided by CSMIP are shown in Figure B.1. The building structure consists of a steel frame encased by masonry. The beam-column joints appear to have only steel angle web connectors, however; in some cases seat angles appear to have been provided. The floor slabs above the first floor are clay tile covered with concrete and span between intermediate steel beams. The exterior walls are 13" unreinforced brick at the north and west elevations and 17" unreinforced brick at the south and east elevations.

B2.2 FOUNDATION SYSTEM AND BASEMENT FRAMING

The building has one level below grade with the steel columns continuous to the foundation at the building interior and steel columns dropping approximately 3' below the ground floor at some exterior conditions. For modeling purposes, the building was considered fixed at the first floor and the effects of the basement was not considered.

B2.3 IRREGULARITIES OF THE STRUCTURAL SYSTEM

The building's overall plan dimensions are approximately 117'x 125'. The plan is approximately square up to the 2nd story and then become a 'U' shape above. Bridges were added recently which rigidly connect the legs of the 'U' as shown in Figure B.1. The first story height is approximately 19' with the typical stories above being approximately 11'-6" in height. Above the 6th floor there is an attic level consisting of framing without a floor

system. The roof slab is at a variable height above the attic. The infill appears to be relatively symmetrical in window geometry at the upper floors, however; the brick wall thickness varies from side to side. At the first level, open storefronts exist on the east and the south elevations. The north elevation has a couple of solid panels and the west elevation is almost completely solid with the exception of a few small windows.

SECTION B3

RECORDED EARTHQUAKE RESPONSE OF THE BUILDING

B3.1 RECORDED EARTHQUAKE RESPONSE OF THE BUILDING

Two records were used for comparison on this building. They are as follows:

Landers Earthquake	*June 28, 1992*
Sierra Madre Earthquake	*June 28, 1991*

The Landers earthquake was centered near the city of Landers which is approximately 43 km north of Palm Springs and 80 km east of San Bernardino. The earthquake had a magnitude of 7.5 M_s. The Sierra Madre earthquake occurred under the San Gabriel Mountains approximately 20 km northeast of downtown Pasadena. This earthquake had a magnitude of 5.8 M_L.

B3.2 LOCATIONS OF INSTRUMENTS

CSMIP Building No. 24541 was heavily instrumented by CSMIP. The Location of the 16 stations can be seen on Figure B.1. Numerous locations were selected on the roof level suggesting that rigid diaphragm motion was not anticipated. Below, at the second floor, the instruments cover only the four exterior walls. The basement level has an instrument in the north/south and two in the east/west directions. Also one instrument recorded vertical motion. Two instruments, one on the sixth floor and one on the attic appear

to have been placed to measure the relative out-of-plane motion of the infilled wall.

B3.3 CHARACTERISTICS OF BASE MOTIONS

Time histories recorded at the basement were considered as the input motion. The acceleration, velocity, and displacement time histories for each direction are shown in Figure B.2 & B.3 for the Landers earthquake. A 2% damped response spectrum was created from the acceleration histories to determine the energy content in the frequency domain of the ground motion. These spectra are presented in Figure B.4. It can be seen from the response spectra that the ground motions carry most of their energy below 1.7 seconds. Beyond this the energy drops off quickly with a small increase in the north/south direction in the 2.5 second range.

B3.4 BASEMENT RECORD USED IN ANALYSIS

Two input records were available in the east/west direction at the basement. The instrument at the south wall was selected as the primary input because of its location against a relatively stiff upper wall. It was felt that this instrument would record the least amount of structural feedback and would, therefore be more representative of the true ground motion. In the north/south direction only one instrument was available at the basement.

B3.5 RESPONSE OF THE BUILDING

The response of the building to the ground motions were investigated by differencing the displacement time histories for the different levels and running response spectrums of the acceleration records for each wall of the building. The time history records can be seen in Figures B.6-B.12 and the spectra can be seen in Figures B.13 & B.14. The differenced displacement time histories for the Landers event were used to determine strut properties.

Response spectrums for the ground accelerations and for the upper floor accelerations were determined and differenced from the CSMIP data. Using this procedure, the periods with the greatest energy content or amplification would show as a spike. The spike was used to determine the probable period of the structure at the drift level experienced by the structure since that is where the greatest amplification would occur.

It can be seen in Figure B.13B that when the difference between the ground spectrum and the roof spectrum for the south elevation is plotted, a peak appears at about 1.8-2.1 seconds. This was thought to be the primary mode with a secondary mode rising at about 1.1-1.2 seconds. In Figure B.14A the spectrum was differenced for the west wall. It can be seen that the primary mode drops off and only the secondary mode at 1.1-1.2 seconds remains. This indicates that the primary mode is torsional about the west wall accounting for the low energy content within the primary mode range.

In most cases the spikes noted were over a relatively broad period range. This can be attributed to the torsional nature of the building. Clear mode shapes were difficult to obtain with the instruments available. In some period ranges the energy amplification appeared to be zero indicating that little or no amplification of the ground motion occurred at this frequency and that the building simply moved with the ground. This can be seen particularly well in Figure B.13B at about 1.5 seconds.

SECTION B4

COMPUTER MODEL OF THE BUILDING

B4.1 LINEAR ELASTIC THREE-DIMENSIONAL MODEL

CSMIP Building No. 24541 was modeled on the SAP90 three dimensional beam frame program. The steel beam to column joints were modeled as rigid connections. Originally, the building was modeled with columns continuous to the basement, however; at the level of displacements from these earthquakes,

this proved to greatly underestimate the building stiffness at the first floor. The columns were, therefore, considered fixed at the ground floor restrained by the first floor slab. The encasement on the frame was ignored because it was not concrete but masonry with minimal mortar around the columns. The slab was assumed to act as a rigid diaphragm. Figure B.5 shows the rotation of the building taken from two independent sets of instruments on the roof. It can be seen that the rotation is identical for both cases indicating that rigid body motion occurred and, therefore, validated this assumption. The slab, however was not considered in the beam stiffness due to its clay tile and concrete construction. Only primary beams spanning from column to column were modeled.

B4.2 MODELING OF URM INFILLS

The URM infill was modeled using the FEM program written by Robert D. Ewing, Ahmad M. El-Mustapha, and John C. Kariotis under a National Science Foundation grant. Typical panels were modeled and the force displacement characteristics were plotted as shown in Figure B.15. The effects from the frame were not subtracted from the overall stiffness of the panels because it was thought that they only added a small percentage to the stiffness. The material properties of the masonry was assumed since physical testing was beyond the scope of this research. It was, therefore, determined that adjusting all of the strut properties by a consistent percentage could be used to adjust the building stiffness to account for the uncertainty of the properties. The story drifts calculated for each wall for the Landers earthquake were used to determine the secant stiffness of the crossbraces. The crossbraces were then sized using a modulus for steel and adjusting the area to represent the infill at that drift limit.

B4.3 COMPLETE BUILDING MODEL

The final model was a three-dimensional steel frame with diagonal crossbraces at the exterior representing the infill. Nonstructural interior items such as

concrete stairs and clay tile walls were not considered in this model. Rigid offsets in the frames were not used to modify the stiffness. Supports were raised at the open storefronts as described below to account for masonry bulkheads at the bottom of the columns. The properties of the braces as obtained from the FEM data were reduced by 10% at all locations in the final model and 5% damping was used in all modes of the model. These two parameters were based on the comparisons of the CSMIP data and the SAP90 model.

B4.4 RESULTS OF THE COMPUTER ANALYSIS

Based upon initial runs of the building model, it was determined that the drift at the first floor over the eastern open storefront was about twice the drift recorded by CSMIP. After further examination of the plans, it was noted that masonry bulkheads below the open storefront windows were effectively reducing the story height at that location. An adjustment was made by moving the lower supports up to the top of the bulkheads with better correlation resulting.

As mentioned before, adjustments were also made in the brace properties as well as the modal damping. Because the frame was steel and had no solid concrete encasing, the stiffness properties of the beams and columns were not varied. The 10% decrease of the strut properties caused a variation of 10% to 20% in the building drifts on the elevations with solid wall to the ground. In addition the frequency match of the model improved with the softening. Little change occurred in the walls which were over open storefronts. Varying the damping ratio from 3% to 5% viscous damping resulted in approximately 15% to 20% variation in the drifts as well.

The eigenvalues for the final computer model are presented in Table B.1. It can be seen that the primary mode is 2.02 seconds and it is relatively torsional. In Figure B.16 the first mode shape can be viewed from above which shows that it rotates about the west wall. This is consistent with the differenced response spectrum in Figures B.13 & B.14. The second mode is at

1.15 seconds and is also primarily torsional. Based upon the CSMIP data it appears that the periods of the structure have been accurately modeled using the equivalent struts.

SECTION B5

COMPARISON OF MODEL RESPONSE TO CSMIP DATA

B5.1 GENERAL

The SAP90 model was built using the procedure as outlined above. After running the time history for Landers only two main parameters were varied. First, the damping was varied until the amplitudes converged. The damping was limited to 5% because this was considered a reasonable maximum value for a steel frame building at this drift level. The second item that was modified was the crossbrace stiffness. The properties on which they were based were assumed and, therefore; all brace properties were decreased by 10% for an improved frequency match to the data.

At the open storefront the effective story height was modified to reflect a masonry bulkhead at the bottom of the columns. This accounted for some of the excessive drift at the first floor encountered above the storefronts.

B5.2 COMPARISON OF AMPLITUDE OF DISPLACEMENT DATA

The results of the computer simulations can be seen in Figures B.6-B.10 for the Landers earthquake and in Figures B.11 & B.12 for the Sierra Madre. It can be seen for the east/west direction that good correlation is obtained for the displacement time histories. Particularly the records for the south wall. Zero crossings are well represented, however; displacements run slightly higher for the SAP90 model. In the north/south direction correlation for the west wall is also reasonably good. It can be seen in Figure B.8 that

the zero crossings and the amplitudes are closely approximated by the SAP90 model with the SAP model responding slightly too stiff. In the east elevation the correlation was not as good. It can be seen in Figure B.9 that the zero crossings and the amplitudes are slightly off at the second floor. This inaccuracy then carries through to the roof. Rotational frequency as seen in Figure B.10 correlated very well. Zero crossings were matched at the roof with considerable accuracy. Amplitudes, however, were overestimated by the SAP model. At this location, above the open storefronts, there were limited structural parameters that could be justifiably adjusted. At the first floor there were no crossbraces at this location. It is believed that existing stairs towards the center of the building may have provided additional stiffening in this direction. These were ignored, as is common practice, during building modeling.

Displacement time histories were also compared for the Sierra Madre earthquake. As was the case for Landers the south wall in the SAP90 model revealed good correlation to the actual building motion (see Figure B.11). In the north/south direction, the building immediately experienced nonlinear behavior during the first main pulse of the earthquake. This can be seen particularly well in Figure B.12A. It can be seen that the one particularly large spike occurs within the first 5 seconds of the earthquake. The ground motion then trails off. During this spike the SAP90 model predicted a much smaller response. This can be justified again by the inaccuracies of the damping representation. Hysteretic damping only occurs during the unloading portion of motion unlike viscous damping which is velocity dependent. Therefore, during this first cycle little or no damping was active within the actual structure. For this plot the motion is slightly out of phase, however, the motion appears to fall in step for later time indicating that a close match was made for the Sierra Madre motion as well.

For both the Landers and the Sierra Madre earthquakes the peak displacements were tabulated as seen in Table B.2. It can be seen that the

overall correlation of peak relative displacements (the most important parameter) was very good.

B5.3 COMPARISON OF FREQUENCY DATA

Response spectrums were created from the SAP90 output acceleration time histories as well as the CSMIP acceleration time histories for the Landers input ground motion. A comparison of these can be seen in Figures B.17 & B.18. These spectrums were 2% damped and used to compare the energy content of the motions. In the east/west direction, period correlation was good, however; the magnitude did not correlate well. In the north/south direction, correlation was not as close due to the torsional inaccuracies as mentioned above. The spectrums were only used to determine whether we had matched the building's response characteristics.

SECTION B6

CONCLUSIONS

B6.1 MODELING

The building model response overall correlated well with the recorded response by CSMIP. The steel frame under intermediate interstory drifts appeared to have behaved with rigid beam-column connections and a fixed base support. The crossbraces provided for this building appear to have represented the infill properties adequately. Physical testing would be required to determine how close the assumed masonry properties were to the actual conditions. Better correlation could be attempted by carefully modeling items commonly considered nonstructural such as the stairs at the center of the building. Further adjustments could also be made to better predict the panel's stiffness during cyclic motion. A factor of 80% of strut stiffness has been suggested for future work.

B6.2 FIT OF COMPUTER DATA TO RECORDED DATA

The fit of the model to the CSMIP records seemed reasonable considering the complexities of the building modeled. The building was extremely torsional and had stiffness changes occurring between the 2nd floor and the upper stories. It should be concluded for this building behavior that good correlation between the building model and the actual building can be accomplished using the proposed infilled brace procedure.

B6.3 DETERMINATION OF DAMPING

The model damping was determined by closely matching the amplitudes of the recorded motion. 5% damping gave the most appropriate drift. The damping was not well modeled as seen by the amplitudes at the end of the records during the trail off. The building appeared to damp much quicker than the model during the lack of input motion such as at the end of the record. It is believed that because viscous damping used in the model is dependent on the velocity of the system and the actual building displays hysteretic damping, which is dependent on drift, the correlation will not work for all levels of drift and, therefore, was adjusted to match at the maximum motion.

Damping was set as 5% for all modes of vibration. It may be appropriate to damp rotational modes differently than translational modes. This did not seem to be a parameter for this structure, however; because all the primary modes were torsional.

B6.4 INSTRUMENT LOCATIONS

Instruments were located at many locations throughout the building. It appeared that rigid diaphragm motion was not anticipated and, therefore, additional instruments were located to determine differential motion within the diaphragm. All instruments were also located in the principal axes of the building. Within this torsional structure instruments could have been oriented to obtain more useful results by anticipating the response of the structure.

BUILDING PERIODS FROM SAP90

Mode 1	2.02 sec.
Mode 2	1.15 sec.
Mode 3	0.68 sec.
Mode 4	0.44 sec.
Mode 5	0.32 sec.
Mode 6	0.22 sec.

Table B.1. Building Periods as Calculated from SAP90

MAXIMUM DRIFTS

Location	Floor	Landers		Sierra Madre	
		CSMIP	SAP90	CSMIP	SAP90
West	2nd	0.24	0.26	0.20	0.20
East	2nd	0.90	1.34	0.90	0.86
North	2nd	0.80	1.05	0.50	0.75
South	2nd	0.75	0.85	0.50	0.60
West	Roof	1.40	1.06	1.60	0.84
East	Roof	2.00	1.97	1.60	1.15
North W.	Roof	2.50	2.00	1.50	1.52
North E.	Roof	2.50	2.00	1.50	1.52
Center M.	Roof	2.02	1.57	0.98	1.05
South	Roof	1.35	1.35	0.80	0.91

Table B.2. Comparison of Maximum Drifts for SAP90 and CSMIP

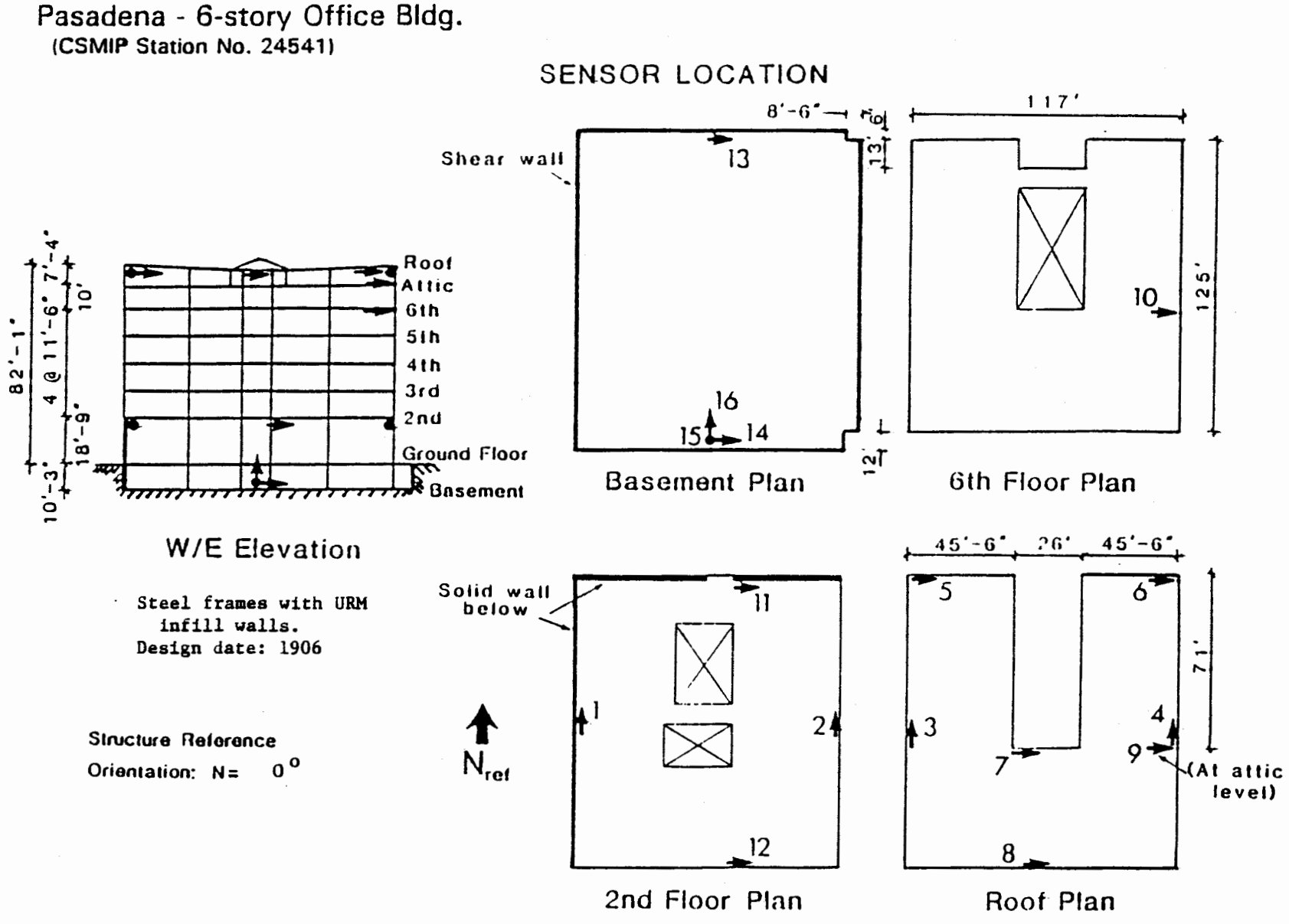

Figure B.1. Plans and Elevations from CSMIP

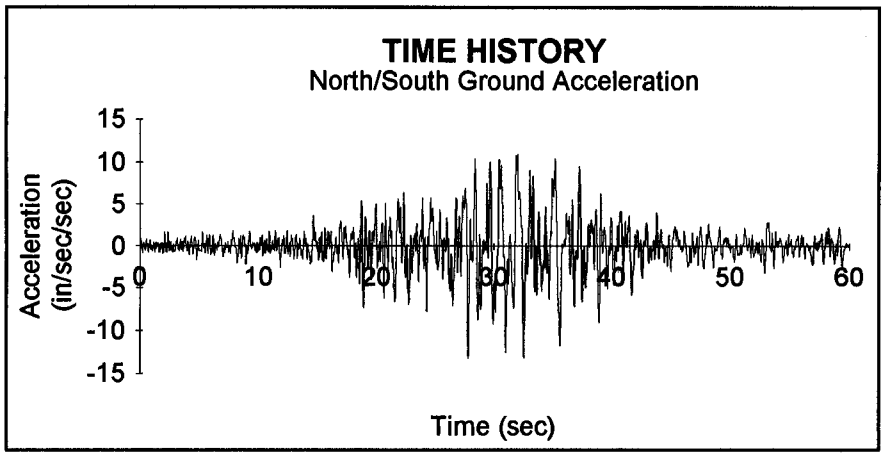

Figure B.2A. Landers Acceleration Time History

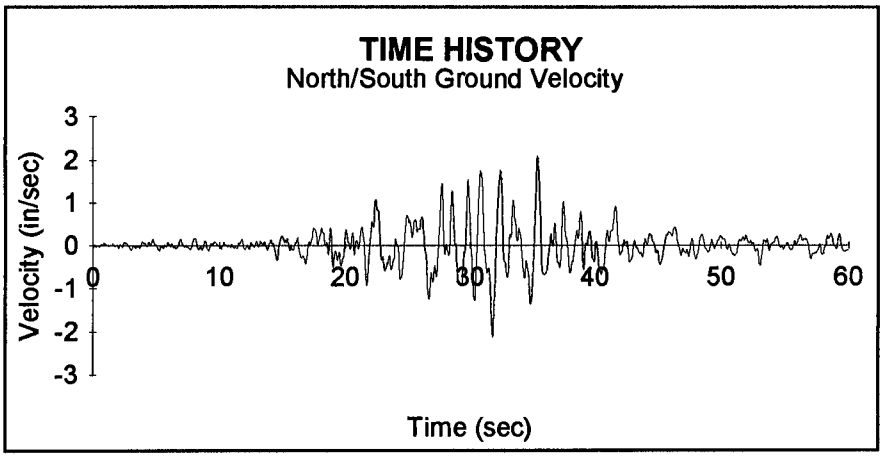

Figure B.2B. Landers Velocity Time History

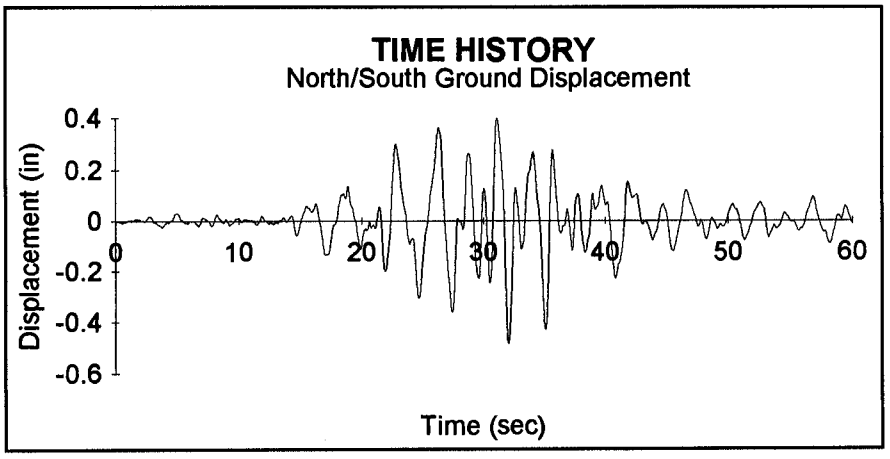

Figure B.2C. Landers Displacement Time History

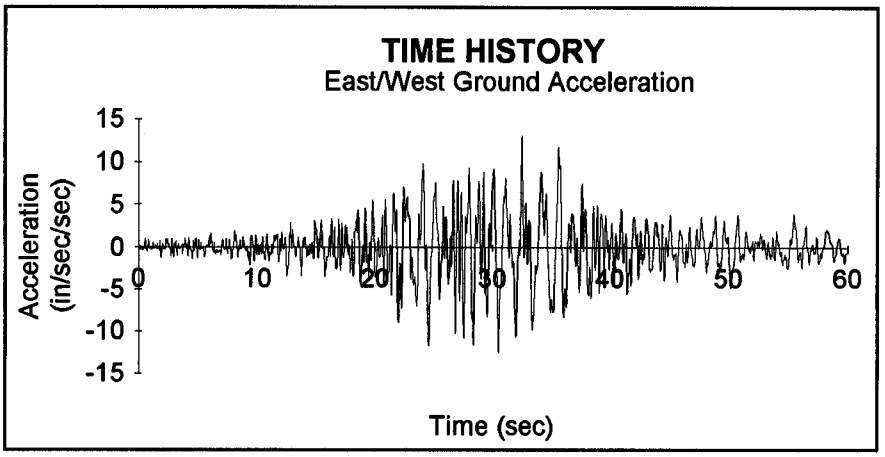

Figure B.3A. Landers Acceleration Time History

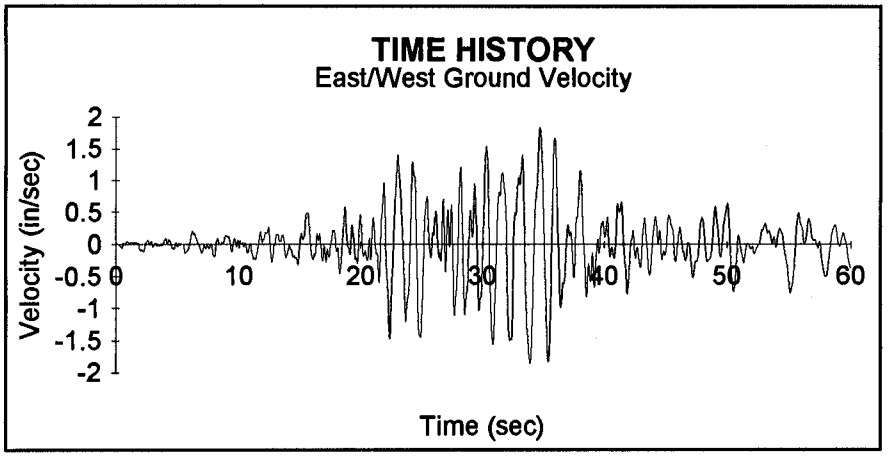

Figure B.3B. Landers Velocity Time History

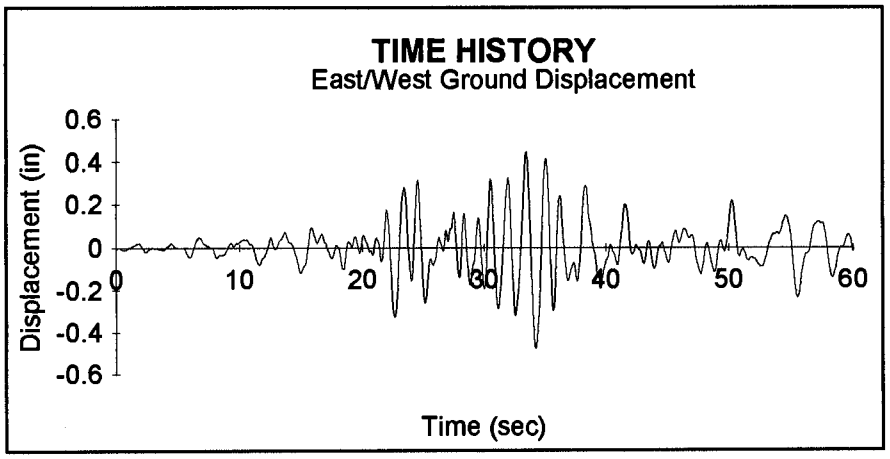

Figure B.3C. Landers Displacement Time History

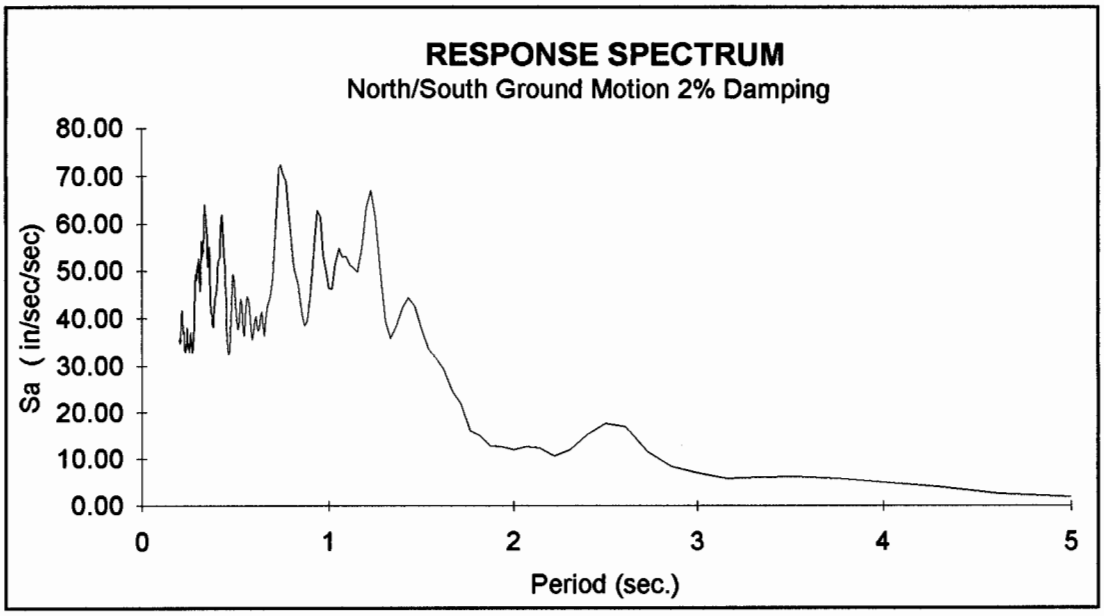

Figure B.4A. N/S Landers Response Spectrum

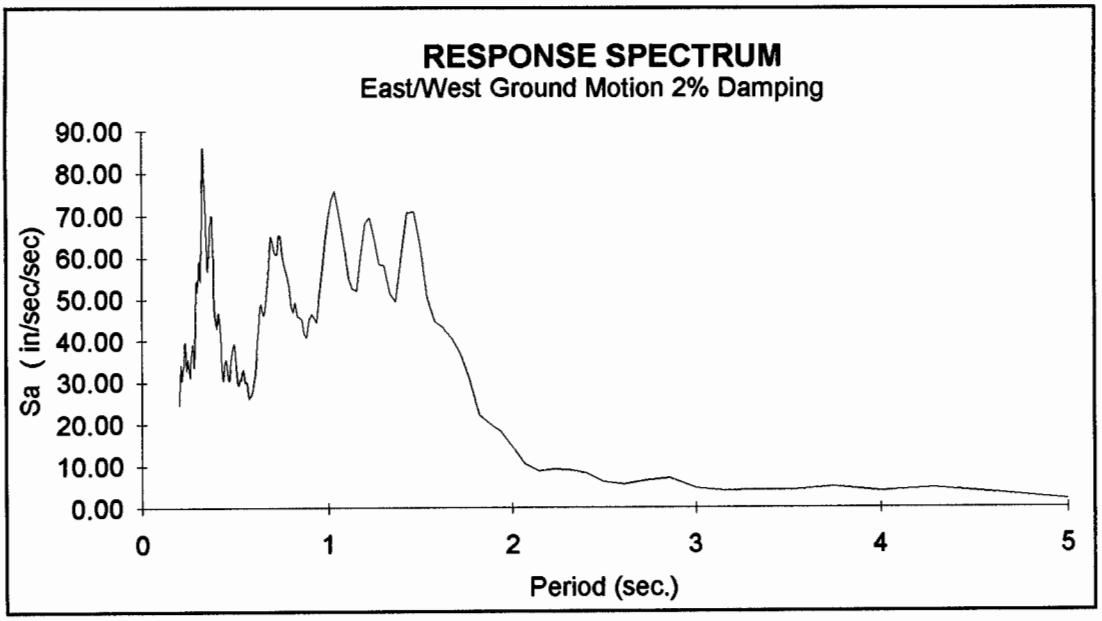

Figure B.4B. E/W Landers Response Spectrum

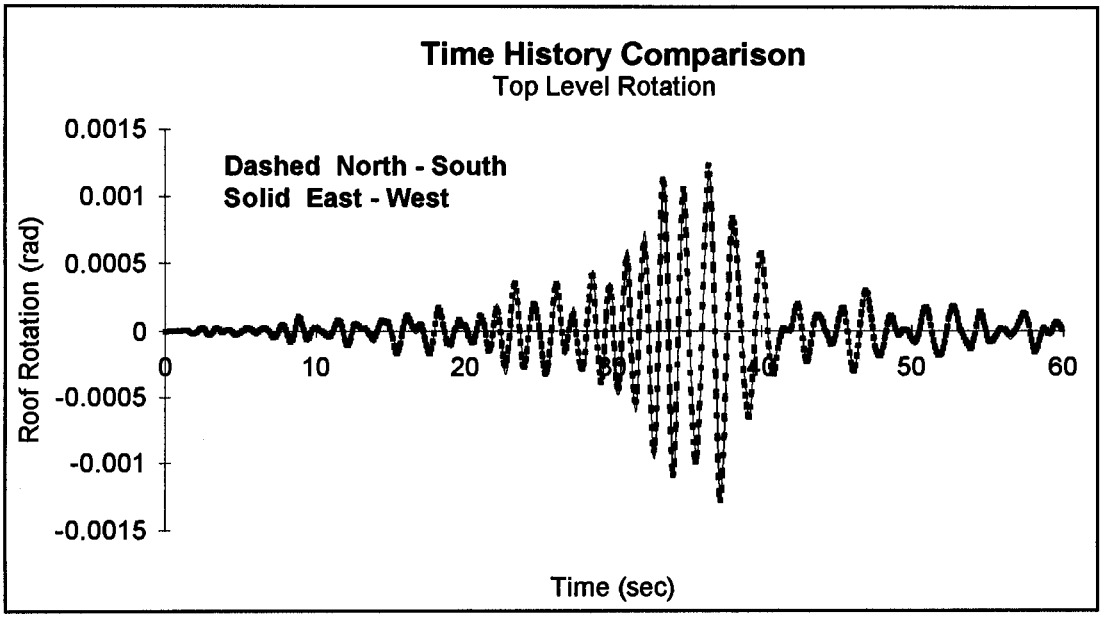

Figure B.5. Landers Rotational Response from two directions

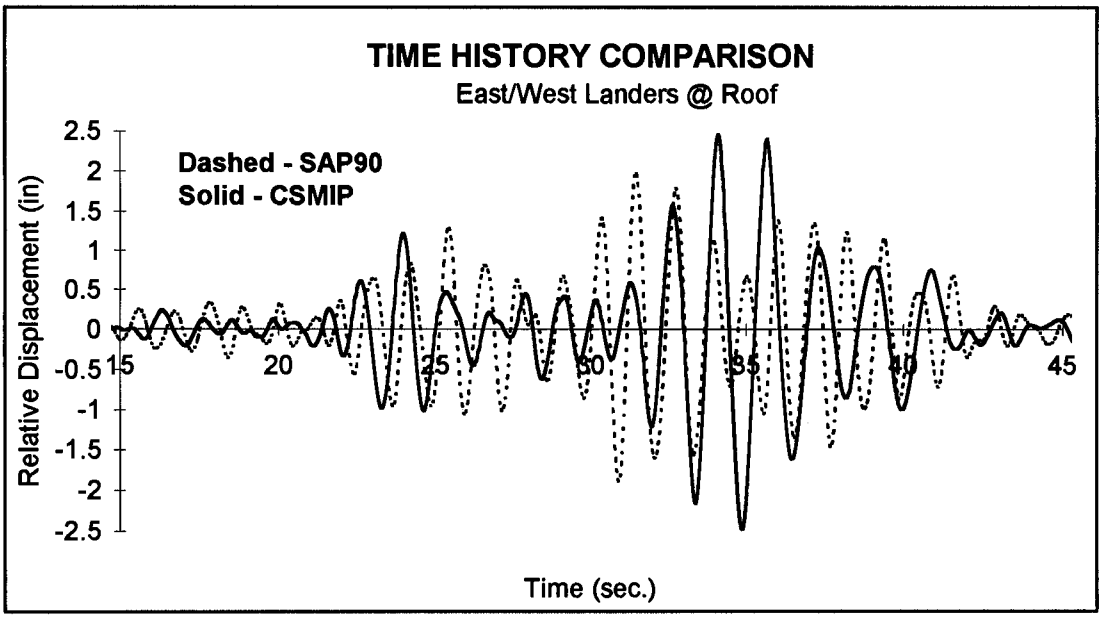

Figure B.6A. North Wall @ Roof Channel 5

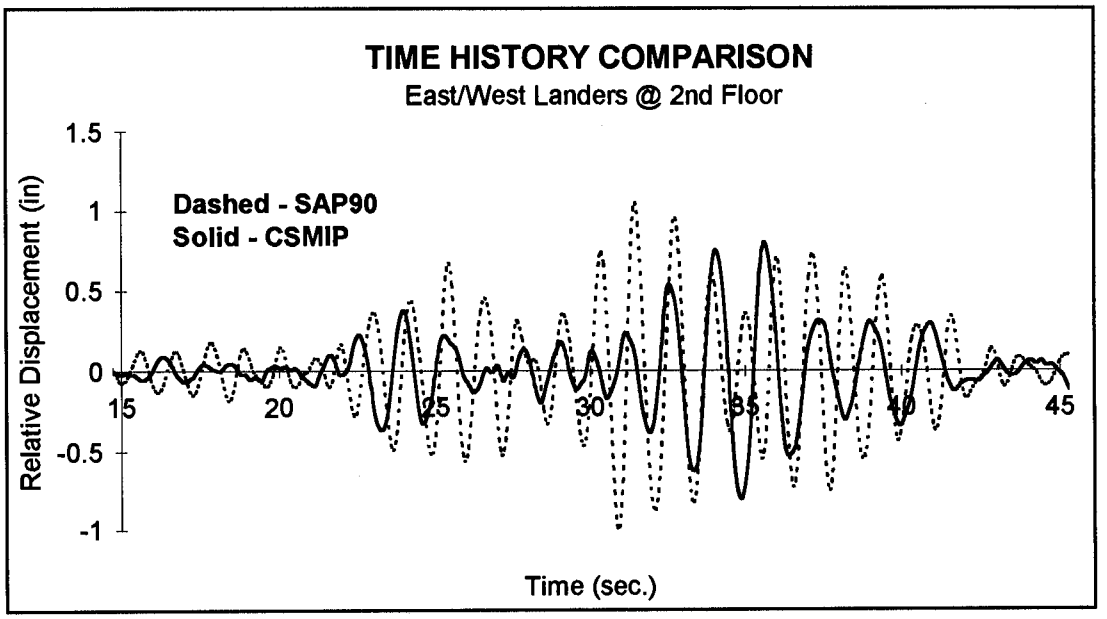

Figure B.6B. North Wall @ 2nd Floor Channel 11

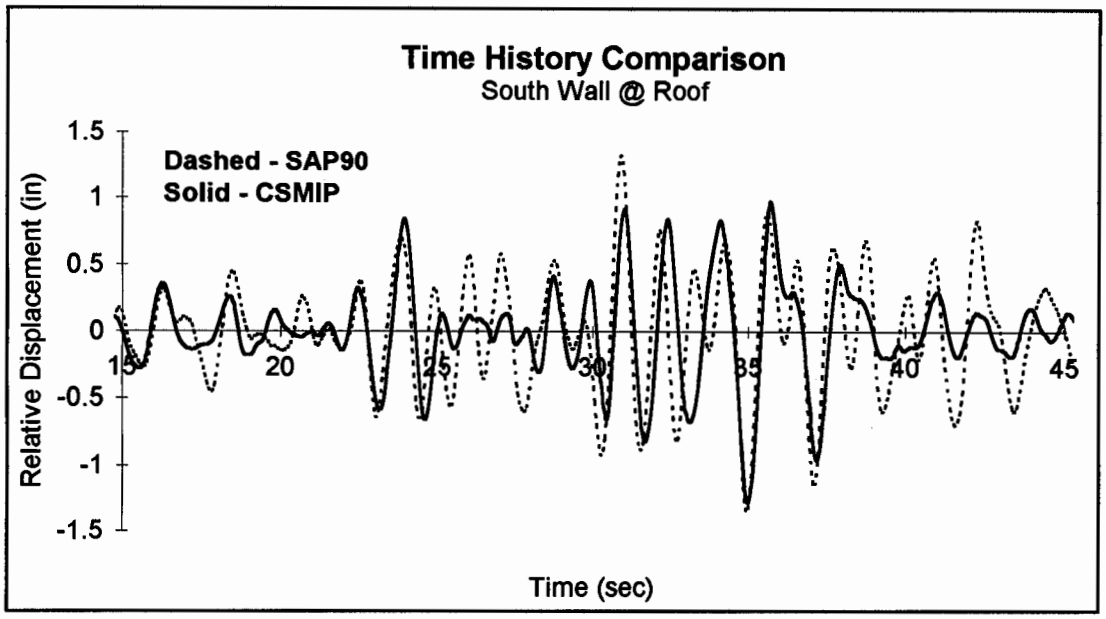

Figure B.7A. South Wall @ Roof Channel 8

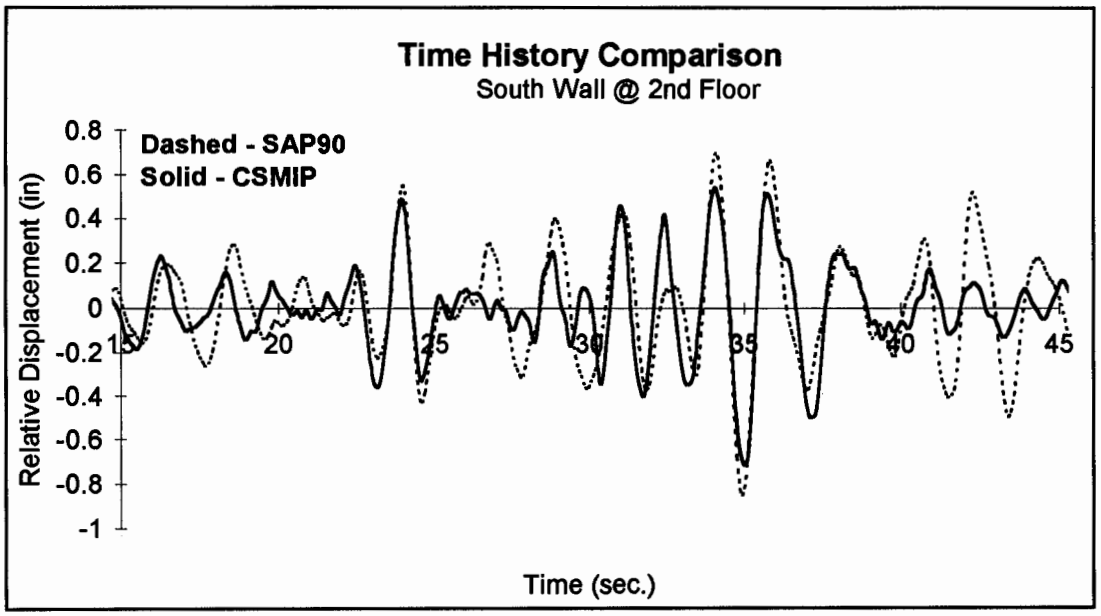

Figure B.7B. South Wall @ 2nd Floor Channel 12

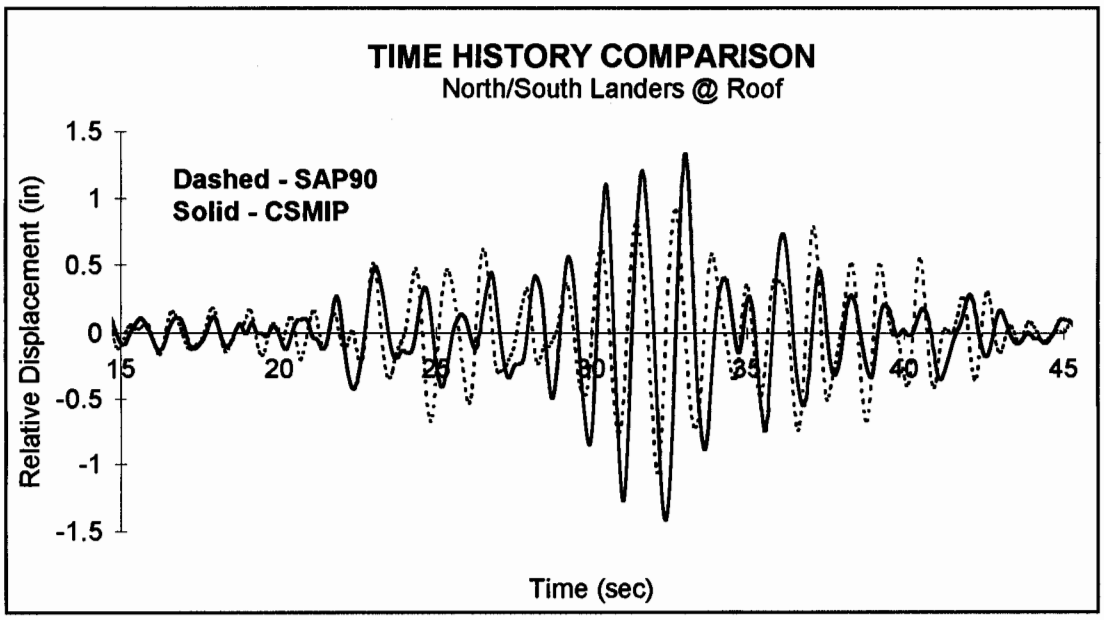

Figure B.8A. West Wall @ Roof Channel 3

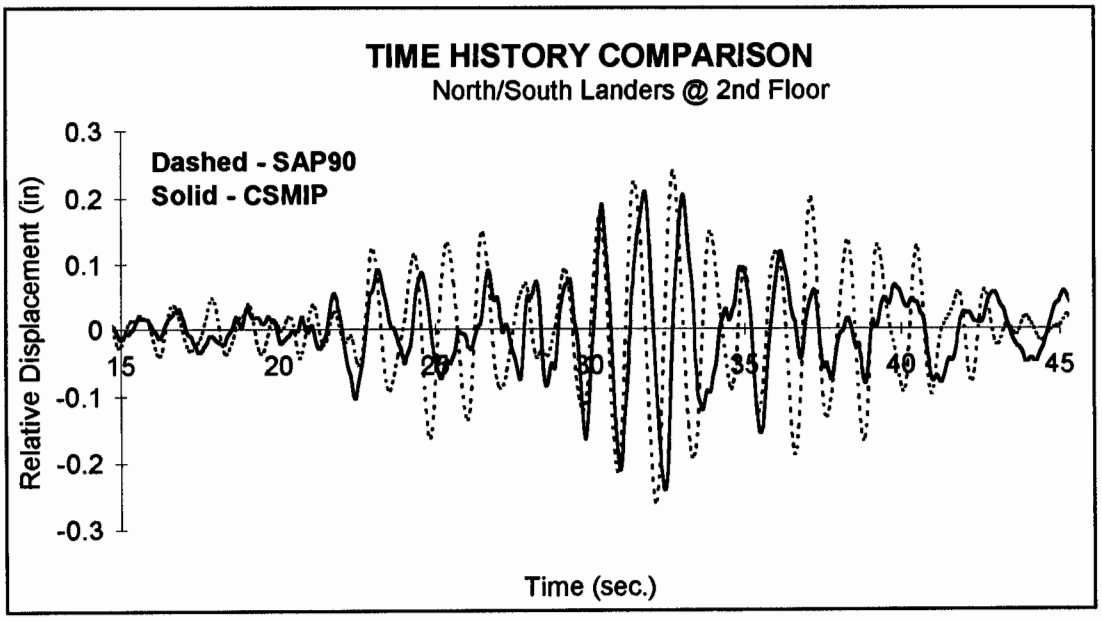

Figure B.8B. West Wall @ 2nd Floor Channel 1

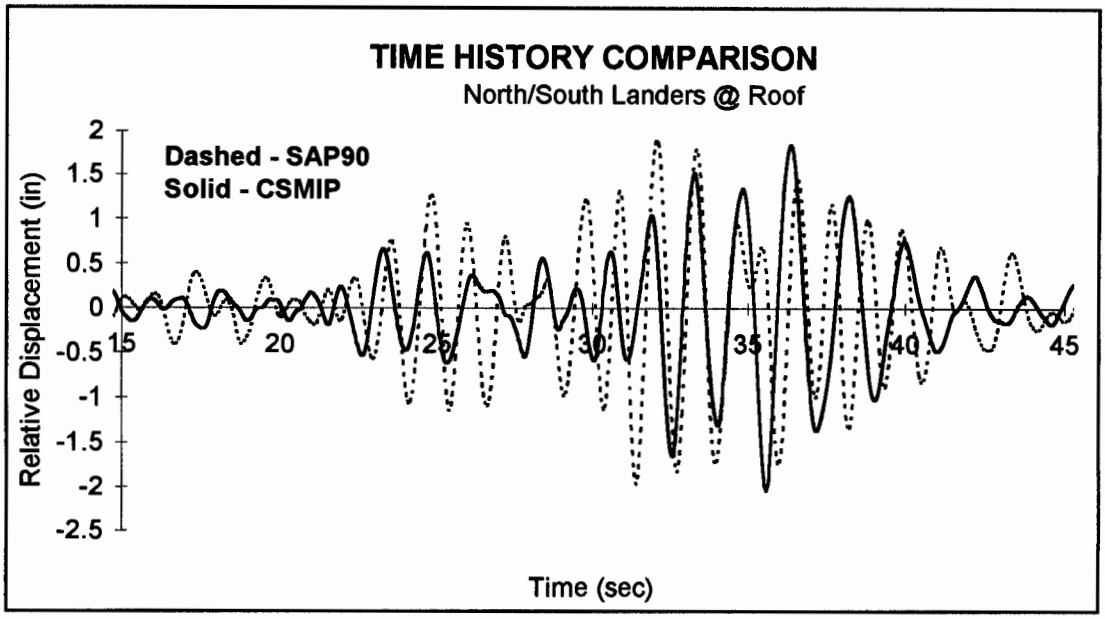

Figure B.9A. East Wall @ Roof Channel 4

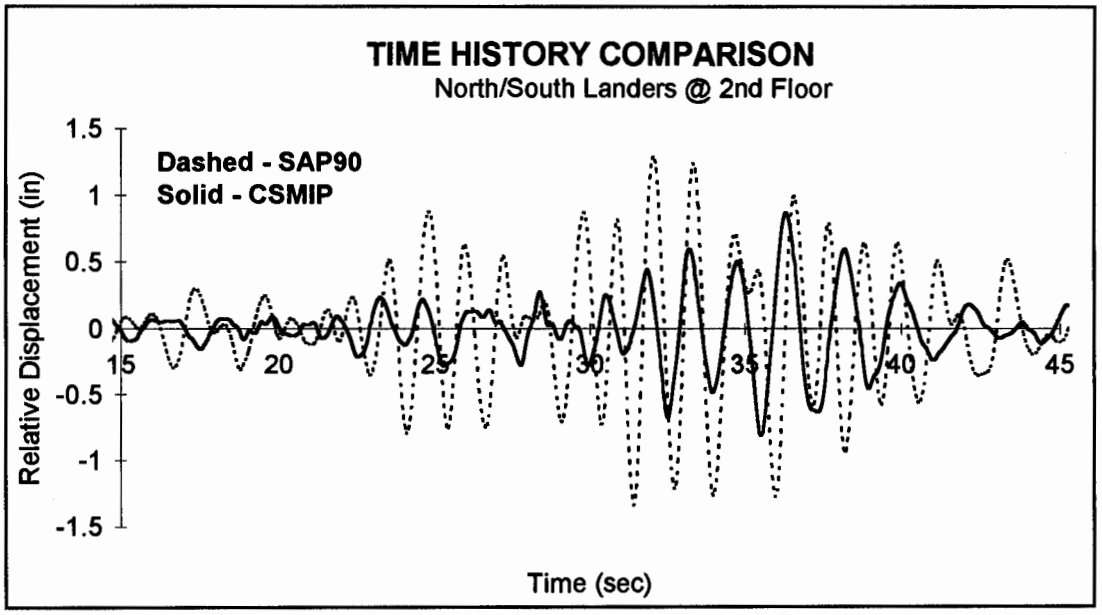

Figure B.9B. East Wall @ 2nd Floor Channel 2

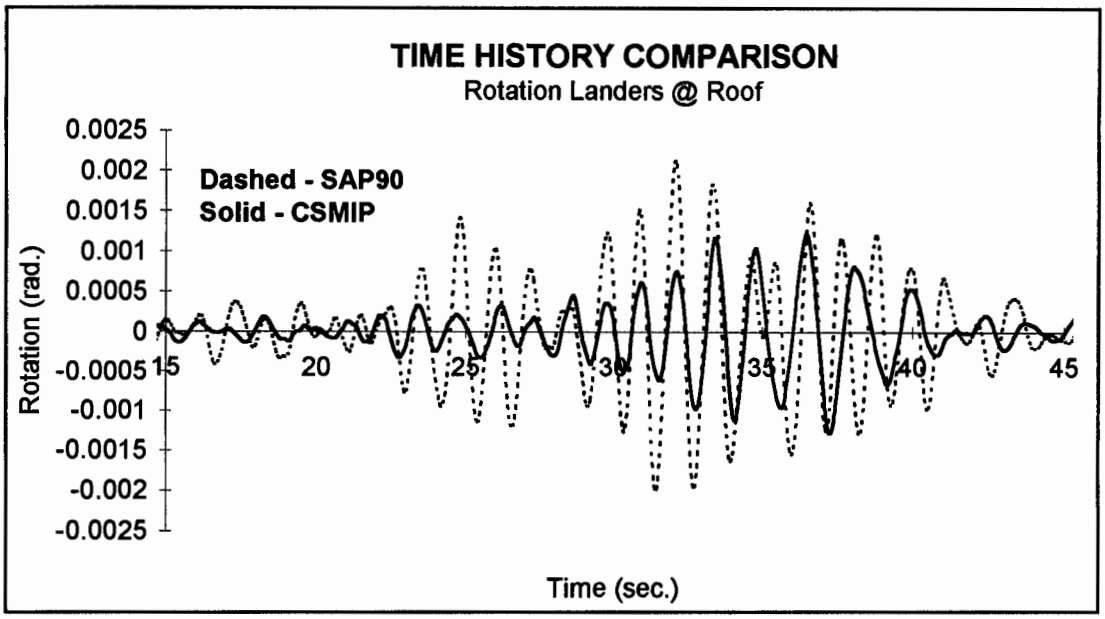

Figure B.10A. Rotation @ Roof

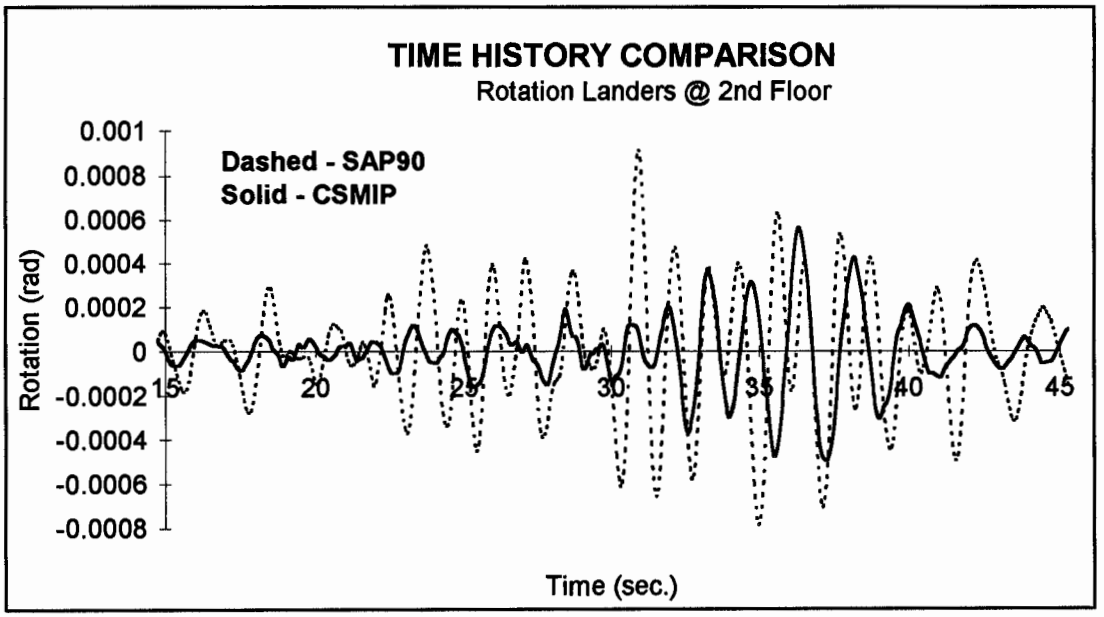

Figure B.10B. Rotation @ 2nd Floor

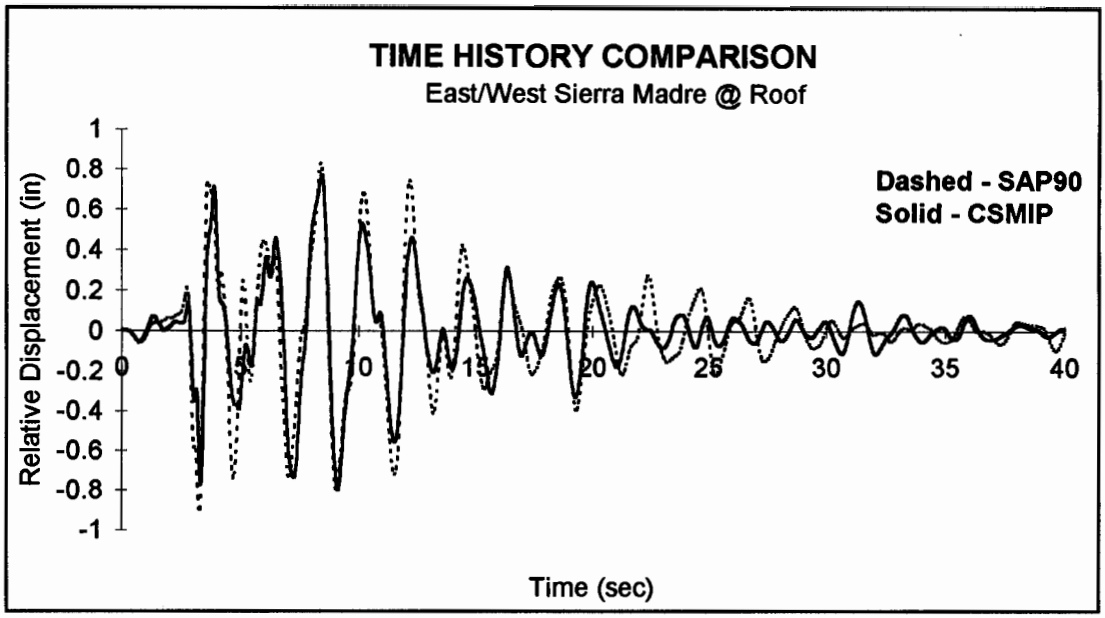

Figure B.11A. South Wall @ Roof Channel 8

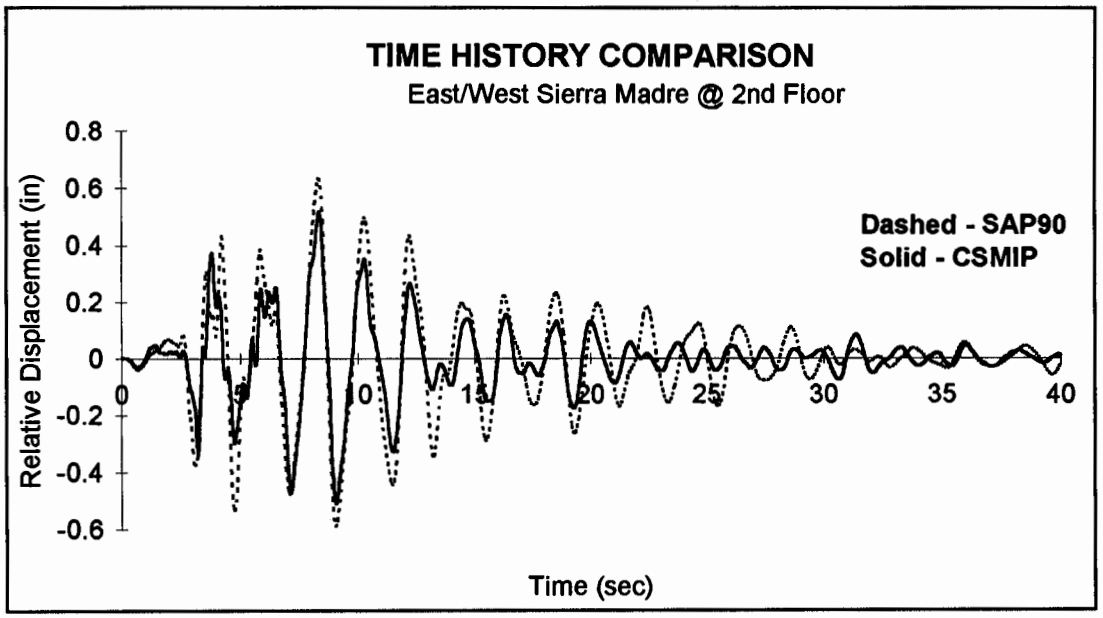

Figure B.11B. South Wall @ 2nd Floor Channel 12

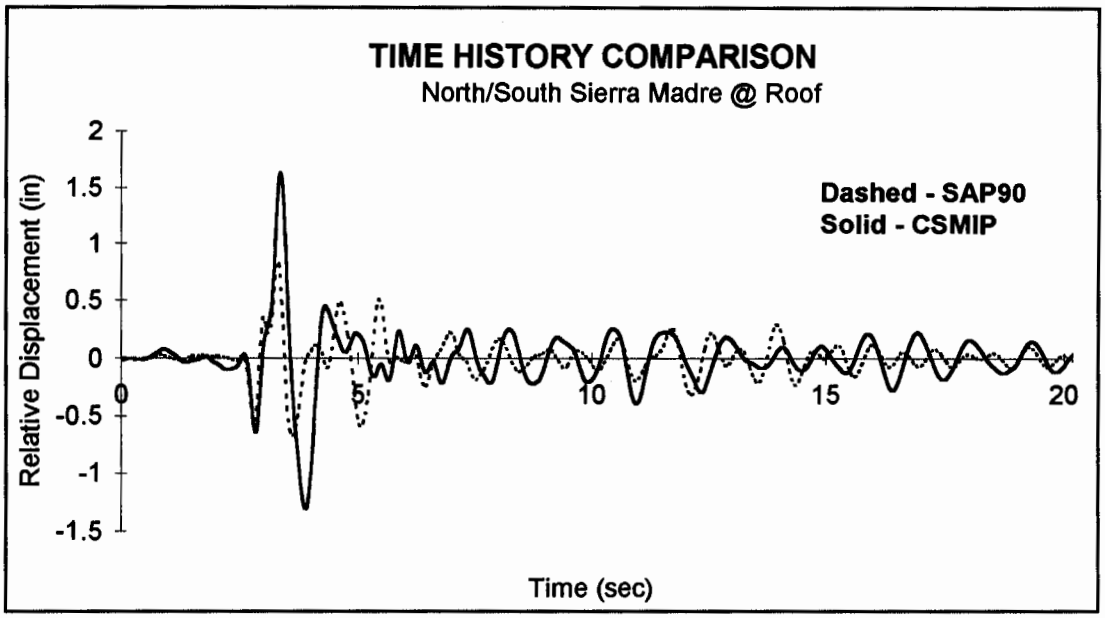

Figure B.12A. West Wall @ Roof Channel 3

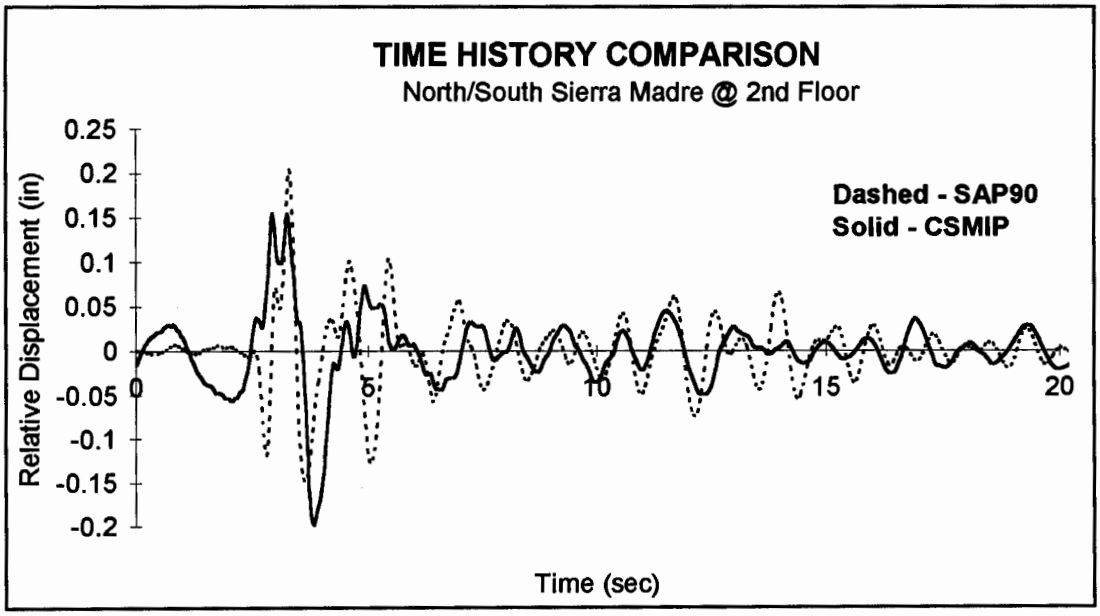

Figure B.12B. West Wall @ 2nd Floor Channel 1

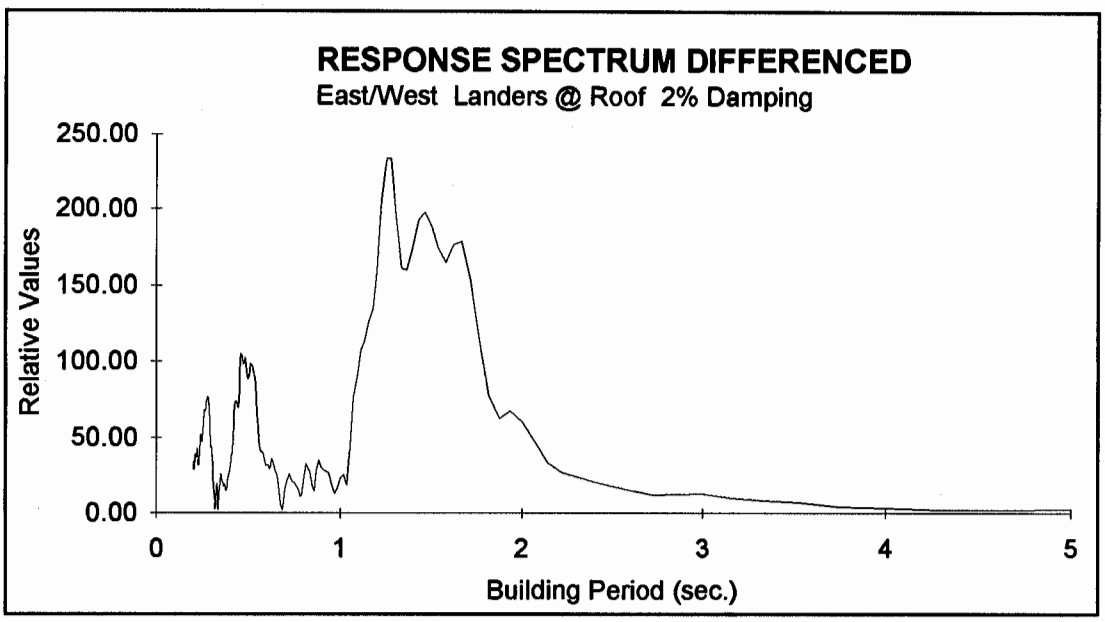

Figure B.13A. North Wall @ Roof Channel 5

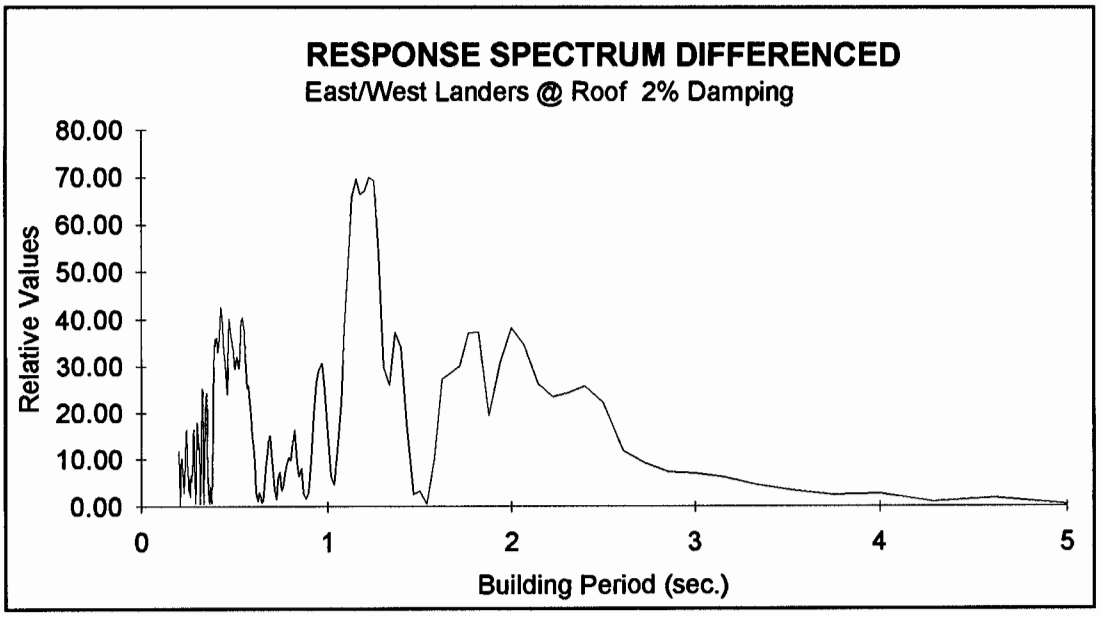

Figure B.13B. South Wall @ Roof Channel 8

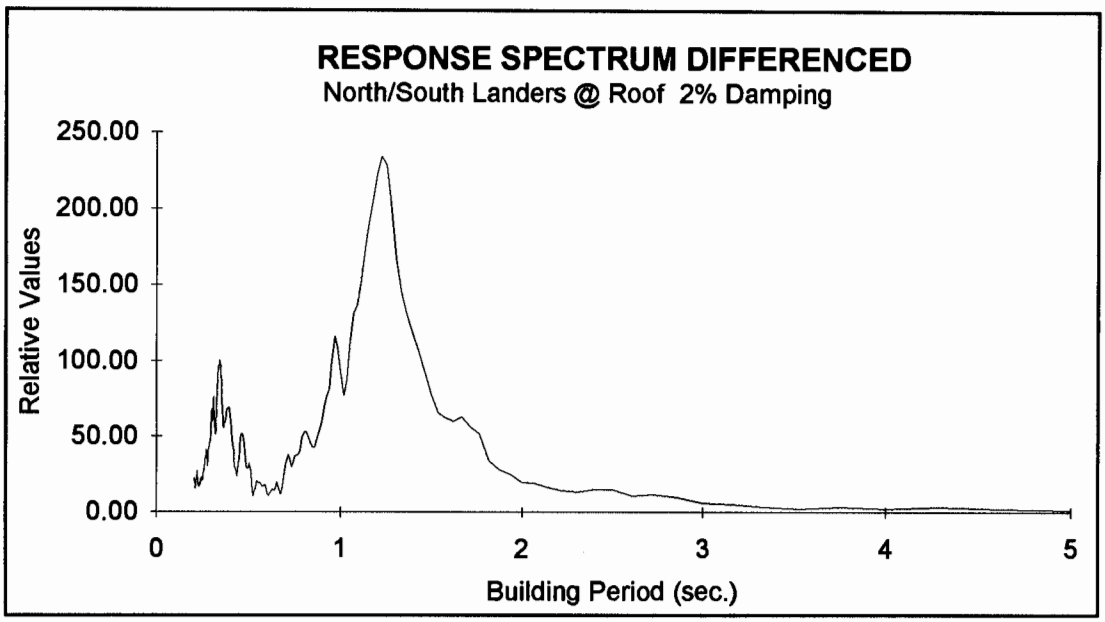

Figure B.14A. West Wall @ Roof Channel 3

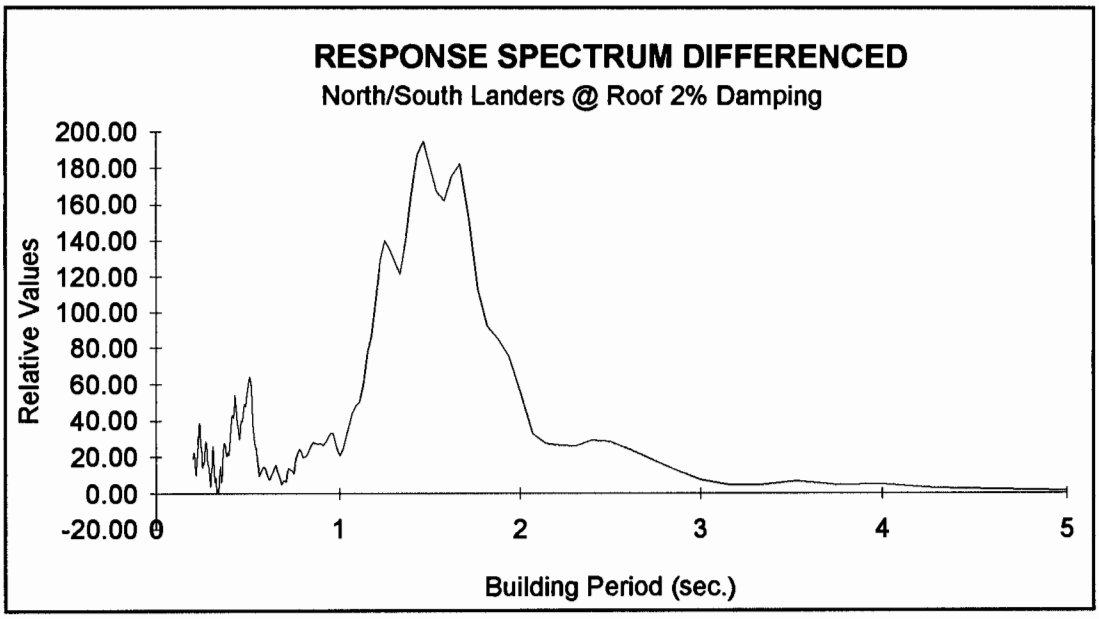

Figure B.14B. East Wall @ Roof Channel 4

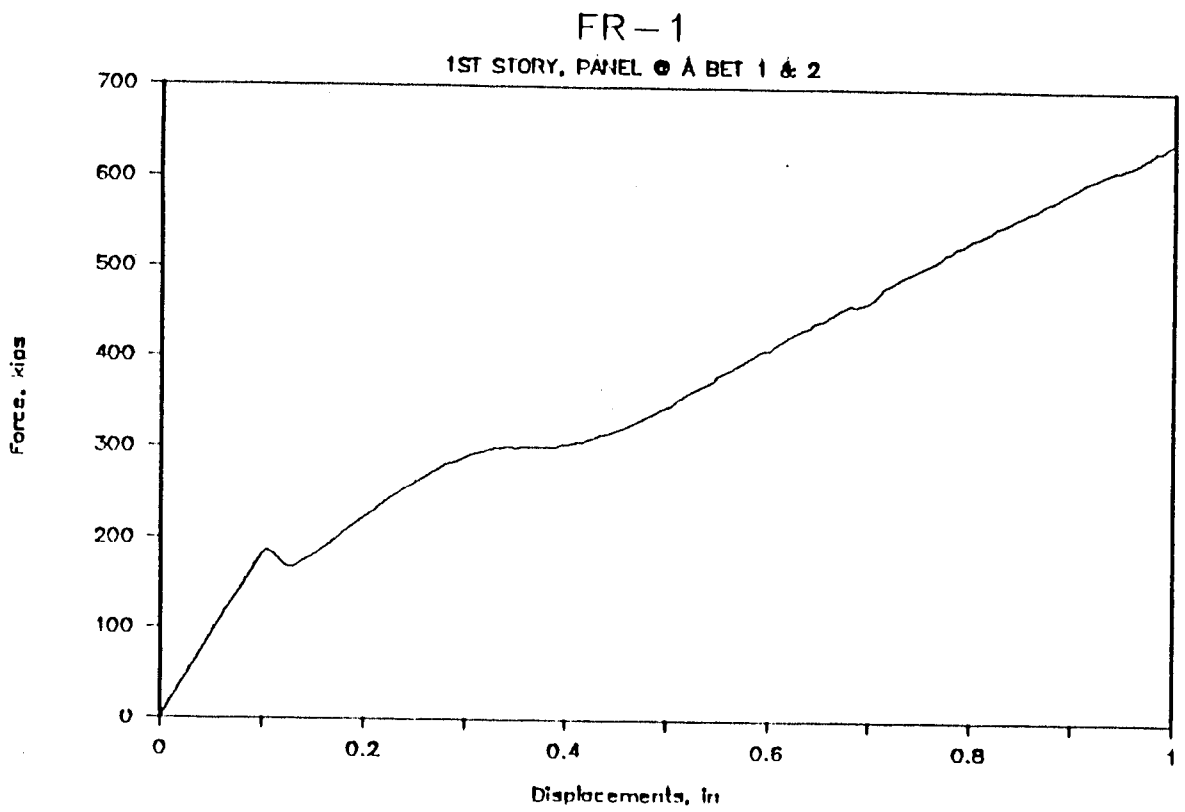

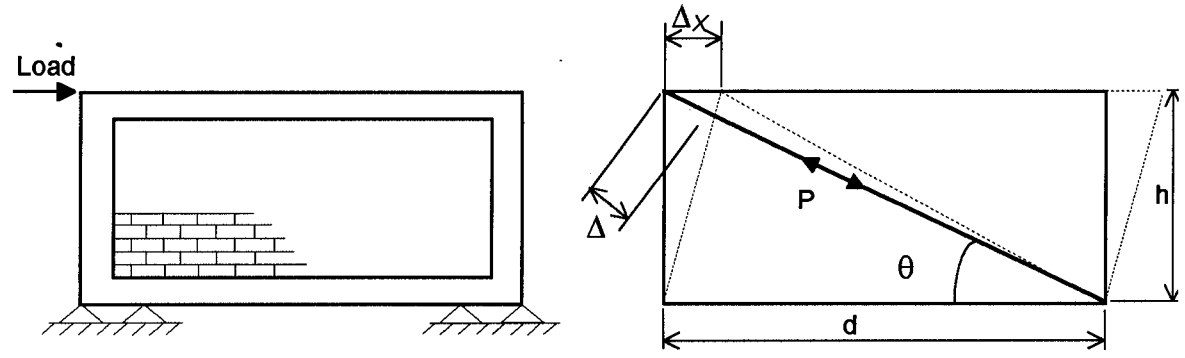

$$\tan\theta = \frac{h}{d} \qquad P = \frac{Load}{\cos\theta} \qquad \Delta x = \frac{\Delta}{\cos\theta}$$

$$\Delta = \frac{PL}{AE} \text{ or } A = \frac{PL}{\Delta E} \qquad A = \frac{Load \times DiagonalLength}{\Delta x \times \cos^2\theta E}$$

$$Area = \frac{1}{2}A \text{ assuming 1/2 area for each brace}$$

Figure B.15. Crossbrace Calculations

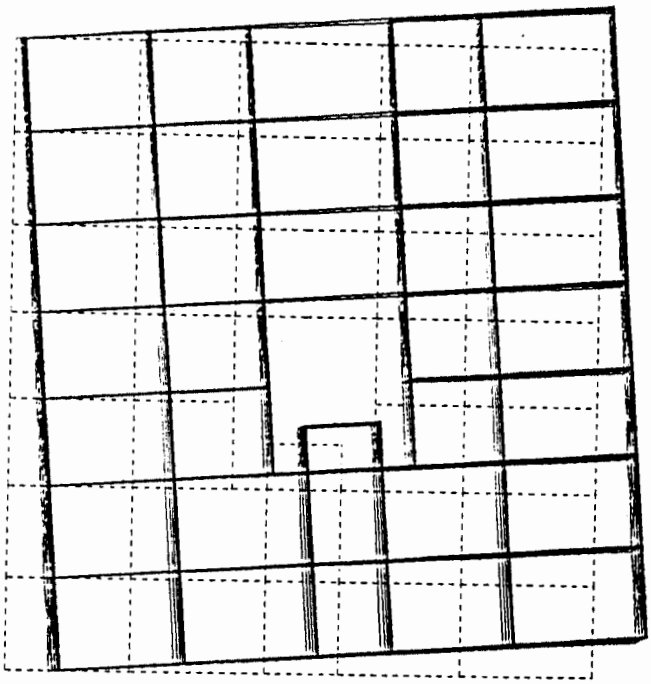

Figure B.16A. First Mode Shape

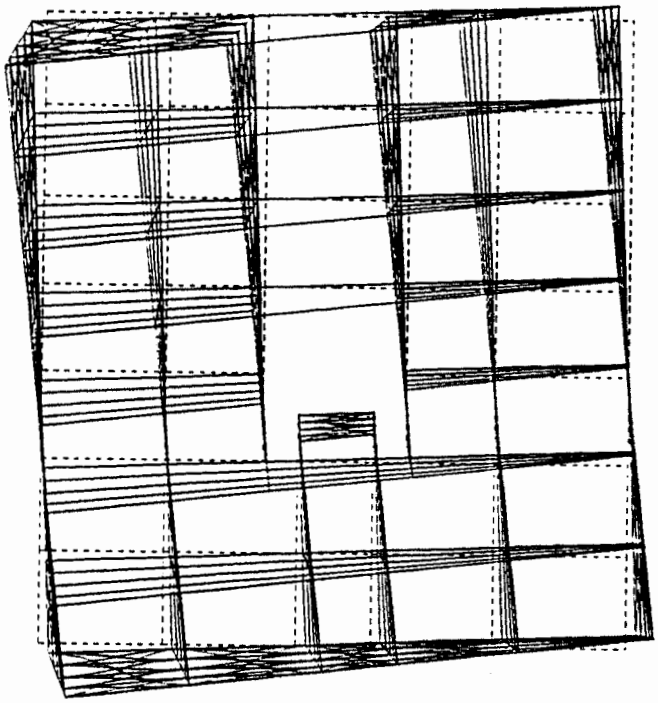

Figure B.16B. Third Mode Shape

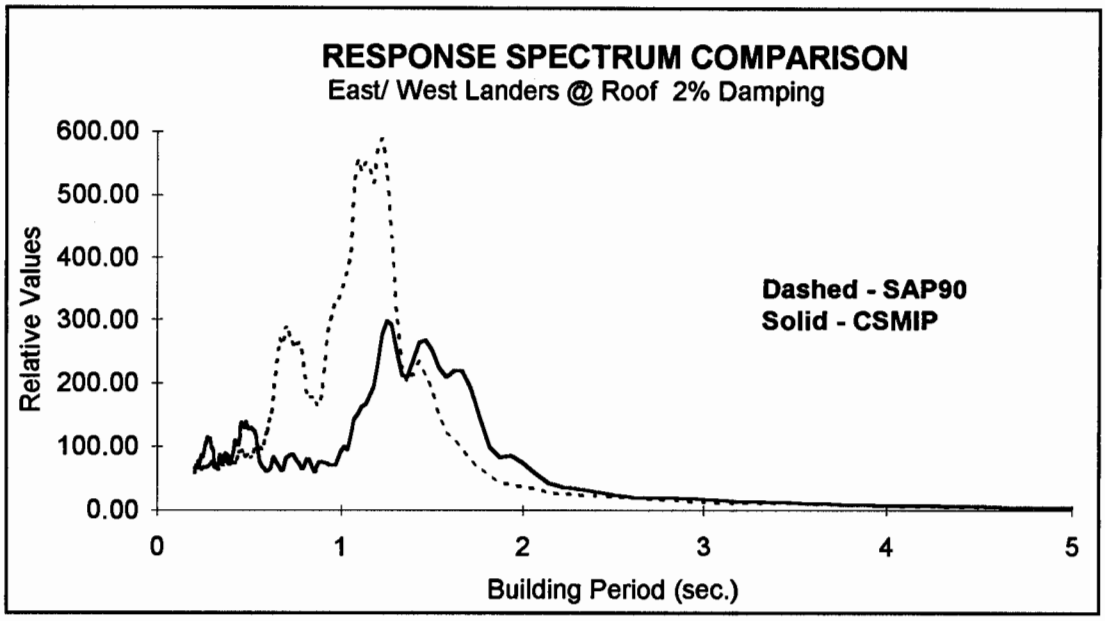

Figure B.17A. North Wall @ Roof Channel 5

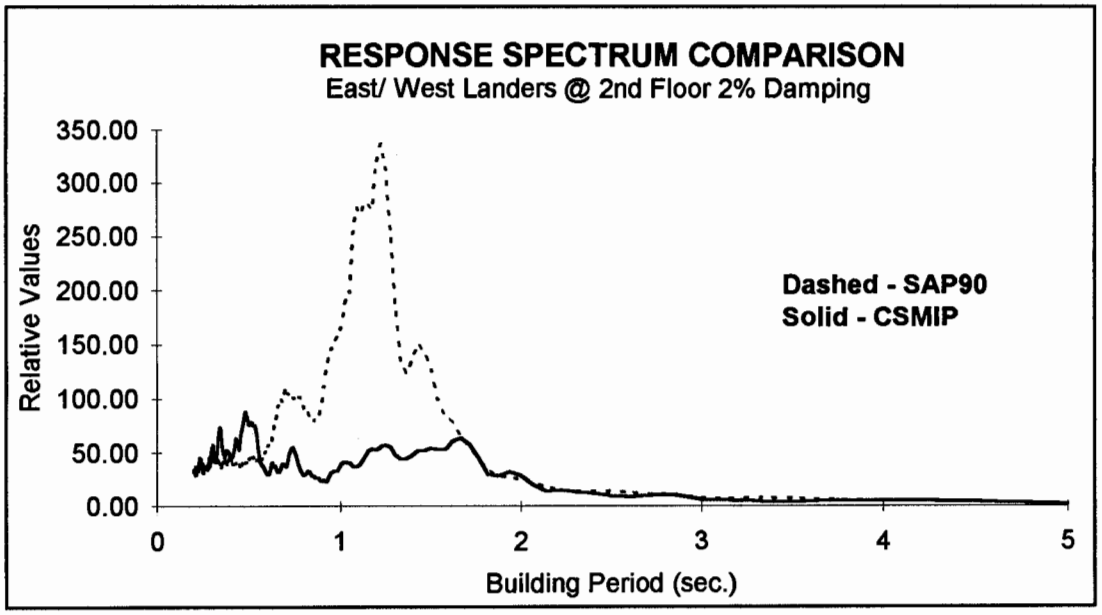

Figure B.17B. North Wall @ 2nd Floor Channel 11

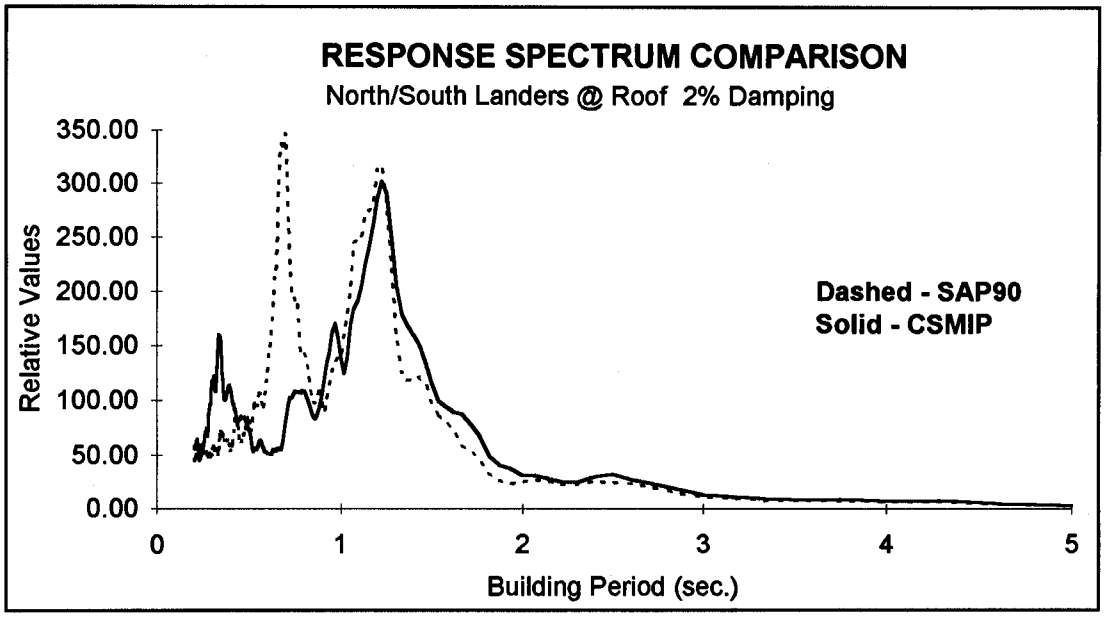

Figure B.18A. West Wall @ Roof Channel 3

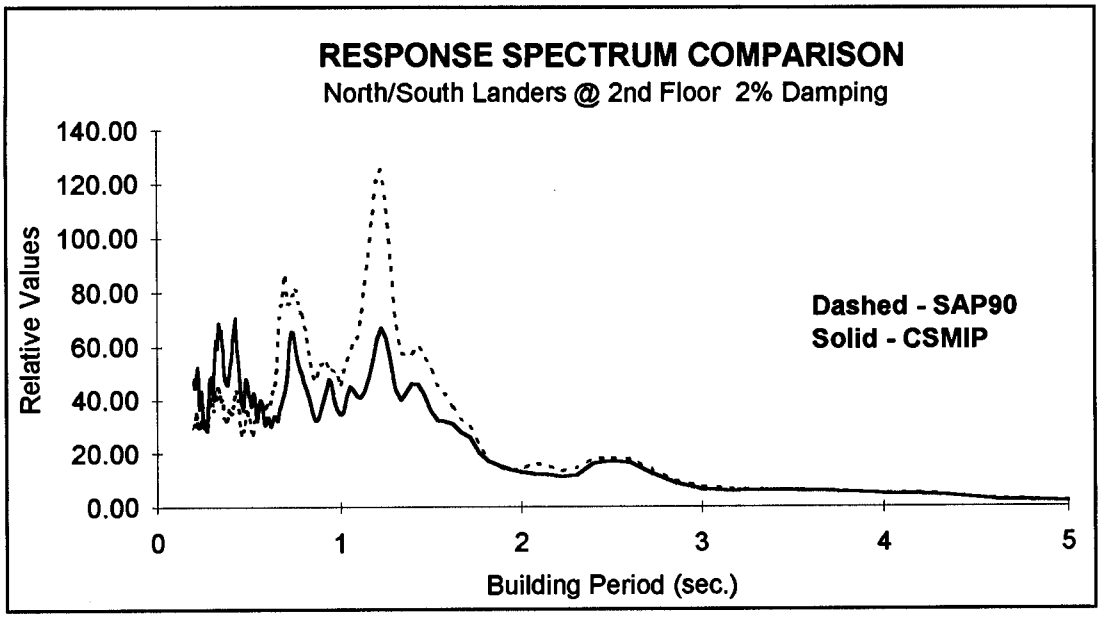

Figure B.18B. West Wall @ 2nd Floor Channel 1

APPENDIX C

SIMULATION OF THE RESPONSE OF CSMIP STATION NO. 24579 TO THE LANDERS EARTHQUAKE OF JUNE 28, 1992

SECTION C1

INTRODUCTION

C1.1 SCOPE OF THE ANALYSIS

The intent of the study is to simulate the response of an unreinforced masonry infill concrete frame building to the Landers Earthquake of June 28, 1992, and to verify the analytical modeling of the infill wall panels as diagonal brace elements using a three-dimensional SAP90 frame element model of the building. The building response records were obtained from CSMIP sensors located in the building at different levels. The analytical SAP90 model was subjected to the basement records obtained from the CSMIP data, then the SAP90 displacement response at the instrument locations were compared with the recorded values.

C1.2 DESCRIPTION OF THE BUILDING

The building is a nine story office building with one story basement level in Los Angeles. The lateral load resisting system consists of a reinforced concrete frame and exterior unreinforced masonry infill wall panels within the concrete frame. The building was instrumented by the California Strong Motion Instrumentation Program (CSMIP), and identified as station No. 24579.

C1.3 COMPUTER MODEL OF THE BUILDING

The three-dimensional SAP90 computer model of the building contained all the concrete frame beams and columns and the infill wall panels. The infill wall panels were modeled as diagonal braces, and their effective linear properties were established from the results obtained from the nonlinear analysis performed using program FEM/I. The concrete floor and roof diaphragms were modeled as rigid, and the floor mass locations and torsional properties were incorporated. The material properties were assumed since no material testing was performed on the building.

C1.4 CSMIP DATA

The building was instrumented with 18 sensors. As the building footprint is "L" shaped, the sensors are located so that both the transnational as well as the rotational motion of the building can be recorded. The sensors are located in the basement, 2nd floor, 5th floor and the roof. CSMIP data were available as time histories of displacement, velocity and acceleration at all instrument locations along with response and Fourier spectra data.

SECTION C2

DESCRIPTION OF THE BUILDING

C2.1 TYPE OF LATERAL FORCE RESISTING SYSTEM

The building is a nine story above ground and one basement level below ground office building in Los Angeles. It was designed in 1923 and constructed in 1924. The height of the building is 128 feet and the floor plan is a "L" shaped and consists of two wings, east wing and south wing. These two wings are similar in plan with a length of 155 feet and a width of 51 feet. However, the south wing has a stair on the north side and the building's main entrance on the south side, which caused the building to be more flexible in the east-west direction.

The lateral load resisting system consists of a reinforced concrete frame and exterior unreinforced masonry infill wall panels within the concrete frame. The vertical load carrying system consists of 4 and 5 inch thick concrete slabs supported by concrete beams and columns. The floor plans and elevations are shown in Figure C.1

C2.2 FOUNDATION SYSTEM AND BASEMENT FRAMING

The foundations are spread footings for the columns, and continuous footings for the walls. The basement walls are typically 12 inches thick reinforced concrete.

C2.3 IRREGULARITIES OF THE STRUCTURAL SYSTEM

The building footprint is "L" shaped in plan. This structural configuration lends itself to a predominantly torsional response. The vibrational modes of the building were therefore strongly coupled and the fundamental mode was torsional.

SECTION C3

RECORDED EARTHQUAKE RESPONSE

C3.1 EARTHQUAKE SOURCE

The response of the building was studied through the recorded motion of the Landers earthquake of June 28, 1992. The Landers Earthquake had a magnitude of Ms=7.5, and was the largest event to occur in California since 1952. The epicenter was located 43 km north of Palm Springs and 80 km east of San Bernardino. The building is located at more than 150 km from the epicenter.

C3.2 LOCATIONS OF INSTRUMENTS

The building is instrumented with 18 sensors, three sensors record the vertical component of the ground motion, and are located at the basement. The other 15 sensors are oriented to record the motion in two orthogonal horizontal directions. These 15 sensors are located as follows: 4 sensors in the basement, 2 in the second floor, 4 in the 5th floor, and 5 in the roof. Figure C.1 shows the location and the orientation of the sensors. These sensors are located so they will able to record the translational and rotational motion of the building.

C3.3 BASE MOTION CHARACTERISTICS

Figures C.2, C.3, and C.4 show the acceleration, velocity, and displacement time histories of the motion at sensors 5 and 6 in the basement. The maximum acceleration at the basement in the north-south direction was 0.031g (sensor 6) and in the east-west direction was 0.045g (sensor 5). Figure C.5 shows the 5% damped spectral acceleration and displacement of the motion

in Sensors 5 and 6. The motion of sensors 5 and 6 were characterized by a long period content with peaks at 0.7, 1.2, and 1.7 seconds, and almost constant spectral displacement between 1.0 to 1.5 seconds for sensor 6 (north/south motion).

Figure C.6 shows the two rotational motions at the base. Figure C.7 shows the 5% damped spectral acceleration and displacement of the two rotational motions at the basement, north-south and east-west, obtained by subtracting the two north-south and the two east-west motions at sensors 4-5 and 6-7. This horizontal rotational motion at the basement was neglected in the SAP90 model because of the program modeling limitations.

C3.4 BASEMENT RECORDS USED IN THE ANALYSIS

The records used as base motion in the SAP90 model were those from sensors 5 and 6. It must be noted that SAP90 can use input motions only in orthogonal directions and thus rotational inputs could not be used.

C3.5 RESPONSE OF THE TOP OF THE BUILDING

The maximum recorded accelerations at the roof were 0.101g at sensor 16 and 0.173g at sensor 14 in the east-west direction, and 0.089g at sensor 17 and 0.141g at sensor 18 in the north-west direction. This large difference in the two building ends in each direction indicated a significant torsional response of the building. Table C.1 shows the maximum displacement and acceleration values of all sensors. The displacement at the corners were in the order of 100% higher than at the center, also indicating considerable torsional response. Figure C.8 shows the torsional motion at the roof obtained by subtracting Sensor 16 from Sensor 14 and subtracting Sensor 18 from Sensor 17.

C3.6 RESPONSE OF INTERMEDIATE FLOOR LEVELS

The maximum absolute acceleration values and the maximum relative displacement values with respect to the ground of the second floor, 5th floor, and roof were obtained, and are shown in Table C.1. The displacement at the corners were in the order of 100% higher than at the center, thus also

indicating considerable torsional response.

The maximum story drifts were also calculated from the building response. The drifts were calculated from the displacement time histories of the sensors at the basement, second floor, 5th floor, and the roof. Then, these drifts were converted to story drifts assuming a straight line deflected shape between the first floor, second floor, fifth floor and roof. These story drifts were used to establish the infill wall panel effective stiffness from the nonlinear FEM/I analysis, see Table C.2.

SECTION C4

COMPUTER MODEL

C4.1 LINEAR ELASTIC THREE-DIMENSIONAL MODEL

A three-dimensional frame element model of the building was developed using the program SAP90. The model contained all the concrete frame beams and columns and the infill wall panels. The concrete floor and roof were modeled as rigid diaphragm, and the floor mass locations and torsional properties were incorporated. The material properties were assumed since no material testing was performed on the building.

The concrete frame effective stiffness was based on using 85% of the gross section properties to reflect the cracked member stiffness at the level of deformations the building has been subjected to. The concrete frame joints were considered rigid, and the columns were fixed at the base.

C4.2 MODELING OF URM INFILLS

The infill wall panels were modeled as diagonal braces. The nonlinear force-deflection relationship of each panel was established from a nonlinear analysis performed using the program FEM/I. The effective secant stiffness of each panel was calculated based on the drift calculated from the building response using the CSMIP data. Then the effective infill wall panels stiffness were reduced to 70% to account for the stiffness degradation during the cyclic loading.

C4.3 COMPLETE BUILDING MODEL

A linear time history analysis was performed using the CSMIP sensors 5 and 6 as input motions at the ground. Only the first 6 modes were used in the analysis. These modes had more than 90% of the building mass participating in the response. Because of the small level of deformation response of the building a critical damping level of 2% was used for the first three modes, and 5% for modes 4, 5, and 6.

The first and third modes of vibration are rotational, and the second mode is translation in the diagonal direction. These three mode shapes are shown plotted in Figure C.9. The corresponding three periods are 1.00, 0.94, and 0.73 seconds.

C4.4 RESULTS OF THE COMPUTER ANALYSIS

The SAP90 maximum displacement results are shown in Table C.3. Time history results are shown in Figures C.10 through C.14 superimposed on the recorded motions from CSMIP data. These displacement-time histories of the response are shown through a 15 to 45 seconds window.

SECTION C5

COMPARISON OF ANALYTICAL RESULTS WITH CSMIP DATA

C5.1 GENERAL

The goal of the analysis was to predict the maximum displacement response of the building. This was to be accomplished by using a combination of linear frame analysis with a nonlinear finite element analysis of the masonry infills in as consistent a manner as possible, and seeking to avoid an empirical "number matching" approach.

C5.2 COMPARISON OF AMPLITUDE OF DISPLACEMENT DATA

These results are shown in Table C.3. The maximum displacement showed a very good agreement with the recorded motions. The displacement time histories of the response are shown through a 15 to 45 seconds window.

North-south motion showed good agreement in the displacement response time history. Sensors 12 and 17 at the 5th floor and the roof are shown in Figure C.13. These motions differed in phase, however, the response maxima occurred at the same time, and were of almost the same magnitude. The corner motion in the north-south direction is shown in sensors 13 and 18, and plotted in Figure C.14. These two motions were of similar magnitude and general shape, however, the building model exhibited a shorter period response.

East-west motion did not show a good agreement in the time history response. Figure C.12 shows the displacement response time history of sensors 11 and 16. The building had a shorter period and the response maxima occurred at different times. The poor matching of the response in this direction could be attributed to the stair well and the building entrance located in the north and south walls of the south wing. Also, the torsional input motion at the base was considerably more significant in the east-west than the north-south direction. Figures C.10 and C.11 show the time history of displacement for sensors 8, 9, 10 and 14.

SECTION C6

CONCLUSIONS

C6.1 MODELING

This research validated the method of modeling masonry infill walls as diagonal struts using a nonlinear finite element program to predict the stiffness at observed levels of displacement. Various adjustments were made to the computer model to account for the actual building condition. The masonry infill stiffness were uniformly adjusted to account for stiffness degradation, and the concrete moment of inertia were adjusted to account for cracking of the sections.

C6.2 FIT OF COMPUTER DATA TO RECORDED DATA

The results were very good in matching the peak displacement values. The time histories of the displacement were not replicated with the same level of

accuracy due to several factors including modeling assumptions, neglecting the input torsional motion, fixing the building at the first floor level thus neglecting the flexibility of the basement effect on the period, and the modeling of the hysteretic damping as viscous damping.

C6.3 DETERMINATION OF DAMPING

The hysteretic damping behavior of the building was approximated as viscous damping. The percent of critical damping considered was 2% in the first 3 modes, and 5% in the modes 4, 5, and 6. The damping value used was based on the level of displacement. Damping values may be varied for each mode also if enough information is available.

C6.4 INSTRUMENT LOCATIONS

The 15 horizontal motion sensors in the building are located as follows: 4 sensors in the basement, 2 in the second floor, 4 in the 5th floor, and 5 in the roof. These sensors are located so they will able to record the translational and rotational motion of the building. Additional sensors could have been located at the first floor level to show the effect of the basement on the response.

TABLE C.1 - CSMIP MAXIMUM ACCELERATION AND DISPLACEMENT RESPONSES

Sensor	Location	Direction	Absolute Acceleration (g)	Displacement Relative to the Ground (in)
5	Ground	West	0.0448	-
6	Ground	North	0.0306	-
8	2nd Floor	North	0.0459	0.181
9	2nd Floor	West	0.0541	0.157
10	5th Floor	West	0.1087	1.151
11	5th Floor	West	0.0663	0.601
12	5th Floor	North	0.0682	0.551
13	5th Floor	North	0.0852	0.913
14	Roof	West	0.1726	2.215
16	Roof	West	0.1008	0.961
17	Roof	North	0.0894	0.872
18	Roof	North	0.1414	1.535

TABLE C.2 - DRIFT CALCULATIONS BASED ON ACTUAL RECORDS

Floor	Total Drift (in)		Story Drift (in)		Drift Used (in)
	X-dir	Y-dir	X-dir	Y-dir	
5th to Roof	0.406	0.327	0.081	0.065	0.08
2nd to 5th	0.447	0.370	0.149	0.123	0.13
Gr. to 2nd	0.157	0.181	0.157	0.181	0.16

TABLE C.3 - MAXIMUM DISPLACEMENT RELATIVE TO THE GROUND

Sensor	Location	Direction	CSMIP Maximum Displacement (in)	SAP90 Maximum Displacement (in)
5	Ground	West	0.000	0.000
6	Ground	North	0.000	0.000
8	2nd Floor	North	0.181	0.159
9	2nd Floor	West	0.157	0.167
10	5th Floor	West	1.151	1.125
11	5th Floor	West	0.601	0.541
12	5th Floor	North	0.551	0.494
13	5th Floor	North	0.913	0.943
14	Roof	West	2.215	2.059
16	Roof	West	0.961	1.006
17	Roof	North	0.872	0.877
18	Roof	North	1.535	1.765

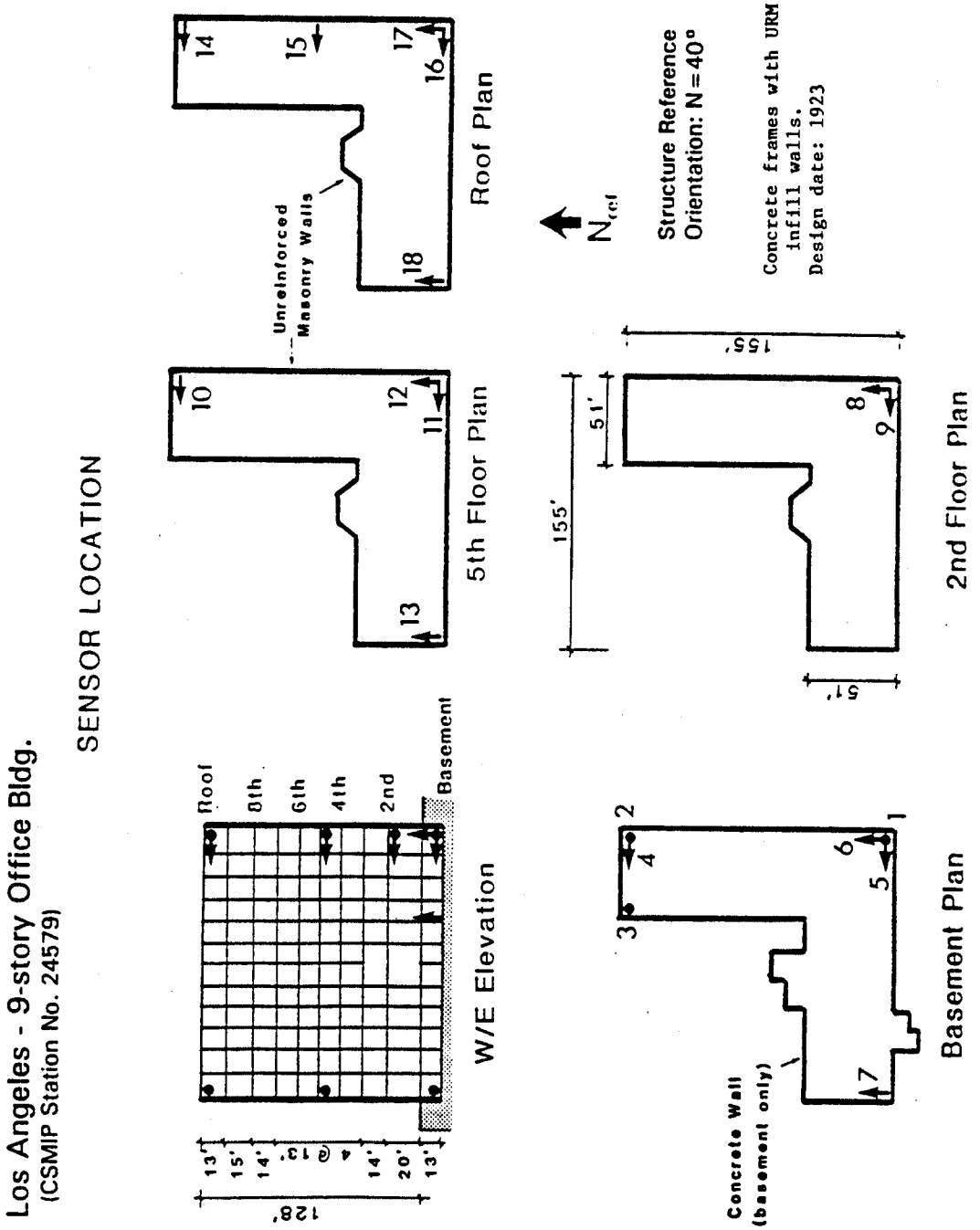

FIGURE C.1 - BUILDING PLANS AND ELEVATIONS, AND SENSOR LOCATIONS

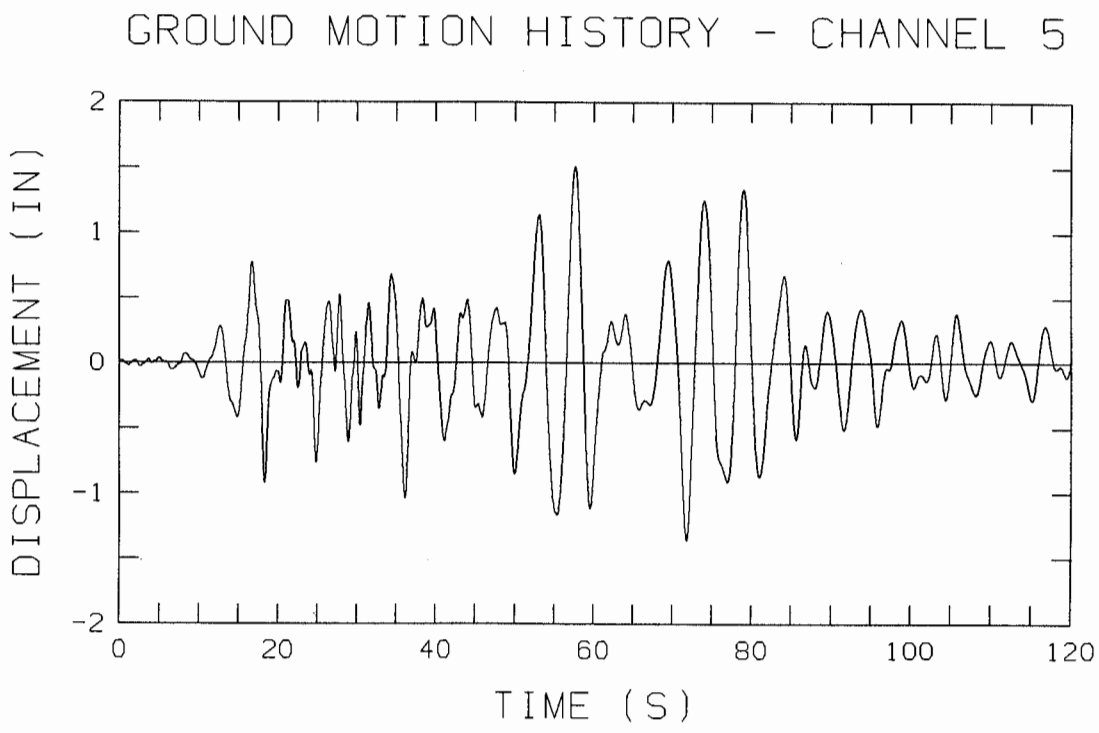

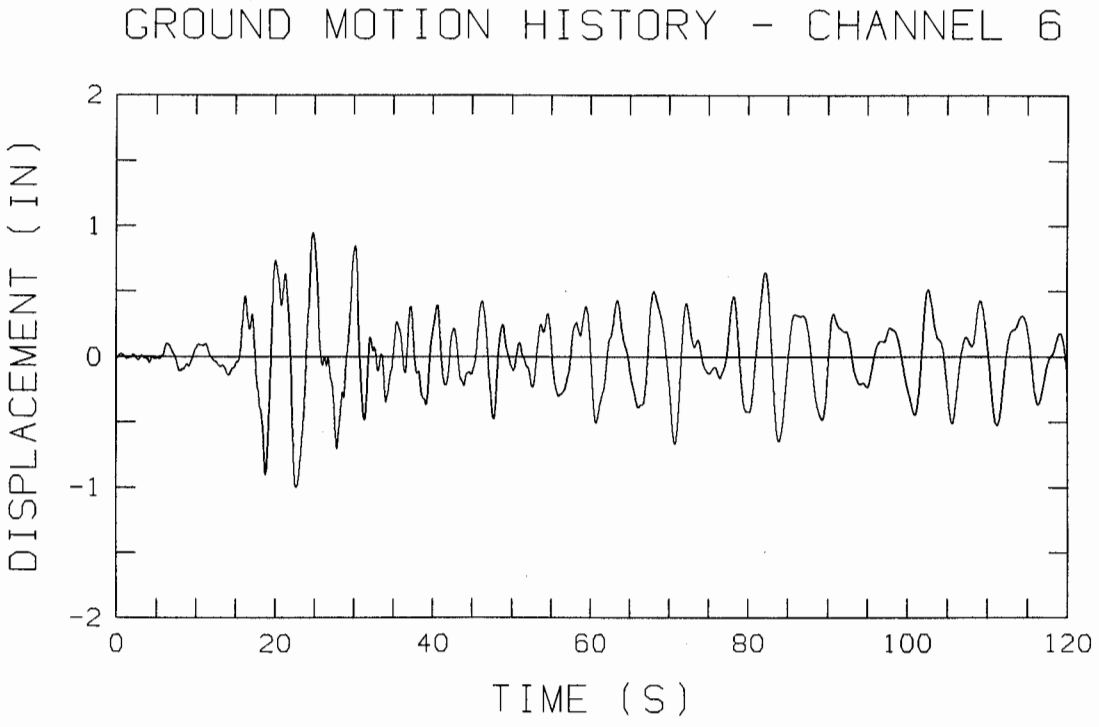

FIGURE C.2 - DISPLACEMENT TIME HISTORY OF BASEMENT MOTIONS

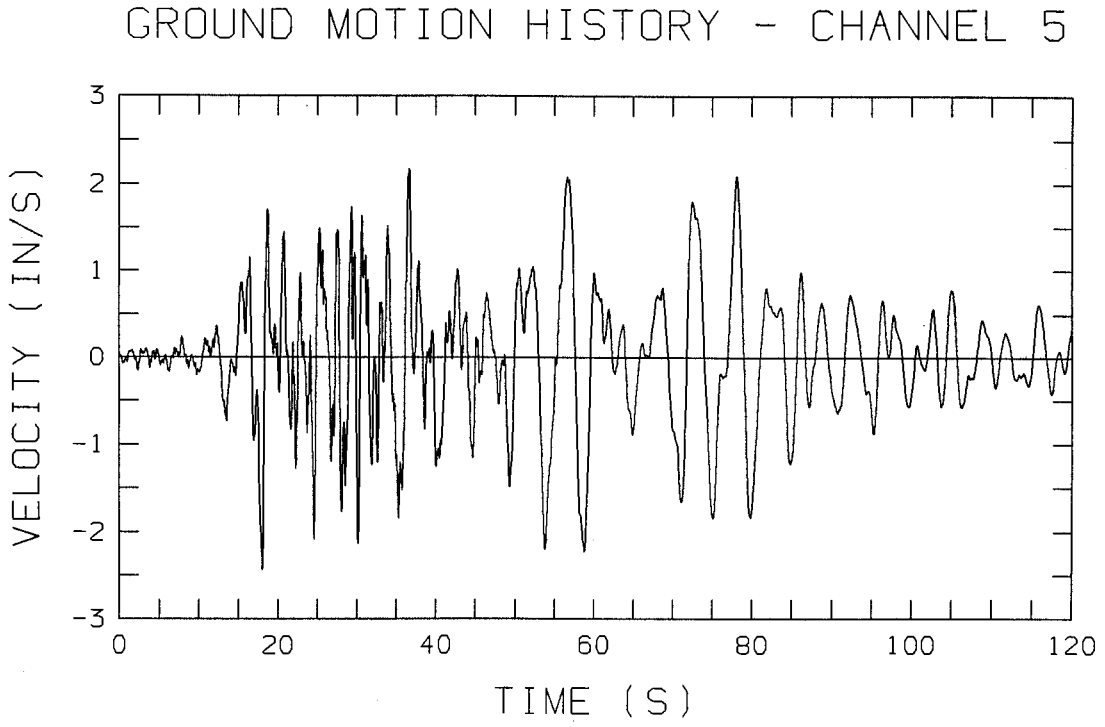

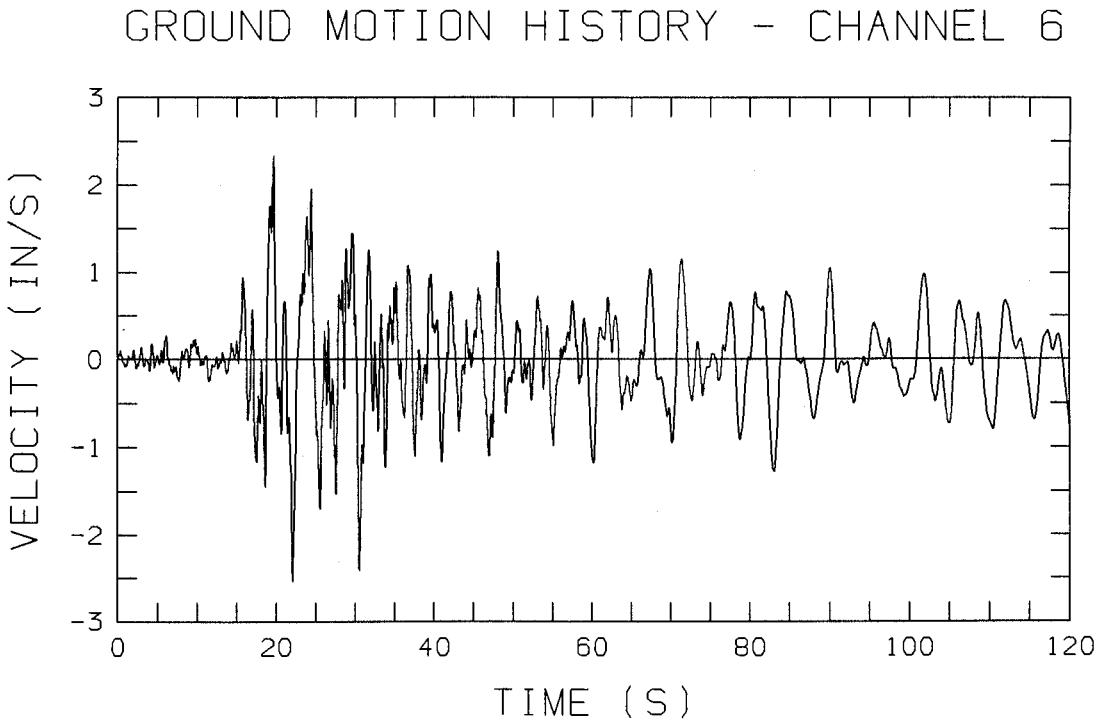

FIGURE C.3 - VELOCITY TIME HISTORY OF BASEMENT MOTIONS

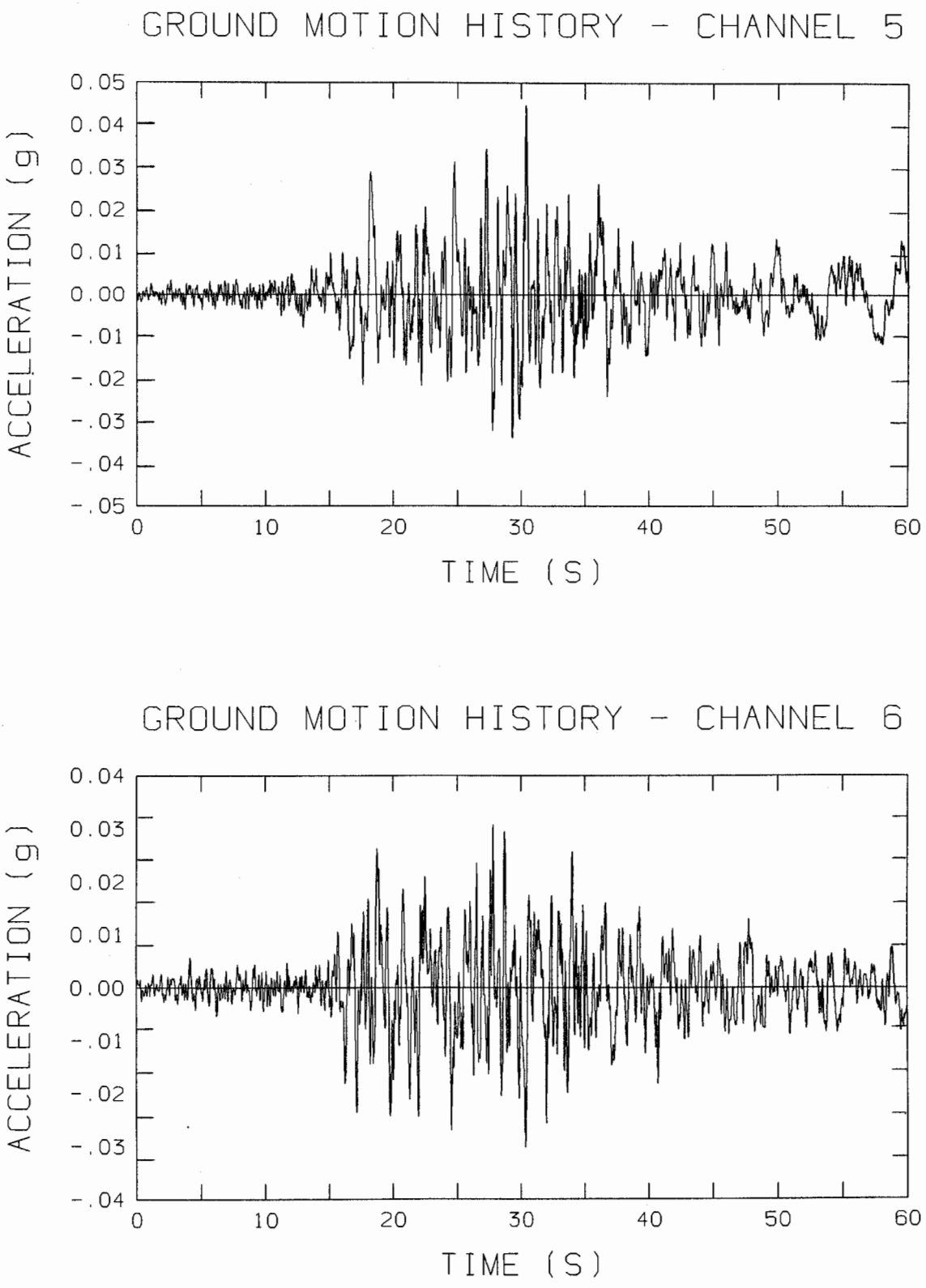

FIGURE C.4 - ACCELERATION TIME HISTORY OF BASEMENT MOTIONS

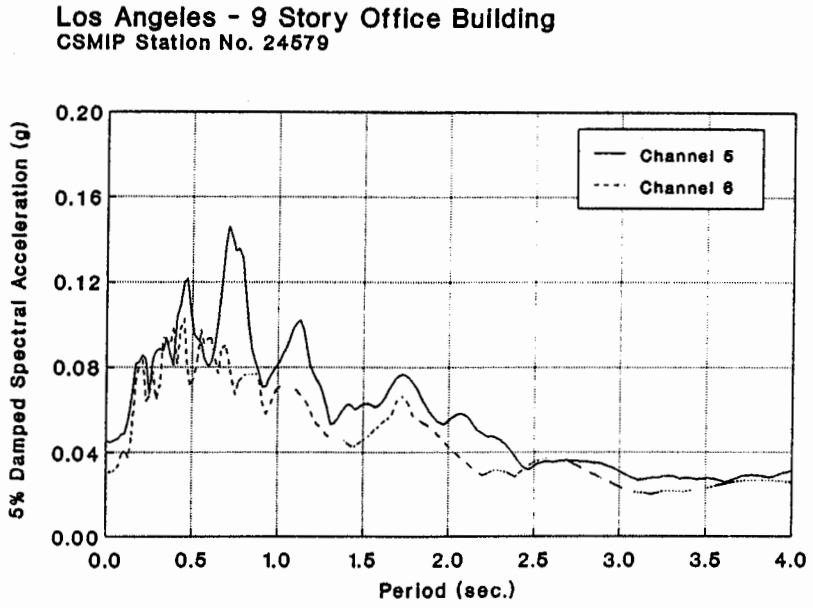

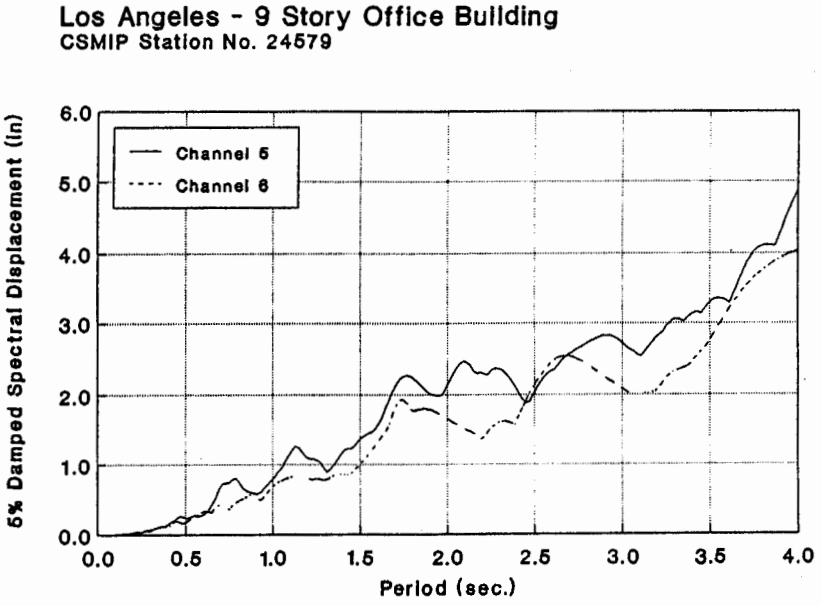

FIGURE C.5 - ACCELERATION AND DISPLACEMENT RESPONSE SPECTRA FOR BASEMENT MOTIONS

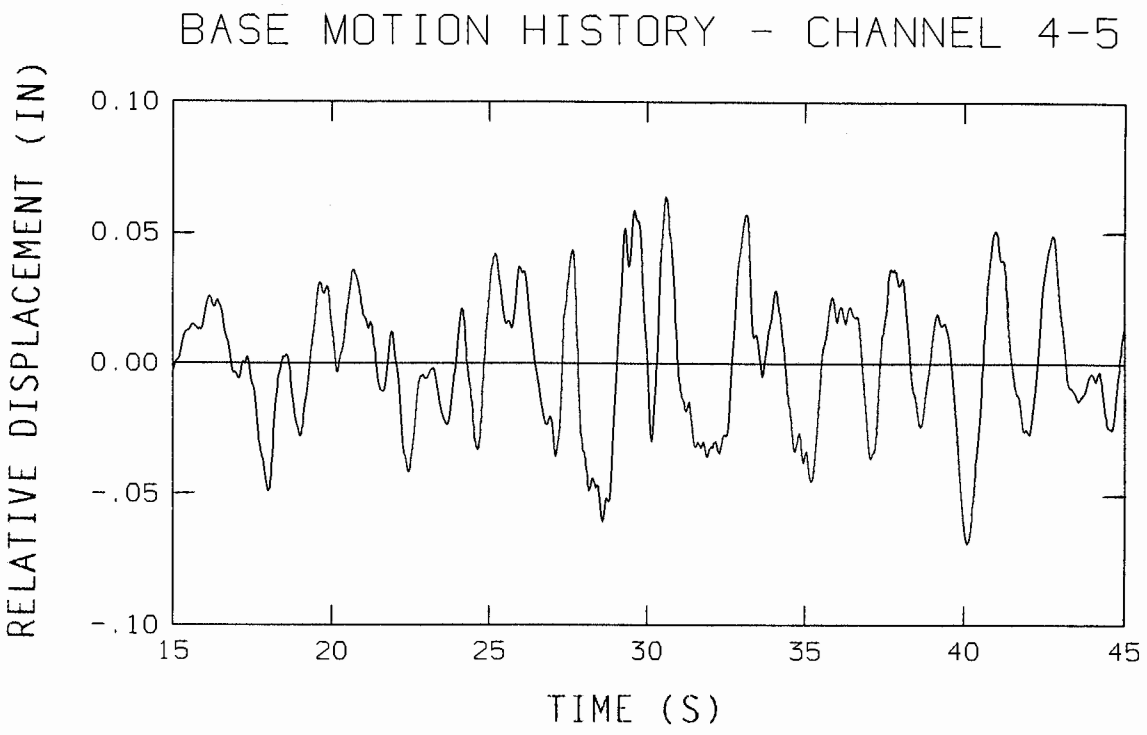

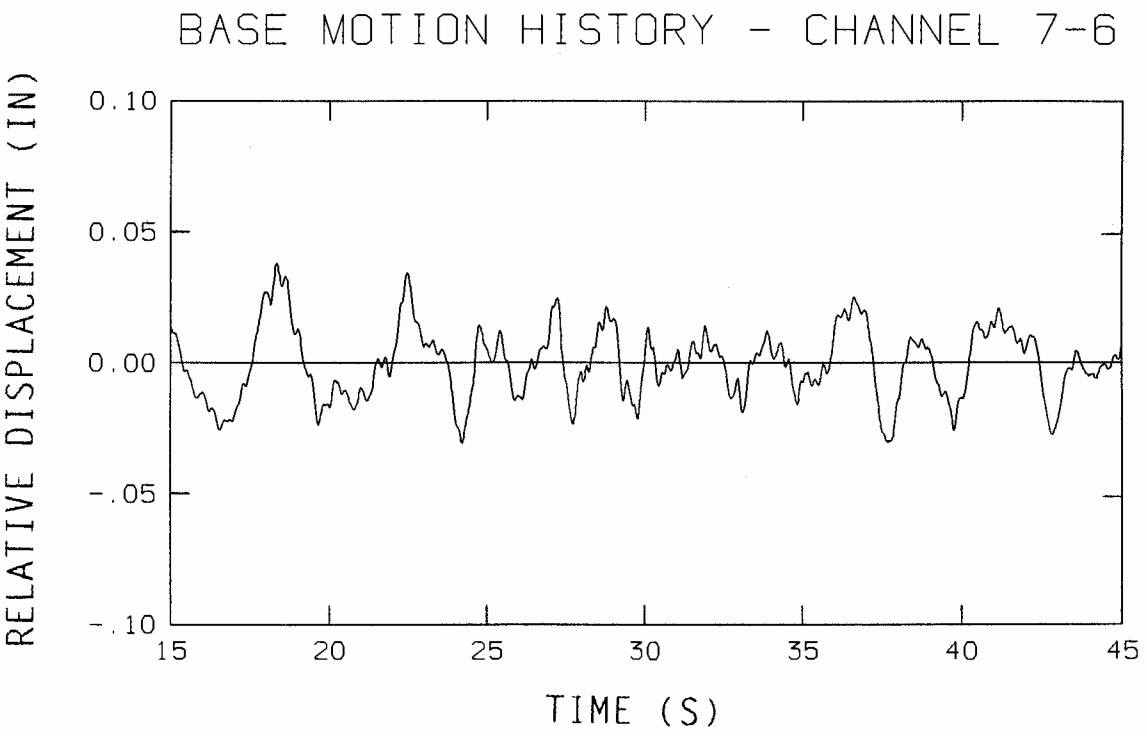

FIGURE C.6 - DISPLACEMENT TIME HISTORY OF THE BASEMENT ROTATIONAL MOTIONS

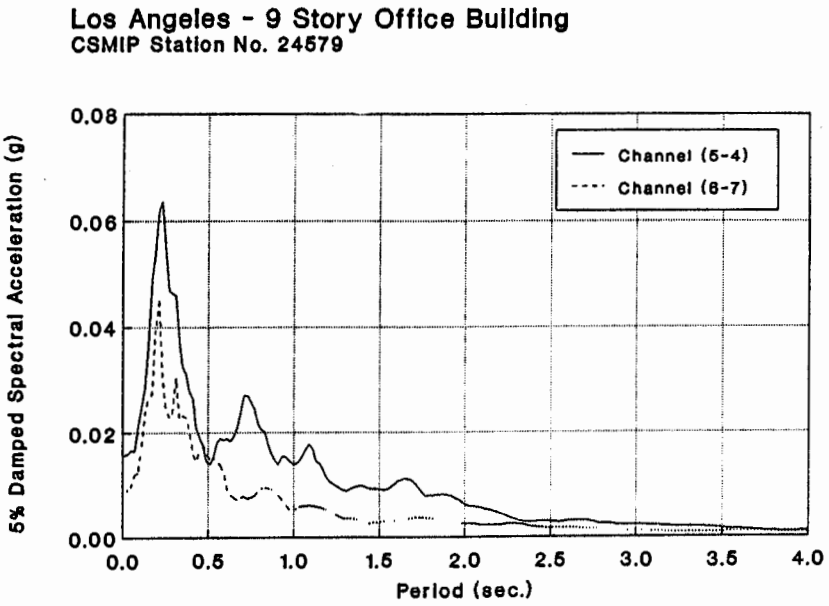

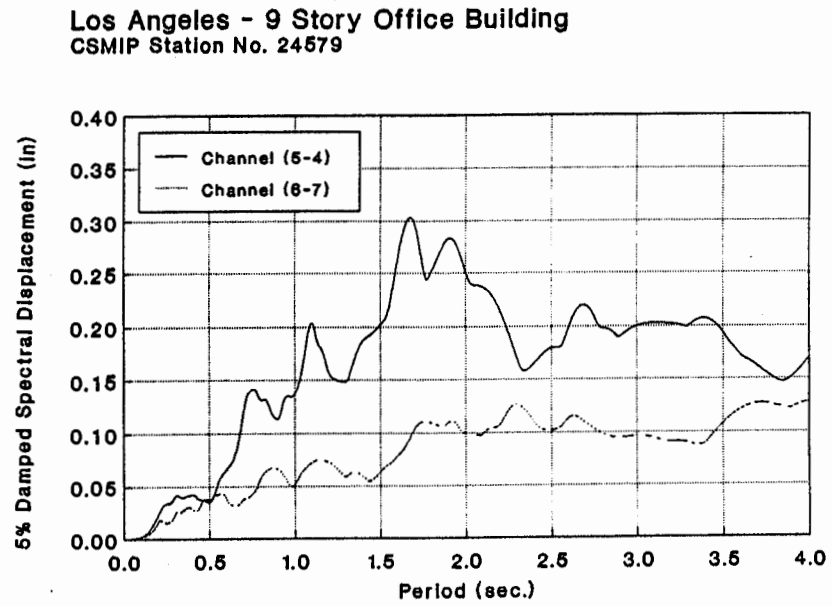

FIGURE C.7 - ACCELERATION AND DISPLACEMENT RESPONSE SPECTRA FOR THE BASEMENT ROTATIONAL MOTIONS

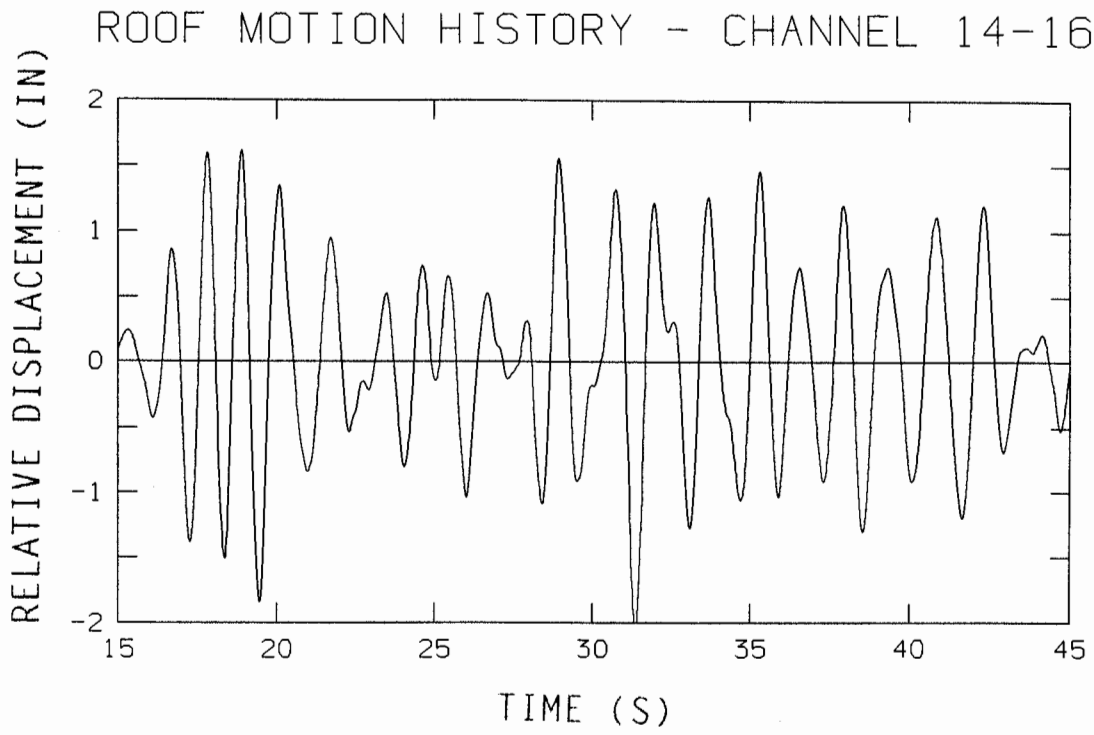

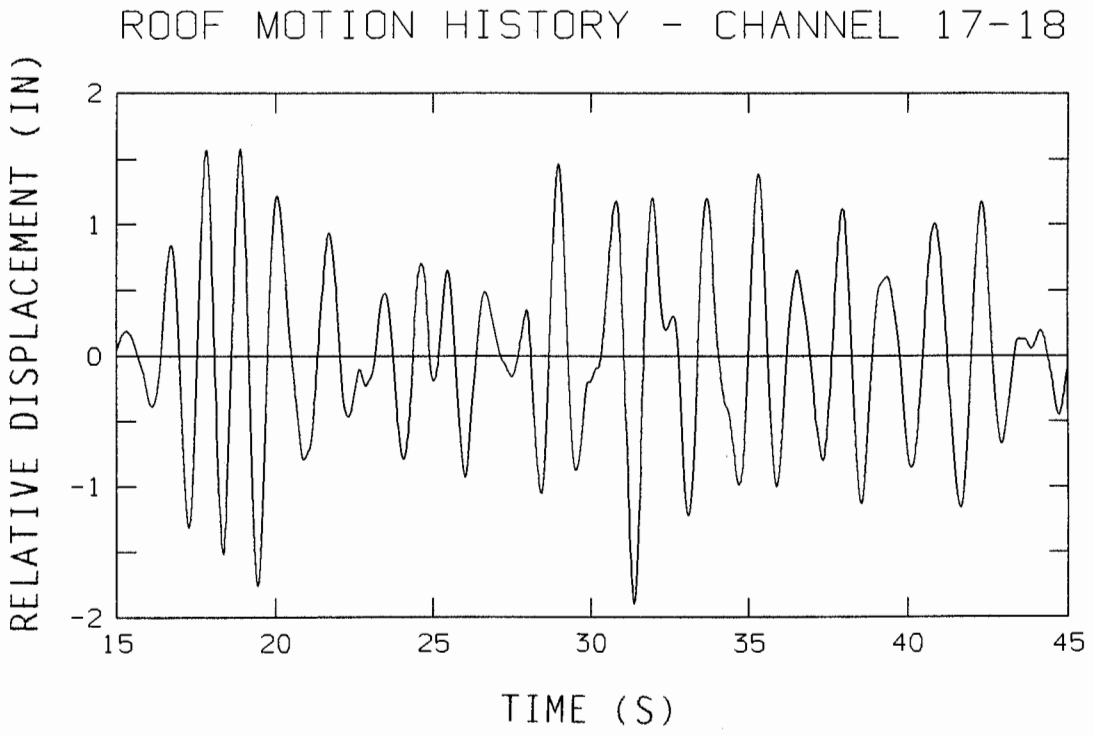

FIGURE C.8 - DISPLACEMENT TIME HISTORY OF THE ROOF MOTIONS

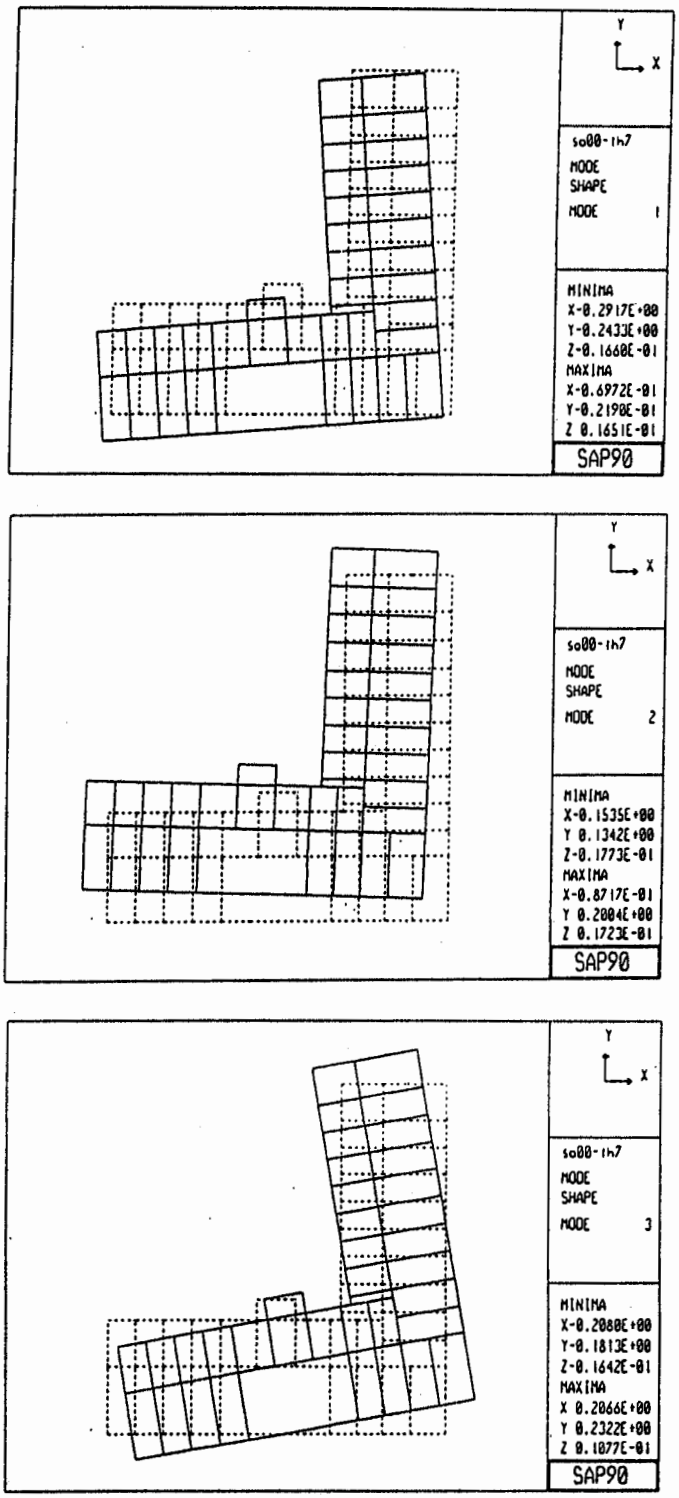

FIGURE C.9 - SAP90 BUILDING MODE SHAPES

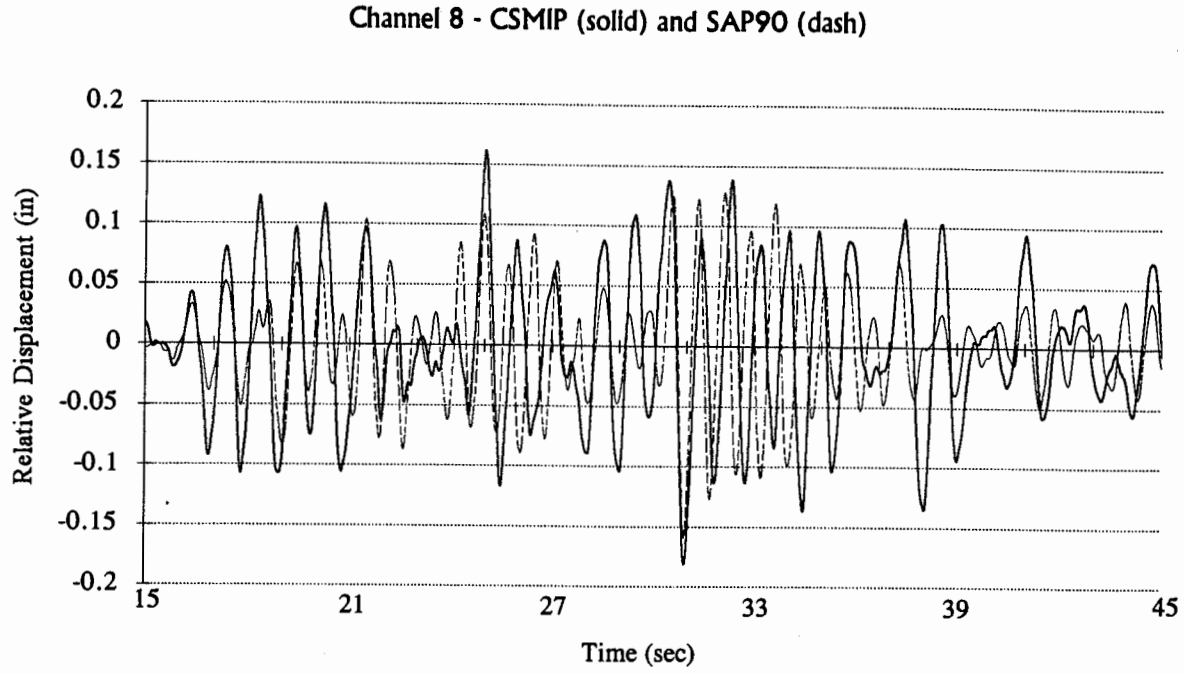

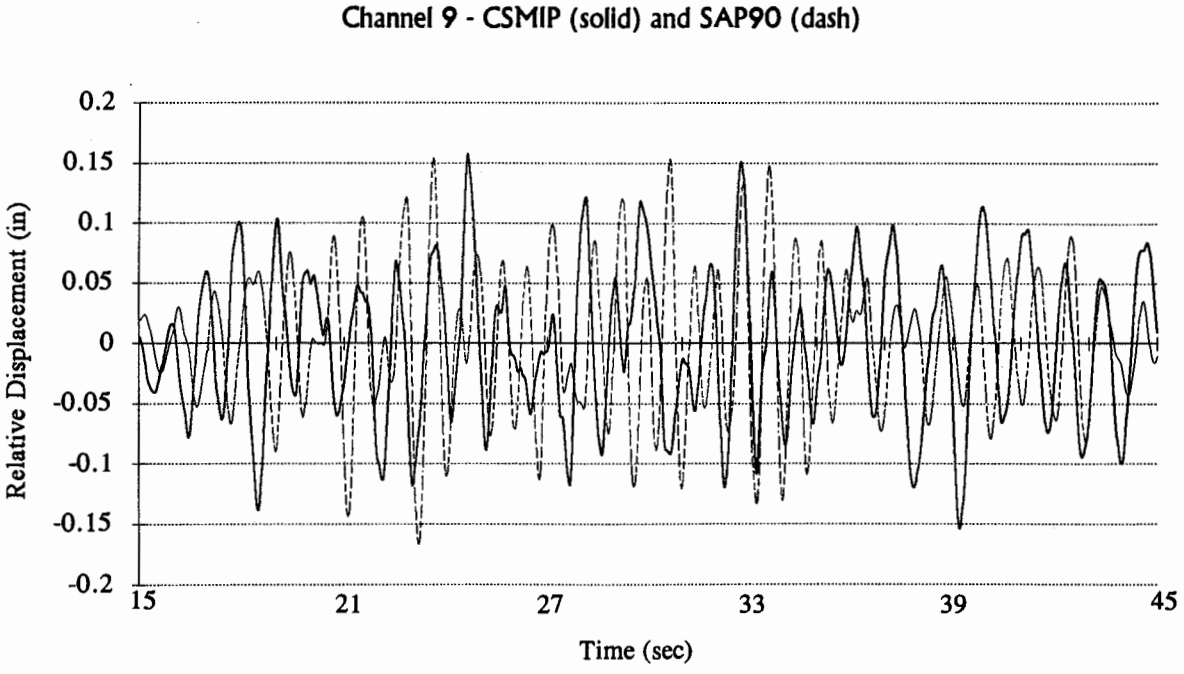

FIGURE C.10 - DISPLACEMENT TIME HISTORY OF CSMIP AND SAP90

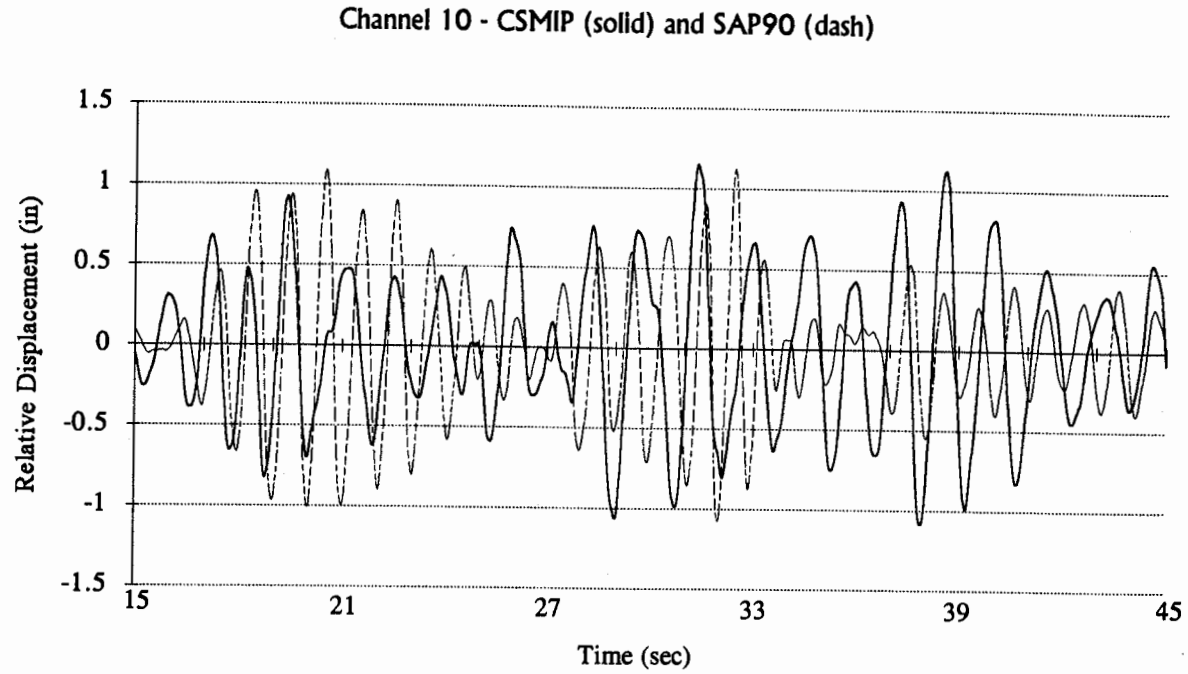

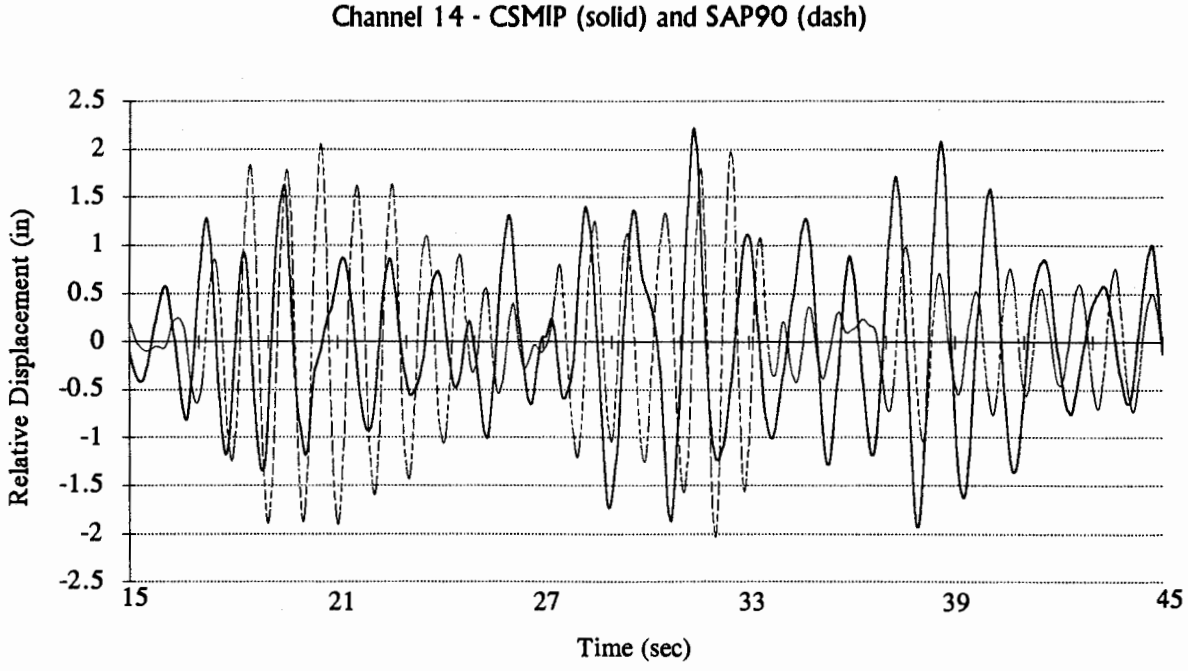

FIGURE C.11 - DISPLACEMENT TIME HISTORY OF CSMIP AND SAP90

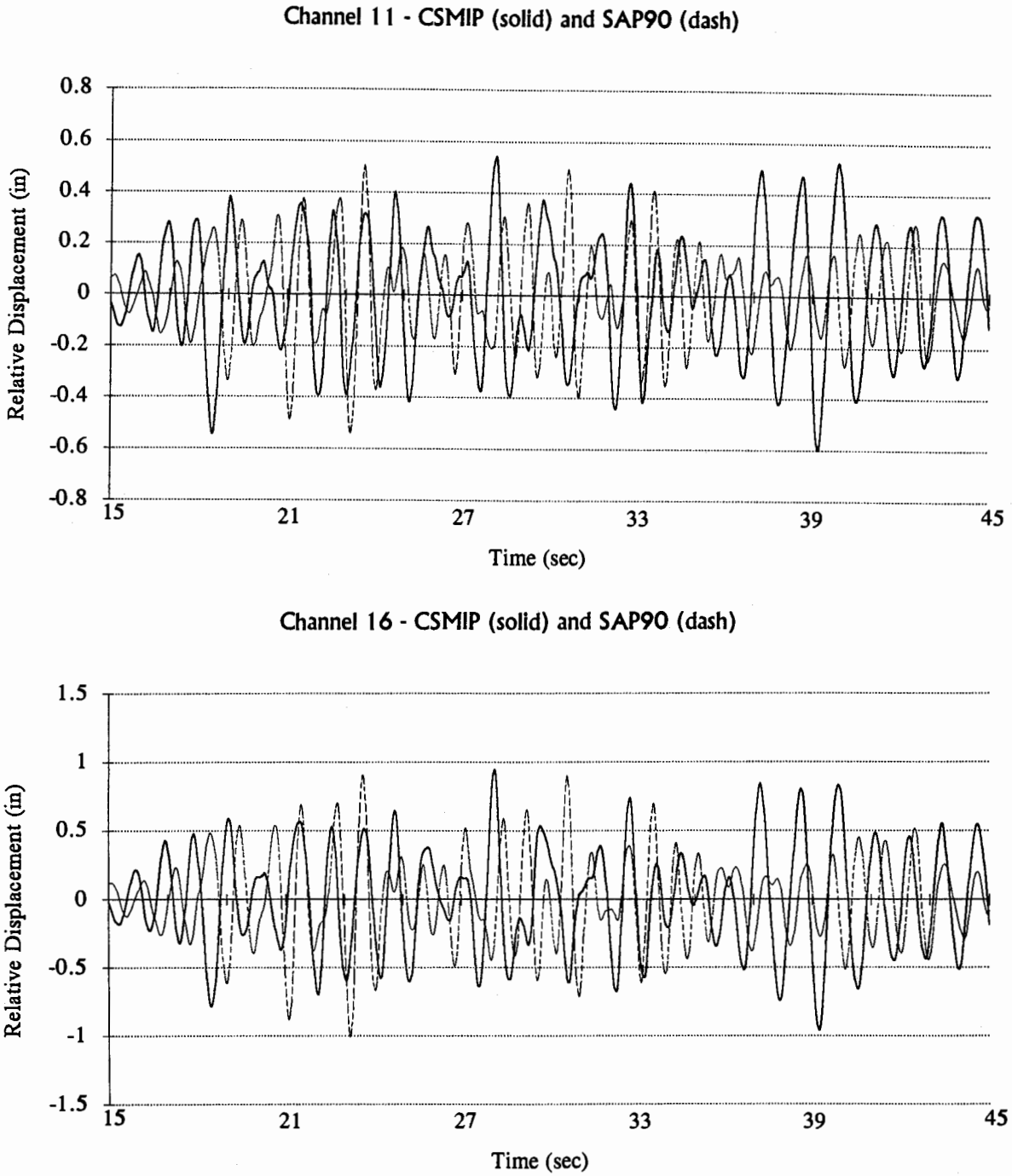

FIGURE C.12 - DISPLACEMENT TIME HISTORY OF CSMIP AND SAP90

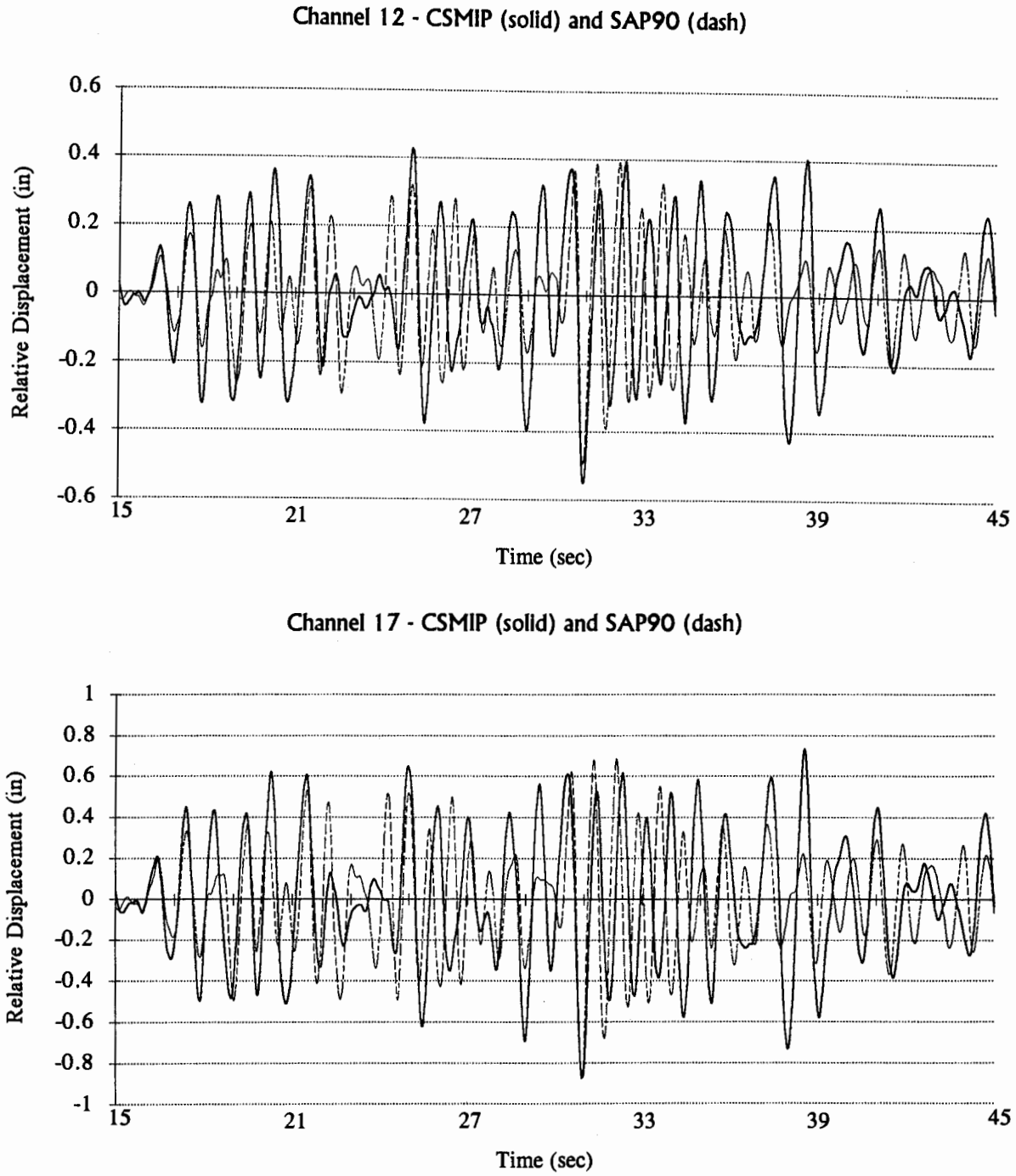

FIGURE C.13 - DISPLACEMENT TIME HISTORY OF CSMIP AND SAP90

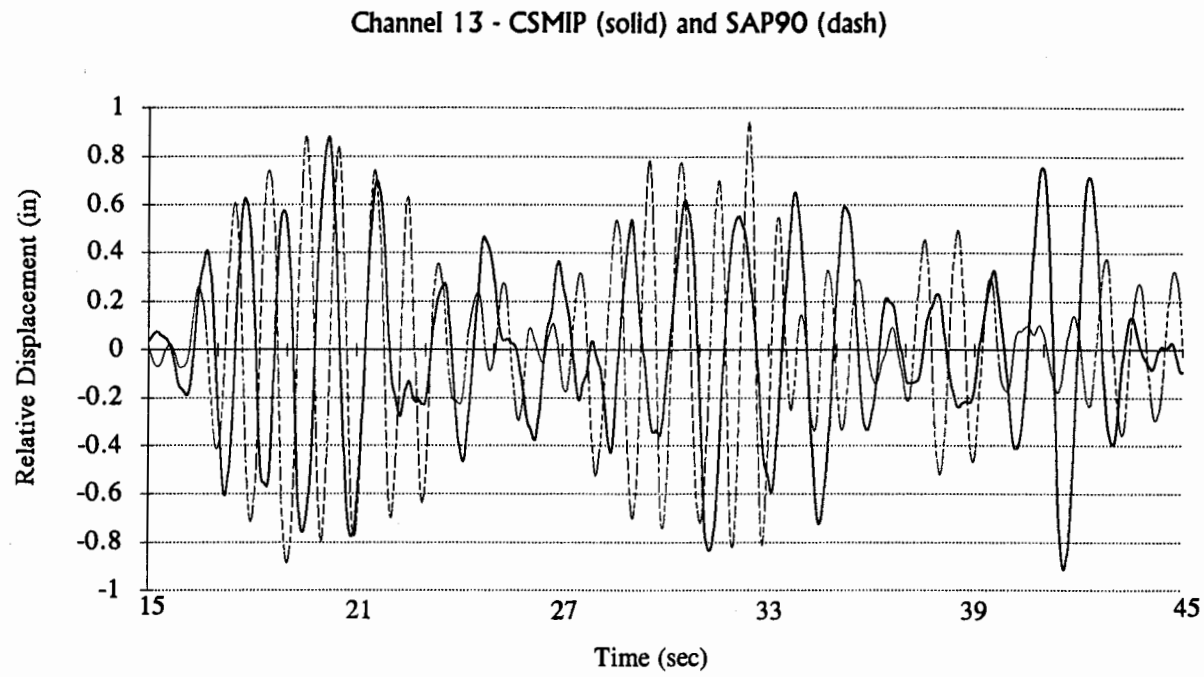

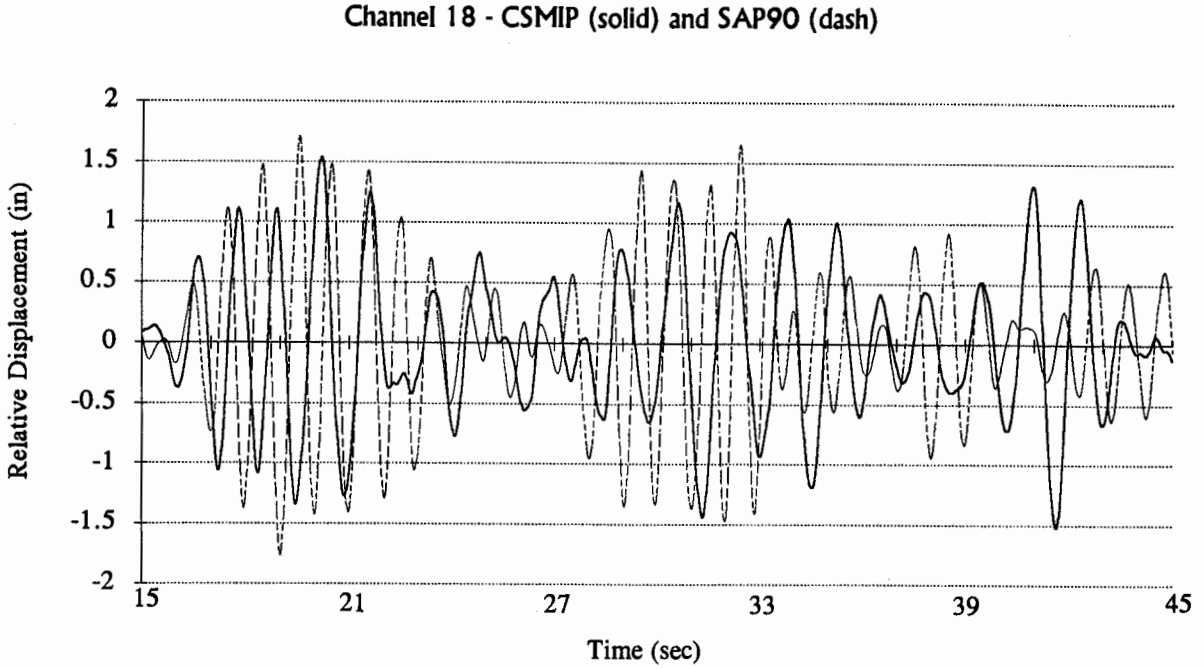

FIGURE C.14 - DISPLACEMENT TIME HISTORY OF CSMIP AND SAP90

APPENDIX D

SIMULATION OF THE RESPONSE OF CSMIP STATION NO. 24581 TO THE LANDERS EARTHQUAKE OF JUNE 28, 1992

SECTION D1

INTRODUCTION

D1.1 SCOPE OF THE ANALYSIS

The intent of this study was to simulate the response of the CSMIP Station No. 24581 building to the Landers earthquake of June 28, 1992. The analysis was done using a 3 dimensional beam element model of the structure with the member properties obtained from the structural drawings. The properties of the masonry infills were obtained from a nonlinear finite element analysis of the various types of panels in the building.

The objective of the analysis was to match the observed displacement response of the building with the analytically computed response using a rational approach towards estimating the structural properties of the building including the masonry infills.

D1.2 DESCRIPTION OF THE BUILDING

The building is a twelve story steel frame building with a rectangular footprint. It is located in downtown Los Angeles. Its primary lateral resistance comes from the masonry infills located along the building perimeter. There are also two basement levels which were not modeled.

D1.3 COMPUTER MODEL OF THE BUILDING

A 3 dimensional beam element SAP90 model was constructed using the member properties of the building columns and beams. The infill properties were obtained from an FEM/I nonlinear analysis and the stiffnesses of the panels were computed from the observed deformation of the building during the earthquake.

Member properties were adjusted to account for the existing building condition. The completed model was then analyzed to compare the CSMIP records with the analytical values of displacement.

D1.4 CSMIP DATA

The CSMIP data was obtained from the 16 sensors that the building had been instrumented with. These sensors were distributed over the height of the building and included instruments on the ends to record torsional behavior. Data available included acceleration time histories and response spectra. The time histories were used to obtain values of story drifts as well as torsional motions.

SECTION D2

BUILDING DESCRIPTION

D2.1 TYPE OF LATERAL FORCE RESISTING SYSTEM

CSMIP Station 24581 is located in downtown Los Angeles. It is a twelve story building designed in 1925. The lateral resistance is provided by steel column frames with URM infill walls. It is rectangular in plan with two basement levels below grade. The building footprint is rectangular with dimensions of 108 feet by 335 feet. The building is 152 feet tall. In addition, there is a penthouse level with a relatively small footprint at the roof and contains a mechanical room also. The building elevation is shown in Figure D.1.

The lateral resistance of the building is provided by a combination of the frame action of the beams and columns in addition to the perimeter frames with masonry infills acting as braces and providing considerable lateral rigidity.

D2.2 FOUNDATION SYSTEM AND BASEMENT FRAMING

The vertical load carrying system consists of concrete slabs with thicknesses between 3 and 7 inches supported by steel beams and columns. The foundation consists of both combined and individual footings. The building has two basement levels with walls that were not included in the analysis. The base of the building in the model was set at the first floor level. However, the input motions used in the analysis were obtained from sensors 3 and 4 which are located in the building sub-basement.

D2.3 IRREGULARITIES OF THE STRUCTURAL SYSTEM

Although the building is symmetric, the rigidity in the east-west (long) direction is moved towards the back (south) wall of the building since the front (north) wall is perforated at its center from the first floor to the roof. Also, the east and west (short) walls are perforated at the first floor. The building has a large aspect ratio of 1 to 3 and torsional modes are further accentuated by the irregularities.

SECTION D3

RECORDED EARTHQUAKE RESPONSE

D3.1 EARTHQUAKE SOURCE

The response of the building is studied through its recorded response to the Landers earthquake of June 28, 1992. The Landers Earthquake had a magnitude of M_s=7.5, and was the largest event to occur in California since 1952. The epicenter was located 43 km north of Palm Springs and 80 km east of San Bernardino. The building is located at about 170 km from the epicenter.

D3.2 LOCATIONS OF INSTRUMENTS

The building was instrumented with 16 sensors, one of which recorded the vertical component of the motion and was located at the basement. The other 15 sensors were oriented to record the motion in two orthogonal horizontal directions.

There are 4 sensors located in the sub-basement, 4 at the second floor, 2 at 4th floor, 4 at the 12th floor and 2 at the roof. Figure D.1 shows the location and orientation of the sensors. These sensors are located so they will be able to record the translational and rotational motion of the building

D3.3 BASE MOTION CHARACTERISTICS

The ground motion from sensors 3 and 4 can be seen in Figures D.2 - D.4 which show the acceleration, velocity and displacement plots. A scrutiny of the

acceleration spectra of the recorded ground motion (from the basement sensors) in Figure D.5 reveals a broad band spectra between 0.5 to about 1.1 seconds from sensor 4. Sensor 3 however reveals a much more peaked spectrum with the strong energy being concentrated around 0.5 seconds with a gradual dying down of the energy for periods over 2 seconds and this is shown in Figure D.6.

The peak accelerations in both the east-west and the north-south directions were about 0.04g at the basement. At the roof, the peak acceleration in the east-west direction was about 0.13g and in the north-south direction about 0.08g. Fundamental translational periods estimated from these response spectra of the sensor accelerations at different levels were about 3.0s for the north-south direction and 2.0s for the east-west direction.

D3.4 BASEMENT RECORDS USED IN ANALYSIS

It may be noted that the records used as the base motion records for the model were the time histories from sensors 3 and 4 which are located in the basement and are oriented in orthogonal directions in the plane of the building. The effect of the basement walls was neglected.

D3.5 RESPONSE OF THE TOP OF THE BUILDING

The peak relative displacements of the roof with respect to the sub-basement were about 2.4 and 2.6 inches in the north-south and the east-west directions respectively. The displacement records from the sensors at the east and west walls (short direction) did reveal the torsional effects present in the building motion particularly due to its aspect ratio as well as the stiffness distributions in the lateral system. Figure D.7 shows the acceleration response spectrum of the torsional motion obtained by differencing the motions of the two end walls at the second and twelfth floor levels.

D3.6 RESPONSE OF INTERMEDIATE FLOOR LEVELS

The CSMIP records for the 2nd floor revealed a strong torsional effect which is caused by the irregularity in the stiffness. As the instrument locations

at the 4th floor were not set for observing torsional motions, this information was not available. The peak displacements at each level were computed from the CSMIP data. Once this was found, a table of peak displacements was used to compute estimates of the maximum drift at each level.

A linear approximation was used at floors between instrument locations. The maximum displacement of the boundary instruments at a given floor (if available) was used in computing the drifts. From this data, a table of drifts for each floor was computed and used in obtaining deformation levels to set the stiffness estimates for each of the masonry infill panels.

SECTION D4

SAP90 COMPUTER MODEL

D4.1 LINEAR ELASTIC THREE-DIMENSIONAL MODEL

A three dimensional beam element SAP90 model of the building was created from the plans of the building provided by CSMIP. The floor diaphragms were assumed to be rigid. The joints of the frames were assumed to be continuous and the base of the columns at the first floor was assumed to be fixed. The two basement levels were not modeled which made the computer model stiffer than the actual building. Therefore, the stiffness of the building was overestimated and this was observed in the computer periods for the building.

The beams and columns were modeled using frame elements. The properties were obtained from the steel tables pertaining to standard shapes in the 1920s. The beams were found to be encased in concrete and therefore could be assumed to be stiffer than the assumed properties. However, it was found on examination that the actual connections of the beam-column joint could not be construed as continuous. To take these two conflicting effects into account, the beam stiffnesses were set at 80% of the actual values. The masonry infills were modeled as diagonal brace elements reaching from a beam-column joint on one floor to a beam-column joint at the diagonal end on the next floor. Two diagonals were

used for each panel for symmetry.

D4.2 MODELING OF URM INFILLS

Figures of force-deformation relationships were computed using the TCCMAR developed non-linear masonry finite element program FEM/I. The CSMIP sensor data was used to compute a maximum deformation level for the building assuming straight line deformation between sensors at different levels. From these drift data, a story deformation was computed. This relative deformation was used to set the secant stiffness for each masonry panel at that level. Once the stiffness was calculated, the diagonal brace properties were then computed and used in the building model.

The material behavior in the nonlinear analysis was assumed and no values were determined from testing. The strut properties were adjusted for the assumed levels of degradation since the finite element analysis yielded properties for monotonic loading.

D4.3 COMPLETE BUILDING MODEL

Six modes of building motion were used in the analysis with over 90 % of the building mass participating. The stiffness of the infills was assumed to be at 70% of the estimated values from the nonlinear analysis. This was done to incorporate the degradation of stiffness over the cyclic seismic loading as well as to account for the influence of the frame stiffness on the overall force-deformation curve in the panel. The stiffness for the panels was adjusted as a whole and not for specific panels or floor levels since the objective of the study was to replicate the building response rather than fitting the data with some best estimates of parameters. Damping in the building was assumed to be 3% of the critical for the first three modes and 5% of the critical in the remaining three modes.

The periods obtained from the SAP90 analysis were 2.4 seconds for the translational mode in the north-south direction and 1.8 seconds in the east-west

direction (CSMIP values were 3.0s in the north-south direction and 2.0 seconds in the east-west direction) and are shown in Table D.1. Figure D.8 shows the mode shapes of the building for the first three modes of the building (two translational and one torsional). The figures are shown from positions which would best show the building behavior.

SECTION D5

COMPARISON OF ANALYTICAL RESULTS WITH CSMIP DATA

D5.1 GENERAL

The objective of the study was to attempt to replicate the CSMIP data through a linear elastic three dimensional analysis of the building using information from a nonlinear finite element analysis of the masonry infills in as rational a manner as possible. The model that was used had masonry infills at 70% of the computed stiffness to take the stiffness degradation into account as well as the influence of the frames. The latter effect arises from the fact that the force-deformation curves for the panel include the frame stiffness - thus the model may doubly add the stiffness of the frame. Even though the building frame is steel, the sizes and the encasement of the columns give it a larger than normal significance in the analysis. The damping values were chosen to reflect the larger damping present in the higher modes. Also, the damping quantity used in the program is a viscous damping as opposed to the hysteretic damping actually present.

D5.2 COMPARISON OF AMPLITUDE OF DISPLACEMENT DATA

The analytical results of the computer simulation are shown in Figures D.9 to D.14 for all the sensors. These are time history plots of the displacement of each instrument location. It may be noted that the instrument location on the model was only approximate due to the paucity of information.

Table D.2 shows a summary of the results of the peak displacements from each sensor from the CSMIP records versus the SAP90 results. It can be seen that

the overall agreement is very good. However, a look at the plots shows some obvious shortcomings. The phase relationships are not very good for sensors 11,13 and 14 while sensors 10,12 and 16 show a better fit. In all the sensors, the fit is better during the earlier part of the record.

The discrepancy in results can be explained by a variety of factors that went into the modeling procedure such as soil structure interaction as well as a lack of available test data to compute material properties for the infill. Also, the procedure is an attempt to model nonlinear behavior with an equivalent linear system and illustrates the difficulties in matching results. However, the procedure is a valid one for modeling in a consistent way the nonlinear behavior of infill panel buildings subjected to seismic loading.

SECTION D6

CONCLUSIONS

D6.1 MODELING

This new method of modeling unreinforced masonry infill panels in existing buildings as diagonal struts can be conveniently used for seismic response computations. This technique was used in modeling the CSMIP station 24581, a twelve story steel frame building with masonry infill panels. A nonlinear finite element analysis was used to compute equivalent brace properties at computed deformation levels in panels and the building model was subjected to the recorded motion. The infill stiffnesses were adjusted for stiffness degradation.

Adjustments were made for the actual fixity in the beam column joints as well as the encasement of the beams in the floor slabs. Therefore, the existing condition of the building was modeled through the careful selection of the building parameters. The analytical results show a good agreement in the peak values of the displacement at various levels. This method may be used in the analysis of buildings with infill panels for seismic retrofitting.

D6.2 FIT OF COMPUTER DATA TO RECORDED DATA

The table of displacements comparing the recorded data and the analytical response shows that on the whole, there was good agreement between the CSMIP values and the SAP90 results. The average percentage difference for the sensors was about 15%. Further, a look at the time history of displacements shows a fairly good agreement in many sensors. However, there is a drift that seems to cause a phase difference towards the end of the time history in the sensors. It should be noted that the locations of the CSMIP instruments on the model are very approximate and based on the available information and this may play some role in the observed differences.

D6.3 DETERMINATION OF DAMPING

The damping values used were broadly applied and were viscous damping values. The actual value of damping to be used is indeed subjective. However, some guidelines may be observed. These include a limiting value based on an estimate of the hysteretic damping and the level of deformation. Further, higher modes will have larger values of damping. Also, damping values may differ mode to mode. These points may be kept in mind during the analysis.

D6.4 INSTRUMENT LOCATIONS

This building has an aspect ratio of approximately 1 to 3. Given this fact and the lateral stiffness irregularities present in the building, it is apparent that torsional motions will be substantial during any earthquake. Therefore, the instrumentation must take this fact into account. The instruments located in this building by CSMIP are fairly reflective of the dynamic motion of the building. However, the basic configuration should preferably (in similar buildings) have four instruments per floor - 2 for the center of the building and 2 to record torsional effects. It is of course not possible due to constraints to follow this for all buildings but such a configuration can prove to be very valuable in obtaining information about the building response.

TABLE D.1

DYNAMIC PROPERTIES

Mode	Period (s) (analytical)	Period (s) (CSMIP Data)	Type
1	2.40		Translation
2	1.80		Translation
3	1.46	2.05	Torsional

TABLE D.2

COMPARISON OF ANALYTICAL AND CSMIP RESPONSES

			CSMIP	SAP90*	
Sensor	Floor	Direction	Max Rel Displ (in)	Max Rel Displ (in)	Percent Difference
3	Basmt	NS	1.06	BASE MOTION	
4	Basmt	EW	1.85		
5	2nd	NS	0.38	0.32	16
6	2nd	NS	0.19	0.25	32
7	2nd	NS	0.38	0.35	8
8	2nd	EW	0.11	0.12	9
9	4th	NS	0.58	0.81	40
10	4th	EW	0.60	0.41	32
11	12th	NS	2.11	2.23	6
12	12th	NS	2.01	2.31	15
13	12th	NS	2.10	2.10	0
14	12th	EW	2.48	2.59	4
15	Roof	NS	2.41	2.38	1
16	Roof	EW	2.57	2.66	3

*** - SAP90 Results are based upon:**

- **Time History Analysis with 6 modes (90% participation)**
- **70% of the Infill Stiffness**
- **3% Critical Damping in modes 1,2 & 3**
- **5% Critical Damping in modes 4,5 & 6**

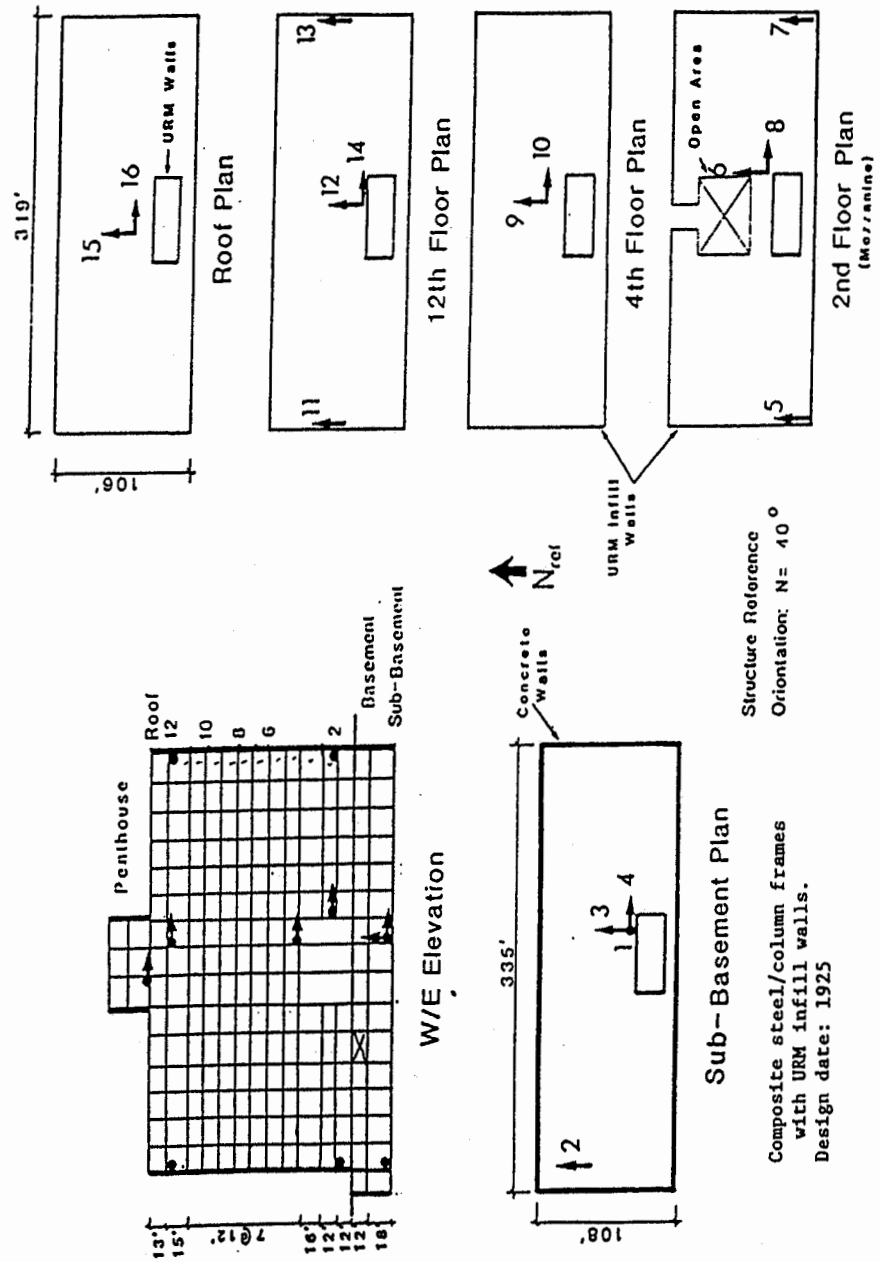

FIGURE D.1 - CSMIP INSTRUMENT LOCATIONS

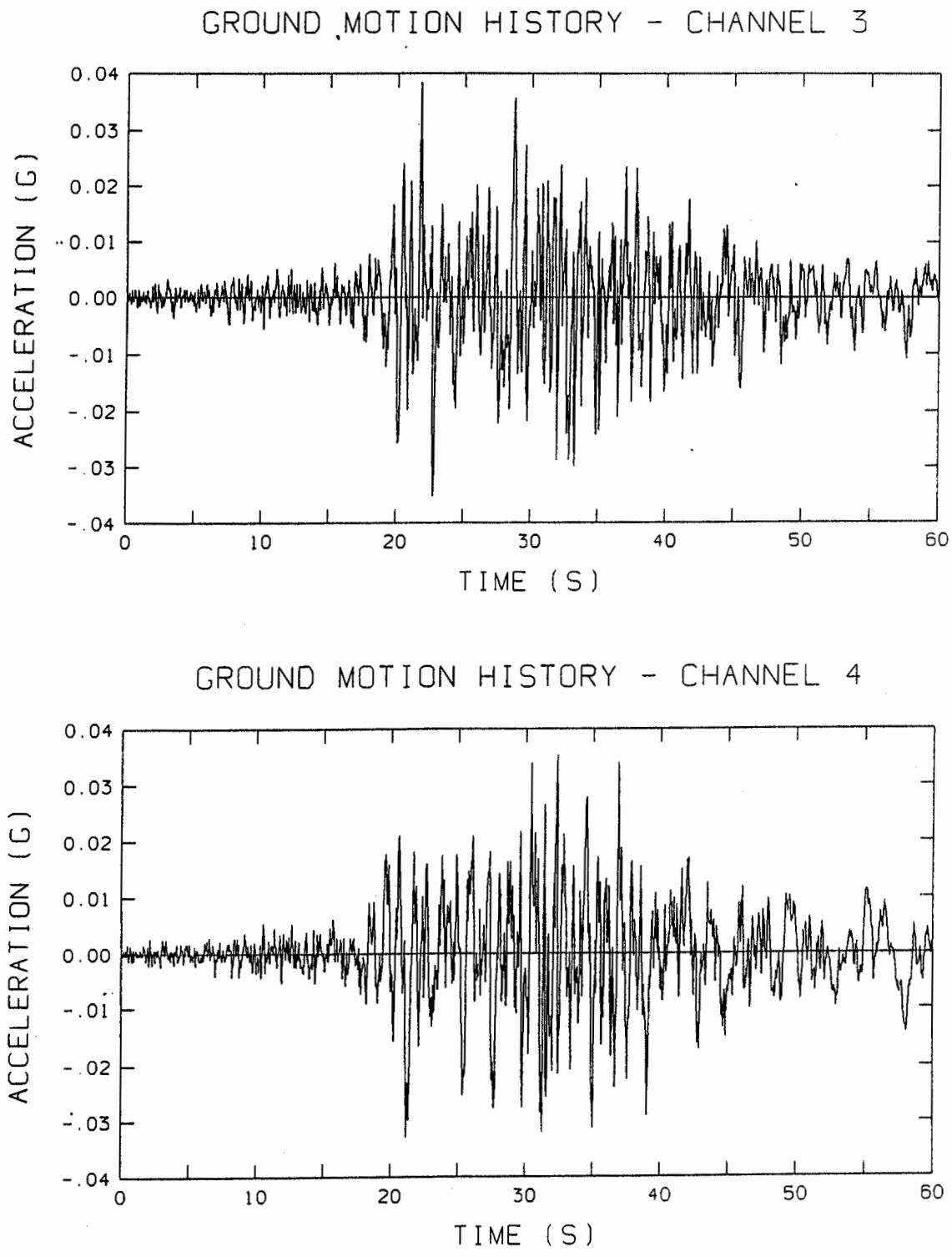

FIGURE D.2 - ACCELERATION TIME HISTORY OF GROUND MOTION

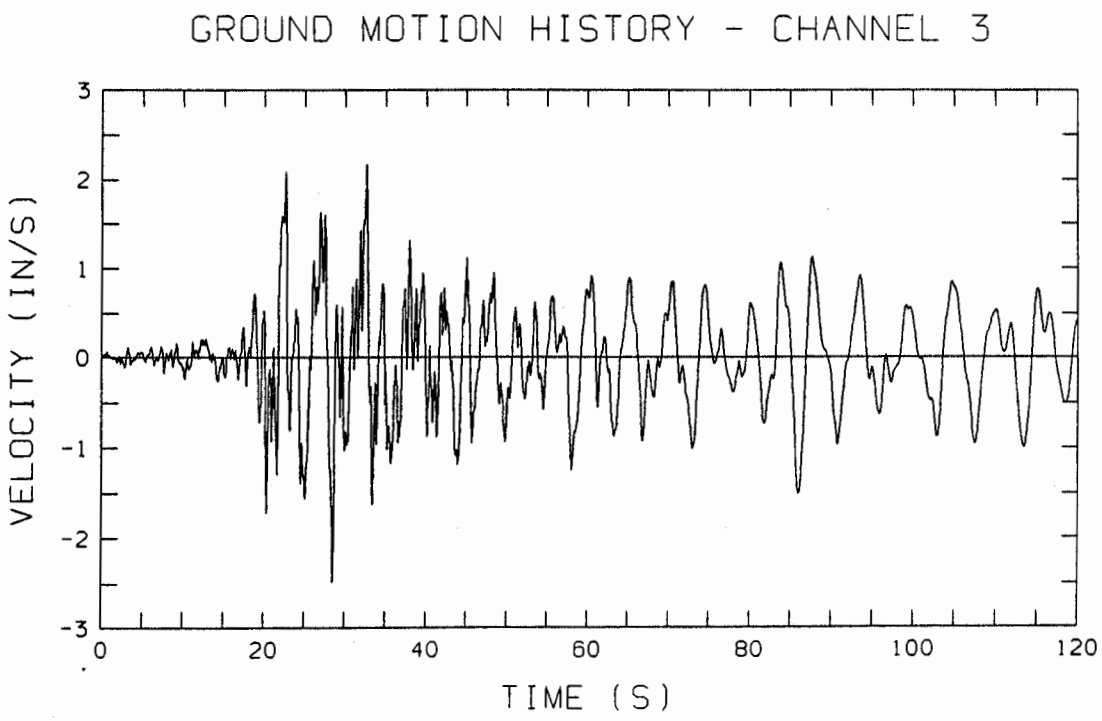

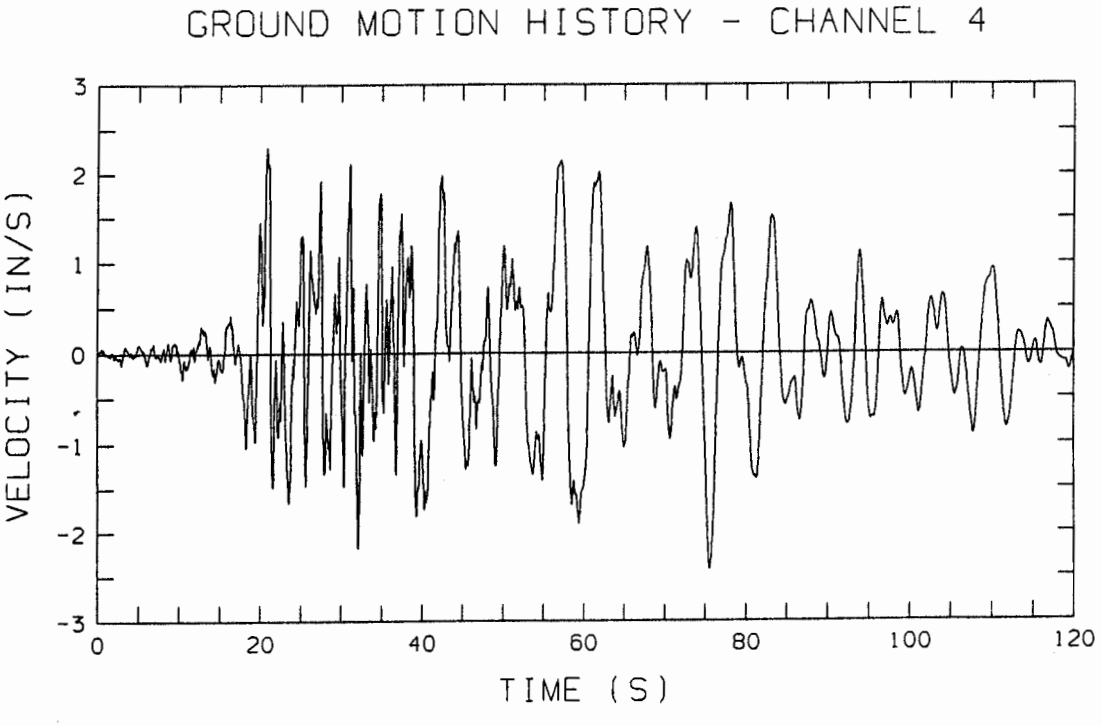

FIGURE D.3 - VELOCITY TIME HISTORY OF GROUND MOTION

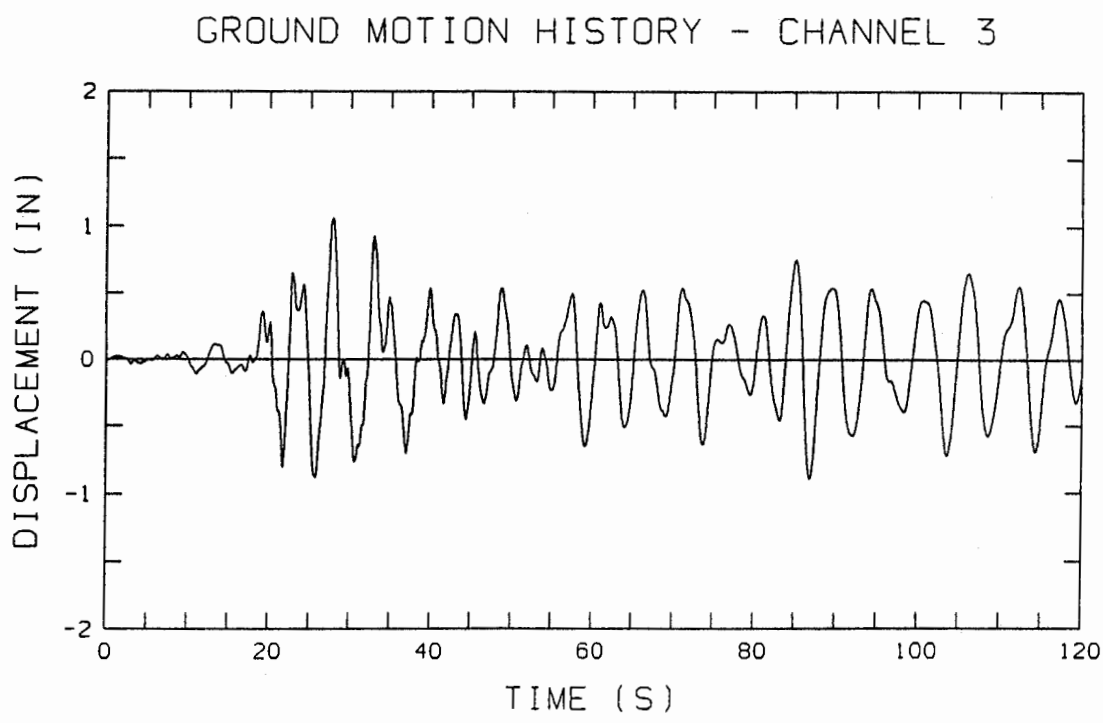

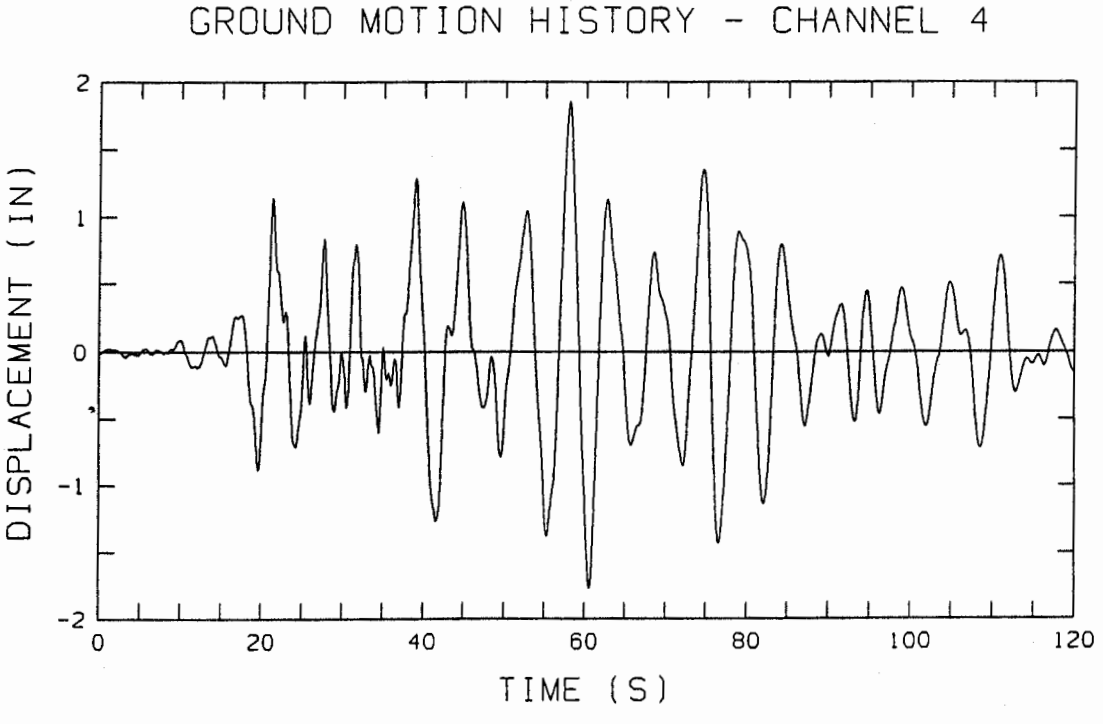

FIGURE D.4 - DISPLACEMENT TIME HISTORY OF GROUND MOTION

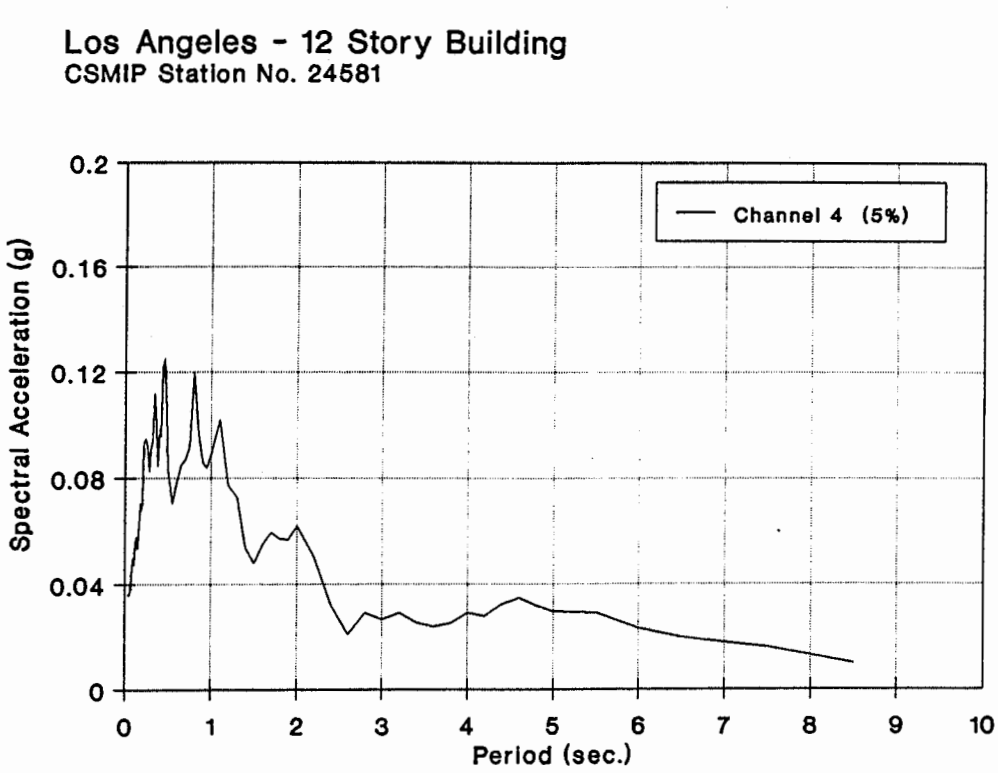

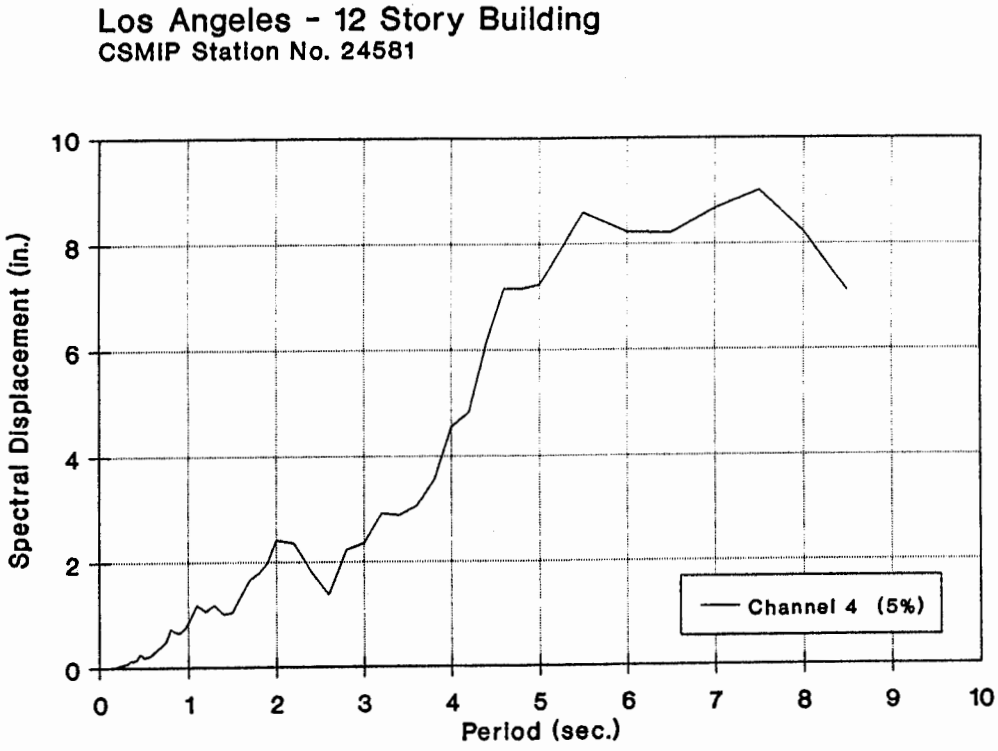

FIGURE D.5 - GROUND MOTION RESPONSE SPECTRUM

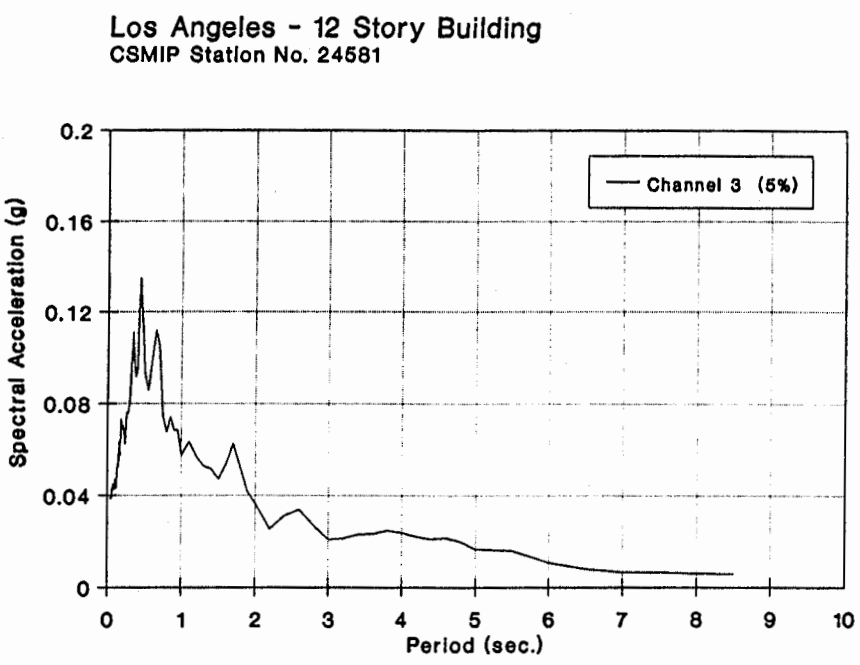

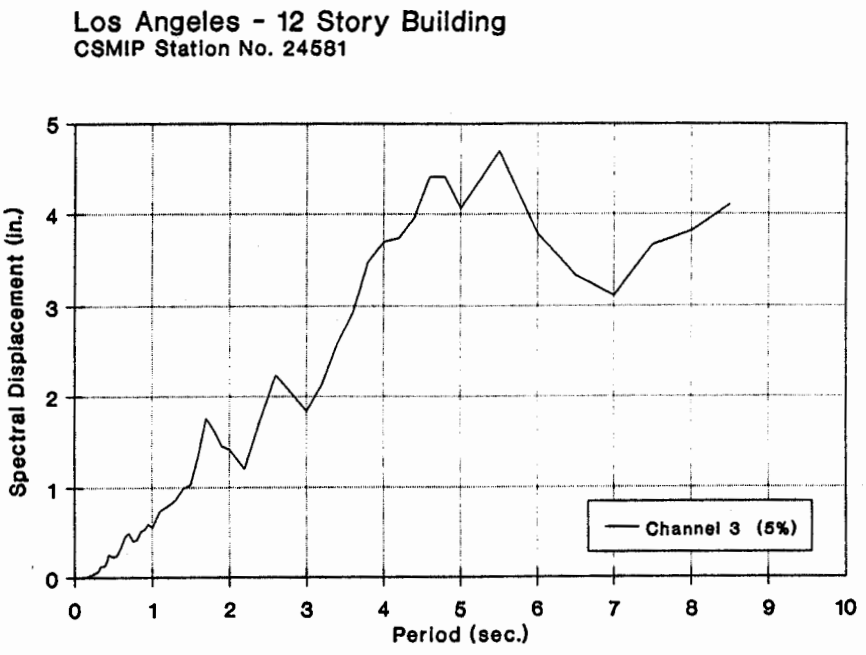

FIGURE D.6 - GROUND MOTION RESPONSE SPECTRUM

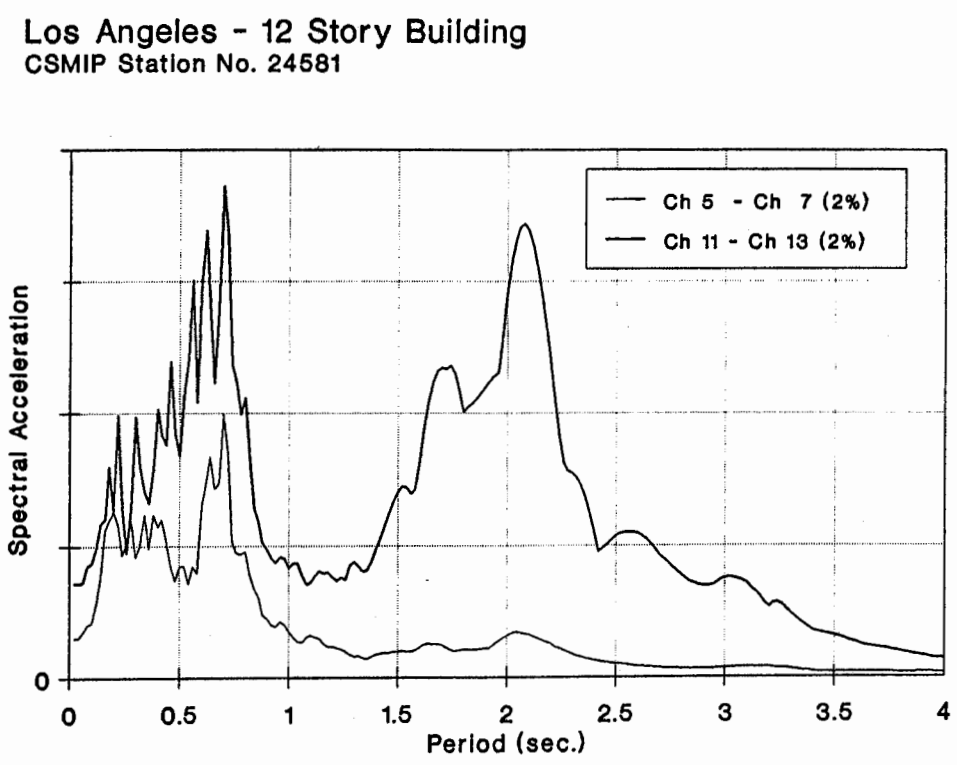

FIGURE D.7 - GROUND MOTION RESPONSE SPECTRUM

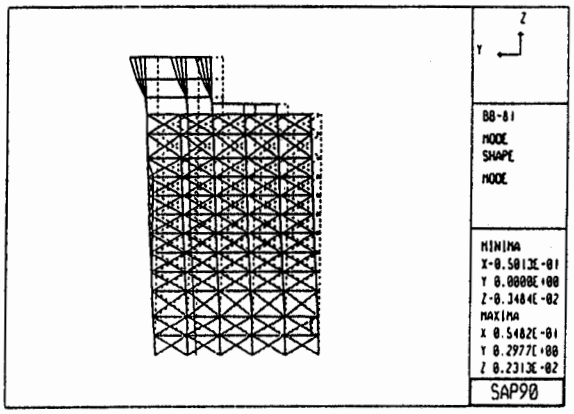

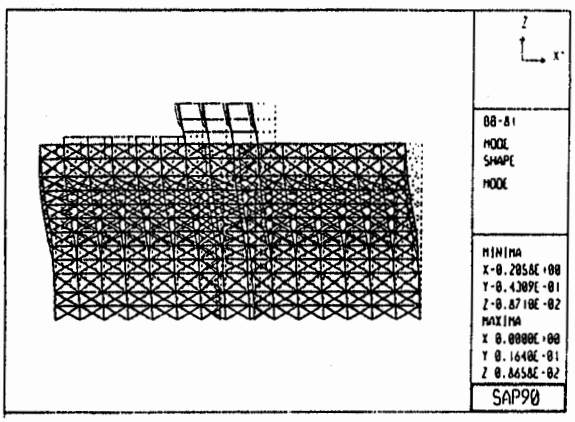

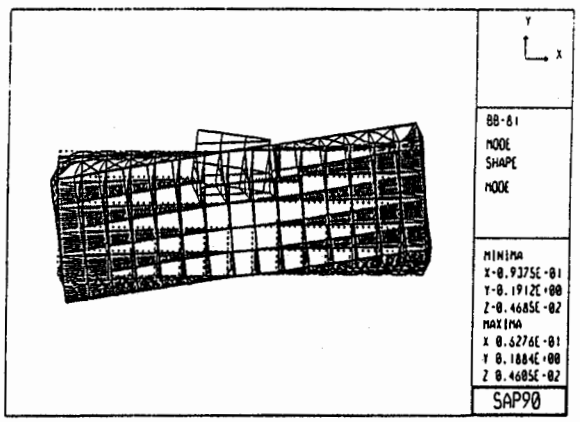

FIGURE D.8 - BUILDING MODE SHAPES

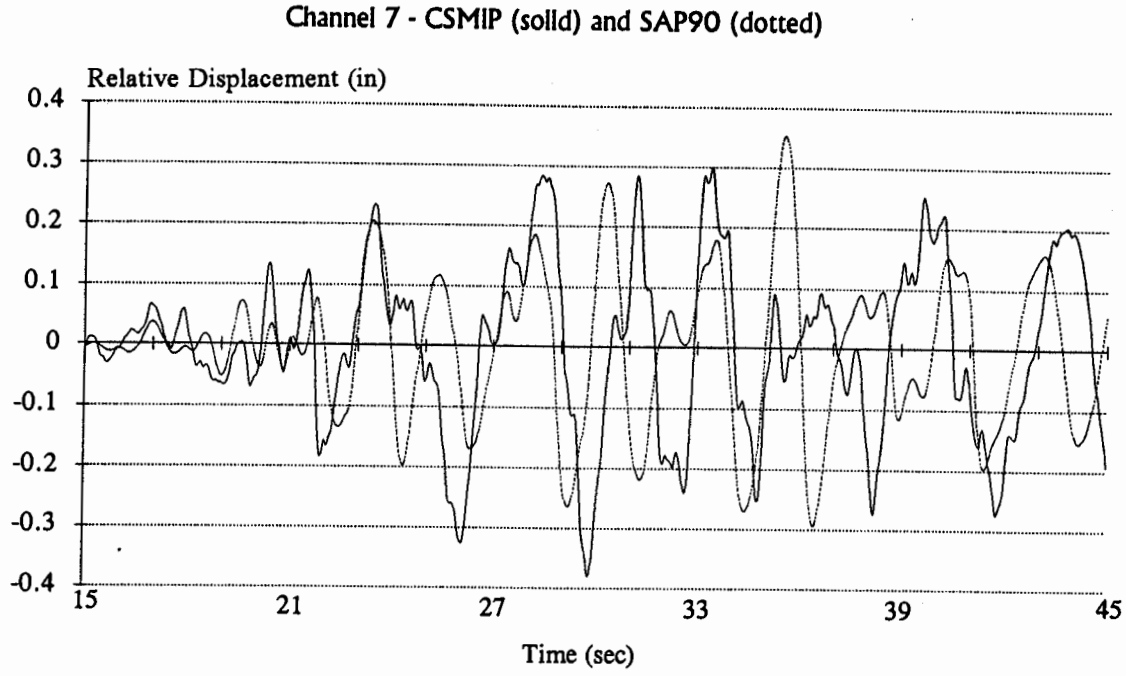

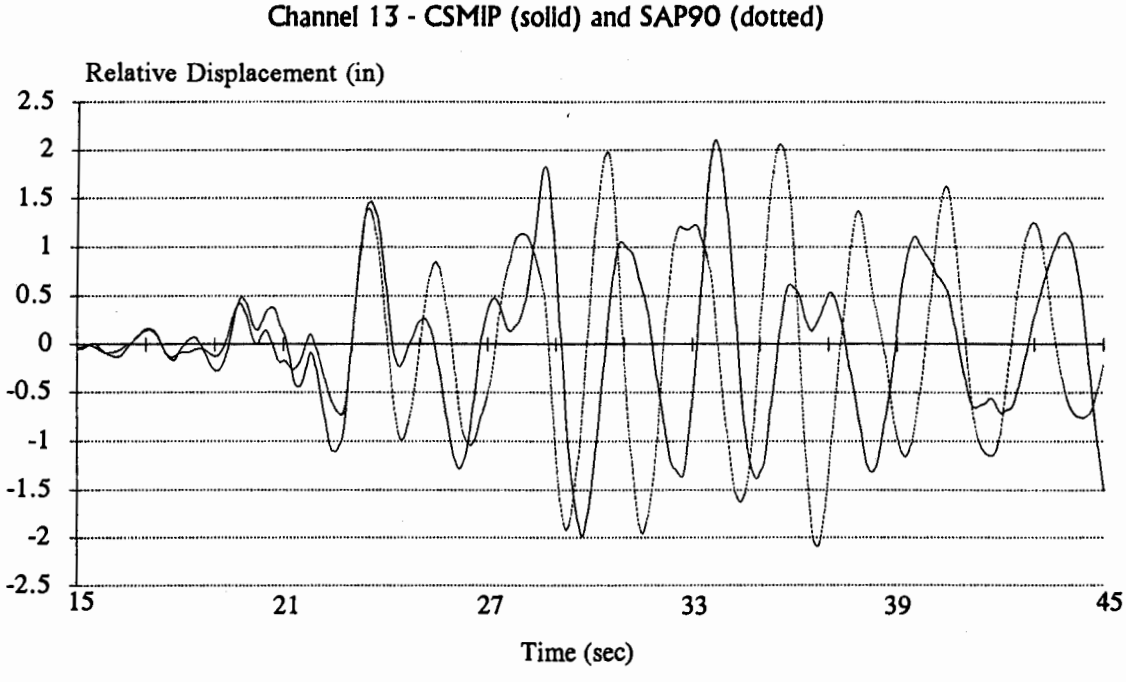

FIGURE D.9 - COMPARISON OF ANALYTICAL VS OBSERVED DISPLACEMENTS

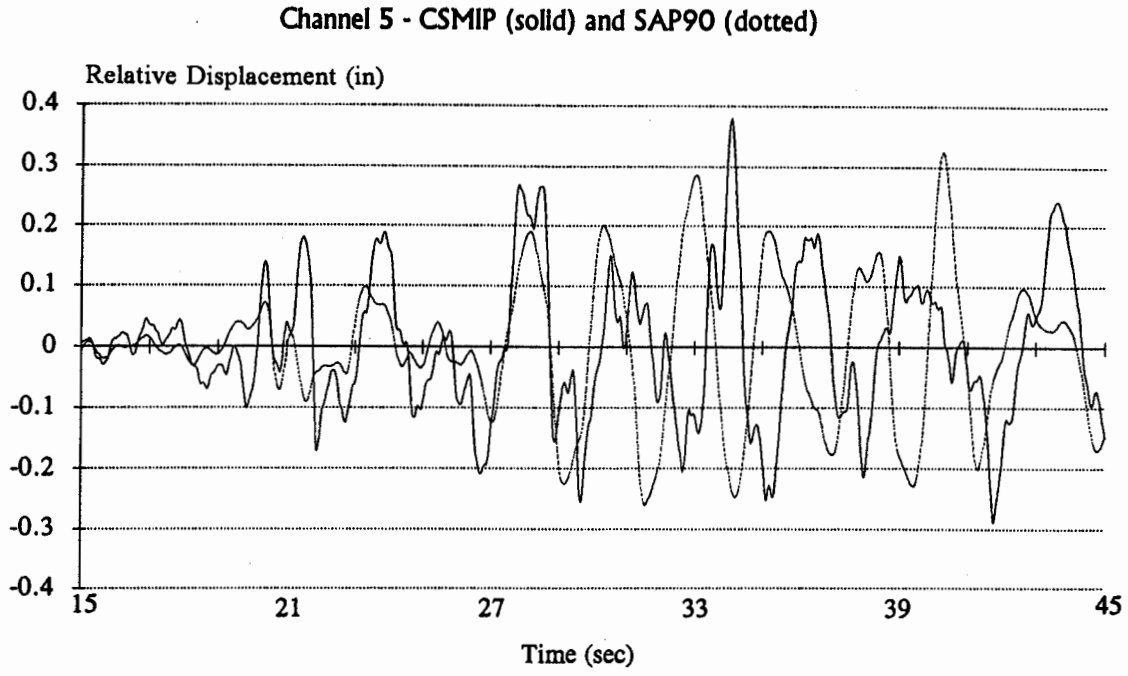

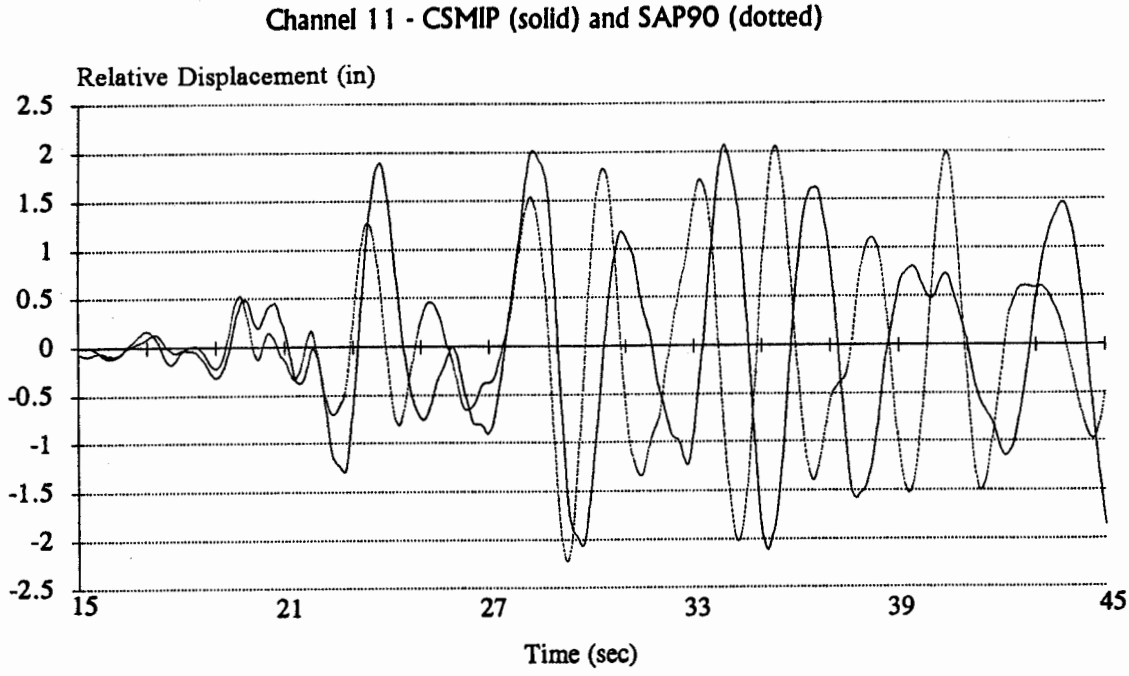

FIGURE D.10 - COMPARISON OF ANALYTICAL VS OBSERVED DISPLACEMENTS

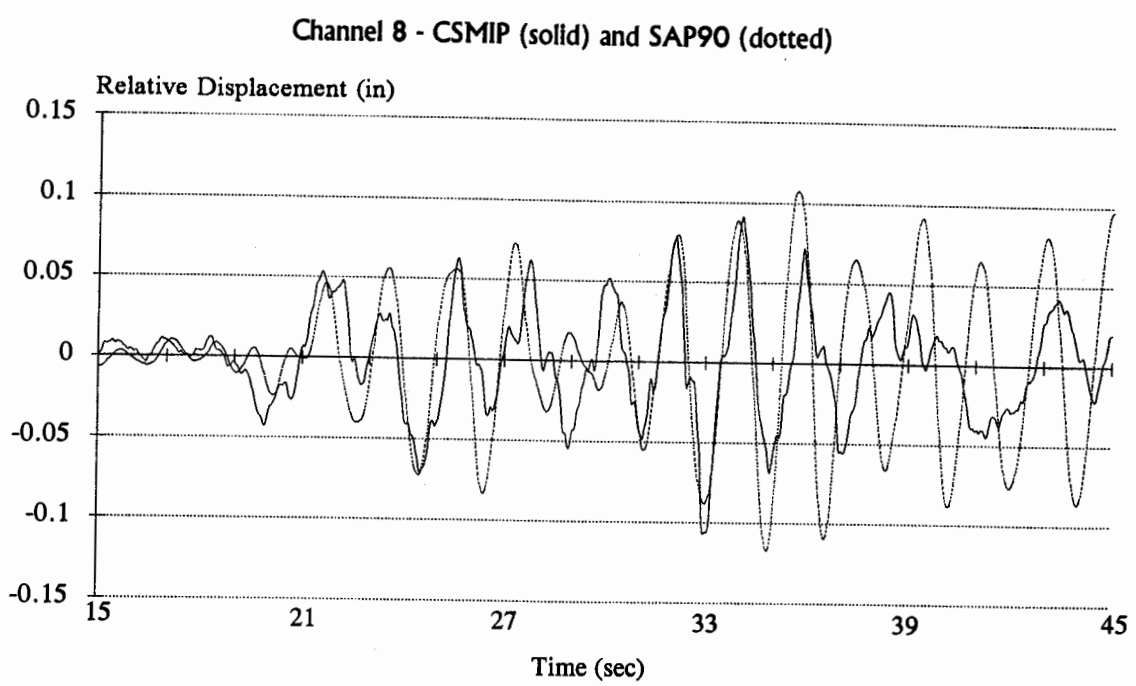

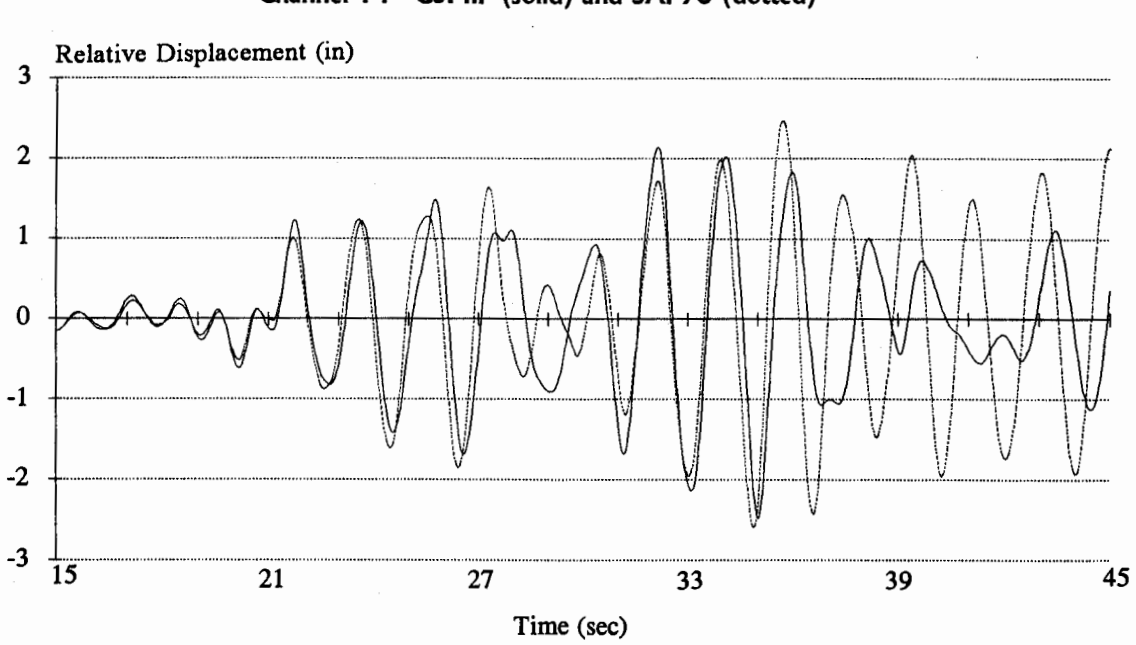

FIGURE D.11 - COMPARISON OF ANALYTICAL VS OBSERVED DISPLACEMENTS

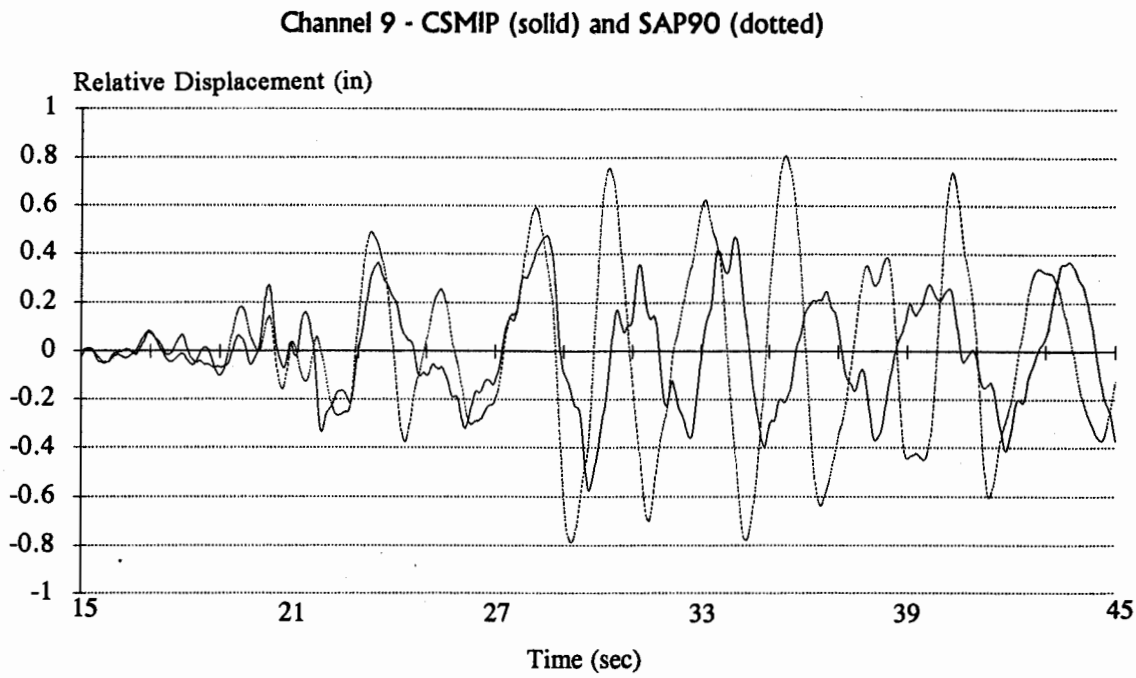

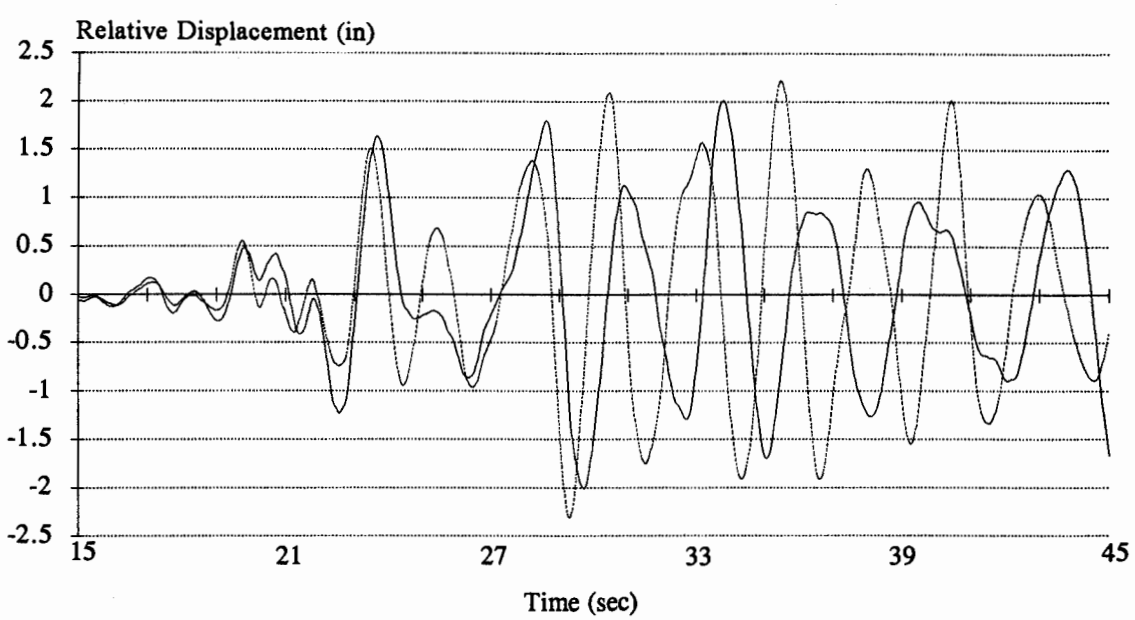

FIGURE D.12 - COMPARISON OF ANALYTICAL VS OBSERVED DISPLACEMENTS

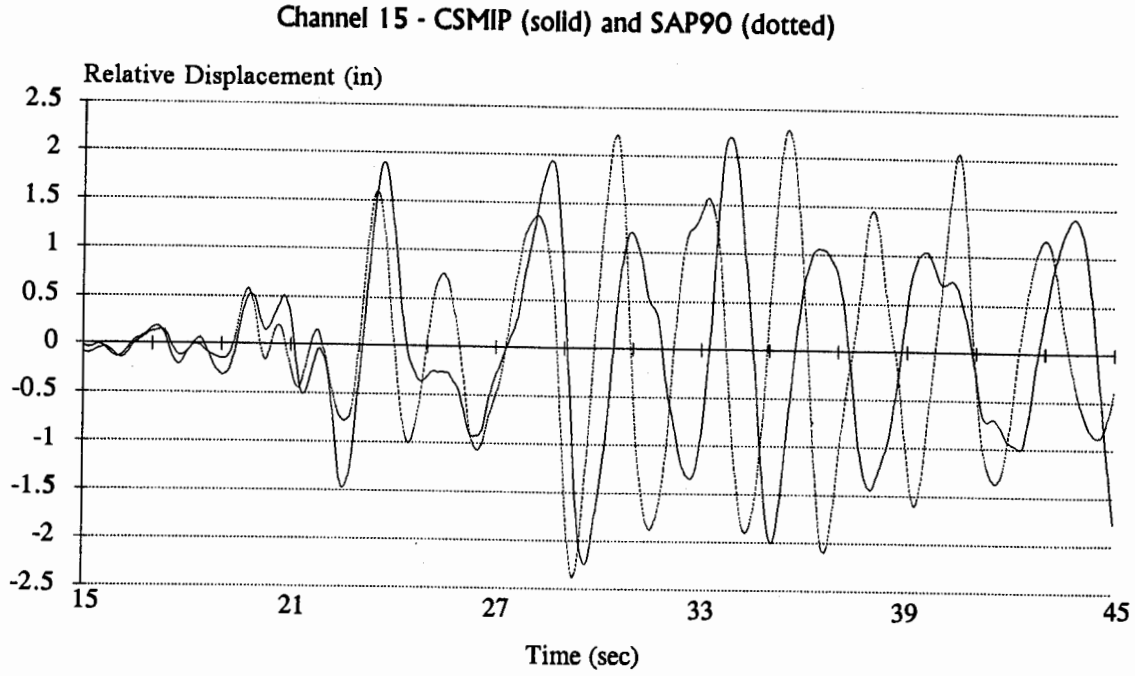

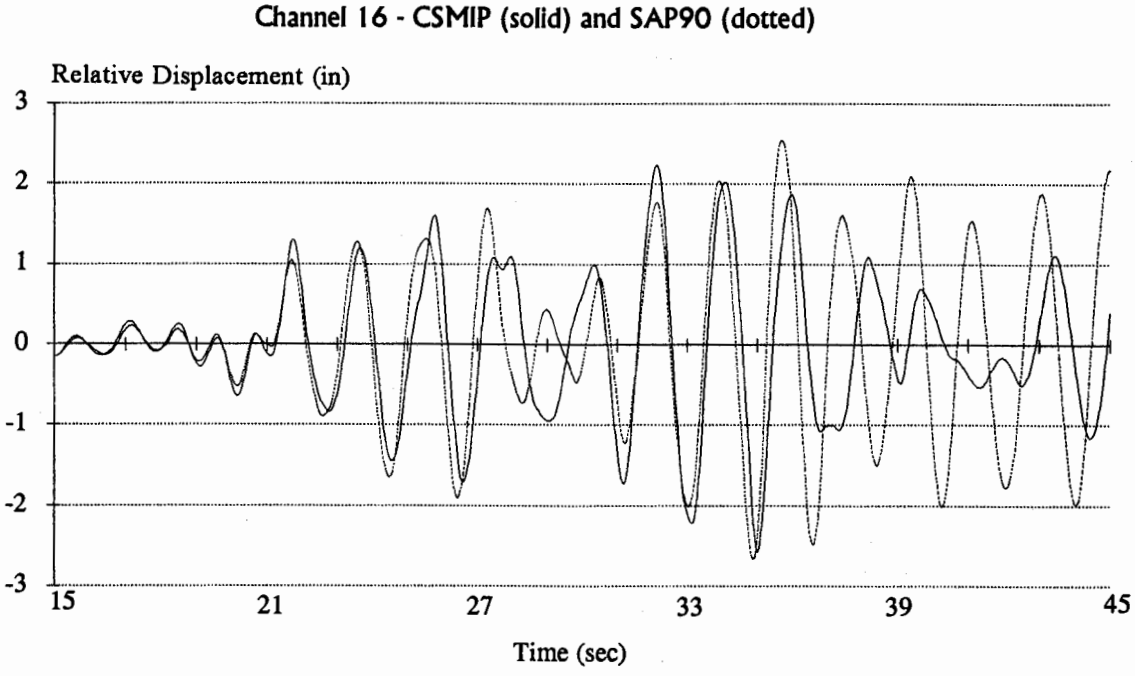

FIGURE D.13 - COMPARISON OF ANALYTICAL VS OBSERVED DISPLACEMENTS

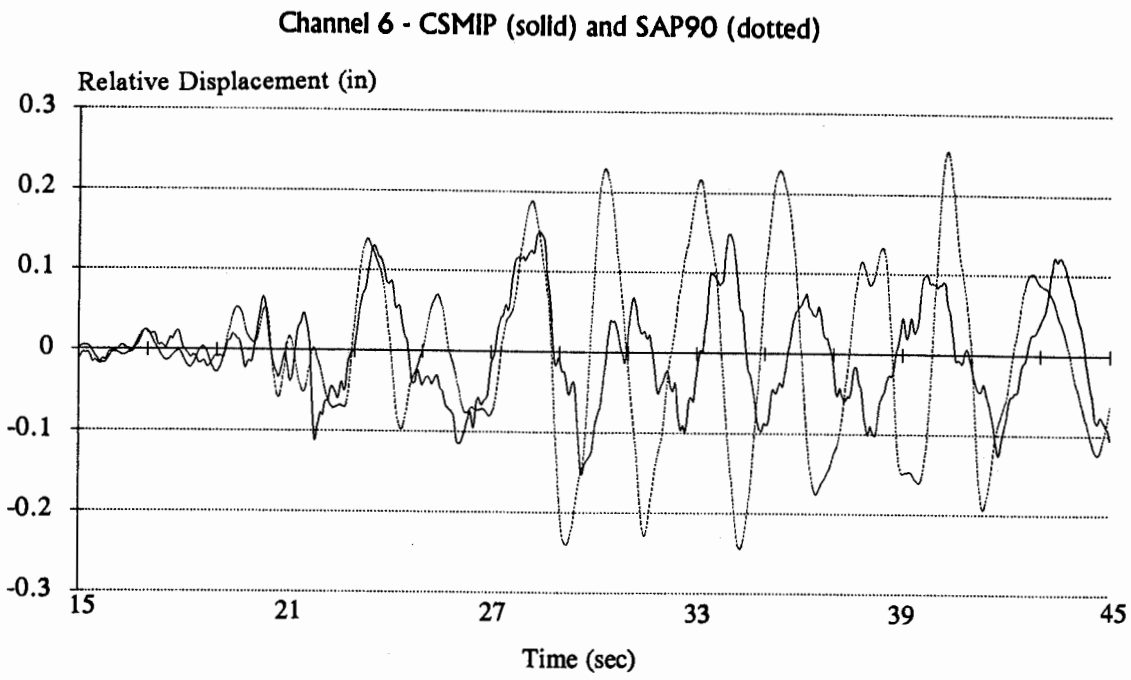

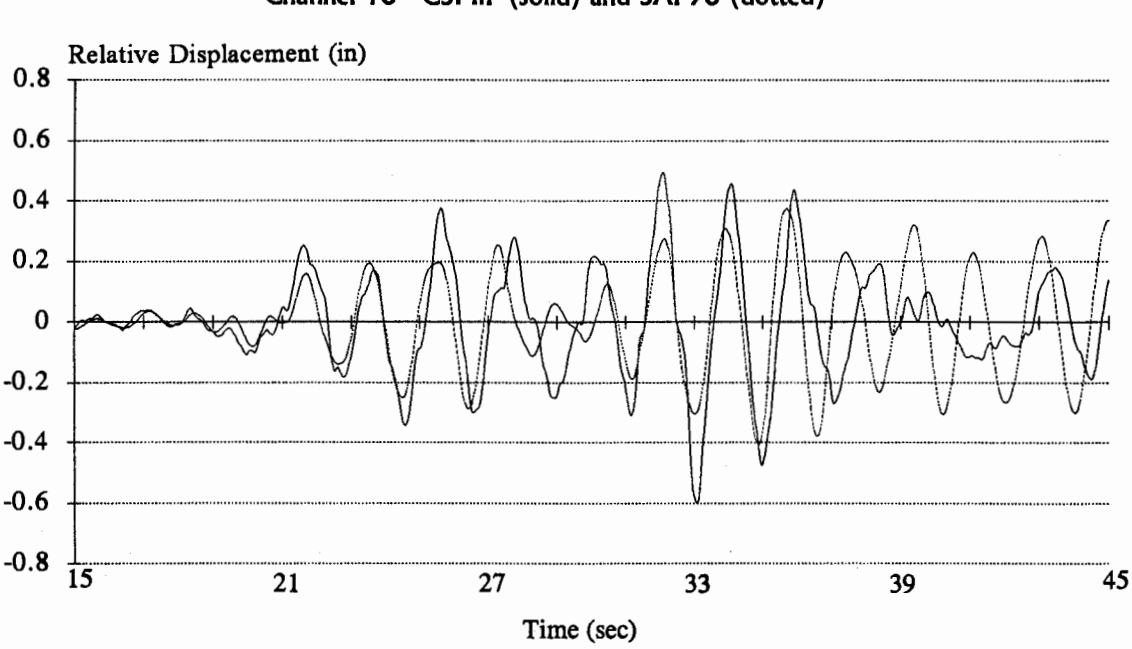

FIGURE D.14 - COMPARISON OF ANALYTICAL VS OBSERVED DISPLACEMENTS